# Investigating the effect of frother type on froth stability, froth recovery and entrainment

Tafadzwa Marozva

B.Sc. (Honours) Chemical Engineering

Dissertation submitted to the Faculty of Engineering and the Built Environment, University of Cape Town

In fulfilment of the requirements for the degree of Master of Science in Engineering


**Department of Chemical Engineering**

**University of Cape Town**

**January 2015**

## Declaration

I declare that this thesis, submitted for the degree of Master of Science in Engineering at the University of Cape Town, is my own work and has not been submitted prior to this for any degree at this university or any other institution. I know the meaning of plagiarism and declare that all the work in this document, save for that which is acknowledged, is my own.

Name: Tafadzwa Marozva

Signature: signature removed

## Acknowledgements

I would like to express my sincere gratitude to my supervisors Dr Belinda McFadzean and Mrs Jenny Wiese who not only served as my research supervisors but also assisted in providing the intuition, understanding and invaluable apparatuses on how to conduct a research. Special thanks are also given to the CMR team in particular the Flotation research group for the technical advice given during the course of the research, and the CMR laboratory staff for bearing with me during the experimental work and providing a conducive environment for my project. Sincere appreciation also goes to SAMMRI for the financial and academic support.

Special mention goes to Christopher Chikochi, Pharaoh Muzanenhamo, Seipati Mabote and Tanaka Shumba for being a good company and their assistance with various works related to this work. This project could not have been completed without your support.

Finally, to my family more so to Netty Marozva: my deepest gratitude. Your encouragement during the times when the journey got rough is much appreciated and duly noted.

*Mwari Baba handigoni kukutendai zvakakwana…..*

# Synopsis

Mineral processing involves liberation and beneficiation operations. Several beneficiation processes exist and one such important process is froth flotation. The flotation process involves the transportation of valuable minerals of a hydrophobic nature into the froth and to the concentrate launder. This hydrophobicity may be natural or imparted by a collector. Froth structure is significant in determining the froth stability which has an effect on the grade and recovery of valuable minerals. The froth structure is dependent on amongst other factors the type of frothers used during the separation process. As a result, frother type and concentration can be used to manipulate the froth recovery and grade of valuable mineral recovered. Upper Group 2 (UG2) ore contains chromite minerals which are naturally hydrophilic. The chromite minerals are usually recovered in the concentrate mainly due to entrainment. This lowers the grade of valuable minerals recovered and poses detrimental effects to downstream operations. Thus, the froth structure plays an important role in the flotation performance of UG2 ore.

This project was aimed at investigating the effect of chain length and functional group of different frothers on the froth stability, froth recovery and entrainment. Froth recovery, entrainment, solids and water recovery, as well as metallurgical recovery, were measured in a laboratory scale continuous column flotation cell. Froth stability was measured in a froth stability column, which is a non-overflowing column in which froth rise rate and equilibrium height were measured. A series of increasing molecular weight polyglycol and alcohol frothers, and their blends, were used to investigate the effect of frother type on froth structure.

Equilibrium surface tension measurements of polyglycol frothers showed an increase in the frother coiling nature and adsorption constants in addition to a decrease in the surface excess with increasing frother molecular weight. Alcohol frother experimental data similarly showed that an increase in molecular weight resulted in an increase in adsorption constant and surface excess. MIBC, which has the similar molecular weight as hexanol, had a lower adsorption constant and surface excess than hexanol due to its branched structure. Blends of polyglycol and alcohols showed no synergistic effects in surface tension or related parameters.

Tests were also performed to investigate the effect of frother molecular weight on foam and froth stability. It was hypothesised that an increase in the molecular weight of the frothers would result in a more stable froth phase. The results showed that for both frother series an increase in frother molecular weight led to a more stable foam phase. The results correlated closely with the surfactant activity trend except in the case of MIBC and hexanol. MIBC resulted in a more stable foam than hexanol, suggesting the existence of a different mechanism apart from surfactant activity to explain the foam stability results. The branched nature of MIBC may result in slower drainage of the thin films, resulting in a more stable foam. Use of frother blends gave a far more stable foam compared to the use of single

component frothers an indication of synergistic interactions between the component frothers. This was hypothesised to be due to an increase in dynamic surface tension, as opposed to the equilibrium surface tension discussed above.

With regards to froth stability tests, the polyglycol frother series showed a peak in froth stability at a molecular weight of 425 g/mol, thereafter froth stability decreased. This was attributed to a higher surface activity of PPG725 in comparison to PPG425. It is hypothesised that the PPG725 molecules adsorbed preferentially at the mineral surface and ceased to act as frothers. Hence PPG425 gave a more stable froth. For the alcohol series, use of pentanol resulted in the most stable froth phase. These findings were attributed to the high frother dosage necessary to maintain the froth in the alcohol experiments. High frother dosages can lead to frothers ceasing to act as a frother due to adsorption of the frother to the mineral surface. The low surface active nature of pentanol resulted in lower amounts of the pentanol being adsorbed on the mineral surface. As with the two phase experiments use of frother blends resulted in a more stable froth phase. This was attributed to an increase in dynamic surface tension with the use of frother blends.

The hypothesis, that an increase in froth stability is associated with a decrease in the grade of the valuable minerals recovered in the concentrate was also investigated. The hypothesis was supported by findings on use of single component frothers. However, the use of frother blends resulted in the desirable outcome of a more stable froth phase together with a higher grade and recovery of valuable minerals. A possible reason could be the existence of an enhanced froth structure, which promotes a stable froth with high recovery potential but good drainage characteristics that promote a low degree of entrainability.

Recommendations to continue this work include dynamic surface tension tests to be carried out with particular interest on the use of frother blends. Frother adsorption density measurements at a hydrophobic solid surface are suggested. The tests would provide valuable insight into the proposed theory of frother adsorption onto the mineral surface at high frother dosages. These recommendations stem from the infinite combination of component frothers that can be used in making frother blends. Further research can be carried out investigating the optimum frother suite that ensures the improved flotation performance to obtain the best technical and economic advantages.

# Table of Contents

# List of Figures

# List of Tables

# Chapter 1

# Introduction

## 1.1. Motivation

Mineral beneficiation processes are often implemented to ensure an increase in potential profits in any ore during the mining operation. Beneficiation is aimed at improving the yield of valuable minerals by ensuring their high recovery during the separation from gangue minerals. Examples of such processes include froth flotation, magnetic separation, gravity concentration and smelting. Froth flotation has been used in the mineral processing industry since the 20$^{th}$ century (Ata, 2012) and is the largest tonnage separation process worldwide (Cilliers, 2006). As the name "froth flotation" suggests the froth phase plays a significant role in the process.

The froth phase assists in transporting valuable minerals from the bulk slurry to the concentrate and in separating valuables from entrained gangue minerals. The froth phase is metastable (Exerowa & Kruglyakov, 1998), but to ensure its role during the froth flotation process it must persist long enough to reach the concentrate launder. To aid froth stability reagents called frothers are commonly added. Different types of frothers which can be used during flotation. Recently there has been a shift from the traditional use of single frother components to dual frother blends (Tan et al., 2005). It is also acknowledged that there has been little research done on the reasons behind shift towards use of frother blends (Laskowski et al., 2003; Tan et al., 2005). This thesis investigated the effect of frothers and their blends on froth stability. Without a generally accepted measure of froth stability use of the maximum froth equilibrium height (Barbian et al., 2003; Barbian et al., 2005), froth decay rate (Iglesias et al., 1995), bubble burst rate (Ventura-Medina & Cilliers, 2002; Ventura-Medina et al., 2003; Morar et al., 2012), water recovery (Wiese et al., 2011) as a measure of stability was implemented.

Not all particles that enter the froth phase reach then concentrate launder; this is due to the eventual bursting of unstable bubbles leading to the fall back of once attached particles. This has a significant impact on the grade and recovery of valuable minerals in the concentrate launder and is expressed as a metallurgical parameter called froth recovery. Froth recovery is the fraction of particles entering the froth phase that reports to the concentrate (Finch & Dobby, 1990). The overall recovery of valuables is a function of froth recovery which in turn is a function of froth stability among other factors. This thesis aims assess the effect of frother type on froth recovery.

In South Africa, due to the increasing costs associated with the required depth in reaching the Merensky reef attention has turned to the Upper Group 2 (UG2) reef (Cramer, 2008).

UG2 ore is comprised largely of chromite (60-90% by volume) (Schouwstra & Kilnoch, 2000).Chromite is not naturally floatable, but significant quantities report to the concentrate during flotation. This is a serious problem to the downstream smelting process, which generally has a 3% chromite constraint to the smelter. Recovery of chromite in the concentrate is due to an unselective transport mechanism referred to as entrainment which has a detrimental effect to the concentrate grade. It is acknowledged that the froth structure in particular water content of the froth has an effect on the degree of entrainment (Savassi et al., 1997; Melo, 2001). Frothers modify the structure of the froth hence have an effect on entrainment which is investigated in this thesis.

Interfacial surface tension measurements in conjunction with adsorption isotherms are usually used to better understand the adsorption of surfactants to the interface which is also conducted in this thesis.

## 1.2. Research Objectives and Key Questions

The objectives of this research are therefore to determine the inter-relationships as a function of frother type between the following parameters:

1. Froth stability,
2. Froth valuable mineral recovery,
3. Entrainment,
4. Pulp zone recovery; and
5. Grade

To meet the set objectives, the following key questions were set:

1. Does changing frother type affect the stability of foam and froth stability?
2. What is the effect of the molecular weight of frothers on the stability of the foam and froth phase?
3. What is the effect of molecular weight of frothers on the froth water recovery?
4. Is entrainment of gangue material related to the stability of the froth phase?
5. Why are frother blends more advantageous to use in comparison to single component frothers?

## 1.3. Thesis Layout

This thesis is structured into 6 chapters and appendices with the structure outlined as follows:

### Chapter 1: Introduction

This chapter introduces froth flotation, with emphasis on the importance of the froth phase and the effect of frothers to key metallurgical performance parameters which is the background of this research. This is followed by the outline of the thesis objectives and key questions.

### Chapter 2: Literature Review

The chapter provides a review of literature concerning the effect of frothers to the flotation process. The scope of the review is limited to froth stability, froth recovery and entrainment at both fundamental and operational level with a review of different methods developed in earlier research to measure the metallurgical parameters also included. At the end of the chapter the proposed hypotheses of this research work are outlined.

### Chapter 3: Experimental Methodology

The chapter gives a detailed description of the experimental approach taken in testing the proposed hypothesis. This includes the set-up of test rigs, conditions under which the experiments were carried out and measurement techniques applied in the tests.

### Chapter 4: Results

Results from the test work performed are given in this section. Results on the effect of frothers on froth stability based on use of the frothing column are initially presented followed by results from the flotation process giving results on effect of frother type on froth recovery and entrainment.

### Chapter 5: Discussion

This chapters aims to discuss the results presented in the preceding chapter.

### Chapter 6: Conclusion and Recommendations

This chapter presents the key findings from this research followed by recommendations of future work.

# Chapter 2

# Literature Review

Over the years extensive research has been done on the effect of frothers on the flotation process. Although the literature covers a wide scope, particularly with regards to the pulp phase, this review will focus on performance parameters related to the froth phase. This review is aimed at three metallurgical parameters: froth stability, froth recovery and entrainment. The scope of the review is expanded to include research done at both fundamental and operational level.

The chapter commences with a brief description of the principles of the flotation process. This is followed by a review of the different types of frothers and their effect on the flotation process proposing theories to explain their mechanism of action. In line with the scope of this research the remainder of the chapter focuses on froth stability, froth recovery and entrainment. A detailed review of different methods developed in earlier research to measure these metallurgical parameters is also included in the review.

## 2.1. Principles of flotation

There are two fundamental operations in mineral processing namely liberation of the valuable minerals from their waste gangue materials, and separation of the minerals from the gangue in a process known as concentration (Wills & Napier-Munn, 2006). Several beneficiation processes exist and one such important process is froth flotation which is the largest tonnage separation process worldwide (Cilliers, 2006). A schematic diagram of the flotation process is shown in Figure 2-1.

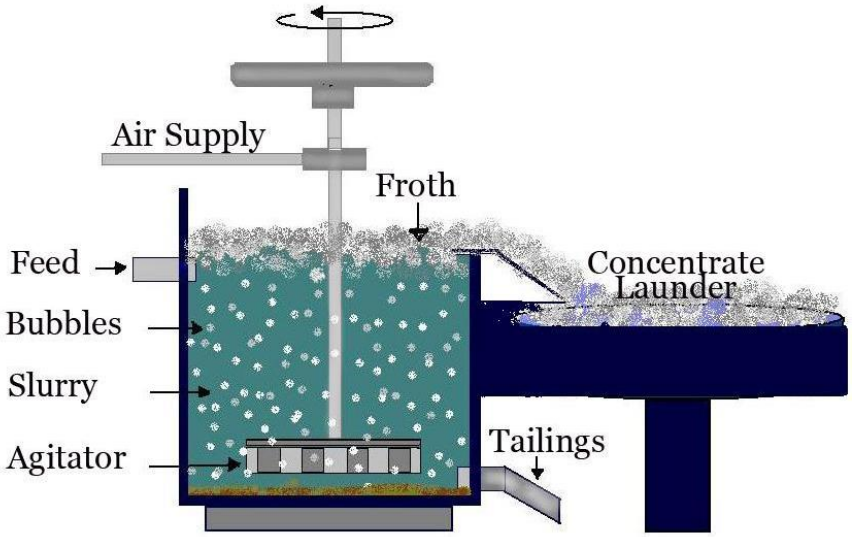


**Figure 2-1: Schematic of the froth flotation process (http://miningeducation.blogspot.com/2012/01/flotation-in-mining.html).**

Froth flotation is a beneficiation process that separates particles on the basis of a difference in the ability of surfaces of different minerals to adhere to gas bubbles in mineral/water slurries (wettability). Mineral particles are either naturally hydrophobic, or they can be chemically treated to induce hydrophobicity. The difference in wettability of different mineral surfaces is mostly achieved by use of chemical reagents.

Froth flotation involves the generation of bubbles by different mechanisms. These bubbles are passed through slurry and as the air disperses through the pulp, the collision of hydrophobic minerals with the bubbles results in the solids adhering to the bubbles and forming a particle bubble aggregate. Due to buoyancy the aggregate rises towards the surface of the pulp phase forming the froth phase which is collected in the launder. In the meantime, particles with a hydrophilic surface remain in the pulp phase and eventually report to the tailings. Perfect separation between hydrophobic and hydrophilic minerals is not feasible. This is due to the existence of transport mechanisms such as entrainment whereby particles are mechanically transferred from the pulp phase to the froth in the flow of water which allows for a fraction of the hydrophilic minerals to report to the concentrate launder.

In summary the role of the pulp phase is to ensure a high recovery of the valuable mineral. The role of the froth phase is to improve the selectivity of the flotation process by reducing the amount of material recovered via entrainment (Wills & Napier-Munn, 2006).

Flotation reagents are used to ensure a highly selective separation process that yields a high recovery of the valuable mineral. Examples of such reagents are collectors, depressants, activators, pH controllers and frothers. Collectors by means of chemisorption adsorb onto the surface of valuable minerals resulting in a hydrophobic surface which promotes the attachment of the valuables to the rising bubbles (Wiese et al., 2011). Depressants adsorb

onto the surface of naturally floatable gangue resulting in a hydrophilic surface which ensures minimum attachment of gangue to the rising bubbles and ultimately a high grade of valuable concentrate. Activators improve the process efficiency due to the formation of precipitates which increase the adsorption of collectors on valuable minerals (Grobler et al., 2005). The role of frothers is the main focus of this research and as such the remainder of the literature review focuses on frothers.

## 2.2. Frothers

Frothers are surface active reagents which adsorb at the air-water interface and whose function in the flotation process is twofold: firstly, to reduce bubble coalescence ensuring smaller bubbles for improved flotation kinetics and, secondly, to promote the formation of froth by decreasing the surface tension at the air-water interface increasing the foamability of the liquid for the separation of valuable minerals from gangue.

### 2.2.1. Types of frothers

Upon examination of literature it is evident that there are several ways to classify frothers. Common classification methods are based on the chemistry of the frother, frother sensitivity to pH, solubility, frothing ability and selectivity relationships (Khoshdast & Sam, 2011). Frothers commercially available to the mineral industry can be classified as follows:

1. Alcohols
2. Alkoxy substituted alcohols
3. Polyglycols

#### 2.2.1.1. Alcohol frothers

The functional group of alcohols is a hydroxyl group. This group can be further subdivided into linear aliphatic, cyclic and aromatic groups.

**Aliphatic Alcohols**

Usually the carbon chain length of such frothers is in the range of 5 to 8. Frothers with fewer than 5 carbon atoms are considered to be too weak and frothers with more than eight carbon atoms are difficult to disperse (Moyo, 2005). They can also be classified as neutral frothers as they are functional in both acidic and alkaline pulps (Bulatovic, 2007). This group of frothers represents the most commonly used frothers and an example of such a frother is MIBC (Methyl Isobutyl Carbinol) (Tan et al., 2005).

**Cyclic alcohols**

These frothers can also be classified as neutral frothers. They are mixtures of different cyclic alcohols produced as synthetic mixtures or from pine resins (Bulatovic, 2007). The most common cyclic alcohols among these mixtures are terpine-ols followed by borneol and pinene (Khoshdast & Sam, 2011).

A major disadvantage associated with using cyclic alcohol frothers is the varying frothing properties due to the inability to ensure a constant composition of the frother (Bulatovic, 2007). Due to their collecting properties these frothers are less popular in the mineral beneficiation industry in comparison to other frothers (Khoshdast & Sam, 2011). Cyclic alcohols are, however, preferred over aliphatic alcohols when a more elastic and persistent froth is required (Moyo, 2005).

**Aromatic Alcohols**

Aromatic alcohols are also known as phenols. These frothers perform relatively well in acidic pulp and have reduced frothing abilities in alkaline pulp and can hence be classified as acidic

frothers. A common example of such a frother is cresol which comprises of a mixture of ortho (35-40%), meta (25-28%) and para (35-40%) cresols (Bulatovic, 2007). Similarly to cyclic alcohol frothers, a disadvantage of using these frothers is their variable composition as they are a by-product formed during the gasification of coal tar and/or the distillation of crude oil (Khoshdast & Sam, 2011).

#### 2.2.1.2. Alkoxy-type frothers

These frothers can be classified as neutral frothers and the most common example of this group of frothers is 1, 1, 3-Triethoxybutane (TEB). TEB is a derivative of the alcohol group and hence they both have the same general characteristics (Moyo, 2005), with TEB tending to be more selective resulting in high concentrate grades. They are not commonly used in the industry as use of these frothers in high concentration does not significantly affect the structure of the froth (Melo, 2001).

#### 2.2.1.3. Polyglycol frothers

These are polymeric derivatives of ethylene, butylene or propylene oxide (Laskowski, 1993) and can also be classified as neutral frothers. Depending on the ratio of the hydrophobic to hydrophilic groups in the frother molecule this group ranges from being completely miscible to partially soluble in water.

Varying the relative length of the hydrophobic to hydrophilic group in the frother molecule results in a change in the molecular molar mass and in hydrophile-lipophile balance (HLB). HLB is defined as the degree to which a surfactant is hydrophilic or lipophilic in nature. This group of frothers offers the flexibility to obtain a required molecule with the desired molecular weight and HLB. The power and performance of these frothers is determined by their molecular weight and carbon chain length (Khoshdast & Sam, 2011). Froth produced by these frothers is more tightly knit and more persistent than froths produced by alcohol frothers (Klimpel & Isherwood, 1991). As the concentration of these frothers is increased, they do not exhibit a strong rate maximum as shown by aliphatic alcohols (Klimpel & Isherwood, 1991).

As a result, the plant recovery possible from a fixed volume flotation cell can be increased with increasing glycol frother concentration unlike in the case of alcohol frothers (Klimpel & Isherwood, 1991). Klimpel and Isherwood (1991) also investigated the effect of changing the molecular weight of glycol frothers on the recovery of particles of different sizes. This work showed that as the molecular weight increased the recovery of and selectivity for fine particles decreased.

#### 2.2.1.4. New frothers

Extensive studies have been conducted on the development of new frothers to produce reagents which are highly hydrophobic in order for the frothers to exhibit collecting properties for coarser particles. Such frothers result in a decrease in the required collector dosages, avoiding the slow floats associated with a high collector dosage (Klimpel & Isherwood, 1991). An increase in mineral recovery as small as 1% due to a change in reagents used during flotation is of great economic benefit at an industrial scale (Harris & Jia, 2000).

The surface activity of frothers is determined by their chemical structure and the functional groups in frother molecules have an effect on their properties (Harris & Jia, 2000). A class of modified alcohol frothers comprising of at least one hydroxyl group has been developed (Khoshdast & Sam, 2011). These frothers are reaction products of various chemical reagents such as a diol, carboxylic acid or an alkylene oxide.

The use of these frothers has resulted in improved recovery of sulphide minerals, improved flotation kinetics and a reduction in the dosage of frother required (Khoshdast & Sam, 2011). There is another group of new frothers with a general chemical formula, ROH.n where R represents an alkylene oxide unit with carbon atoms in the range of 4 to 6 (Klimpel & Isherwood, 1991). Such frothers are a chemical product of direct addition reactions of propylene oxide or butylene oxide and aliphatic alcohols.

### 2.2.2. Effect of frothers on the pulp phase

The flotation process consists of two distinct phases: the pulp and the froth phase. A sub-process of the flotation process is bubble loading which takes place in the pulp phase and involves bubble-particle collisions and the attachment and detachment of the particles from the bubbles (Bradshaw & O'Connor, 1996). Selective attachment of the solids to the bubbles is the most important sub-process as without it separation would not be achieved (Sherrel, 2004).

Solid particles submerged in liquid and in contact with air have interfacial forces exerted on each interface as shown in Figure 2-2.

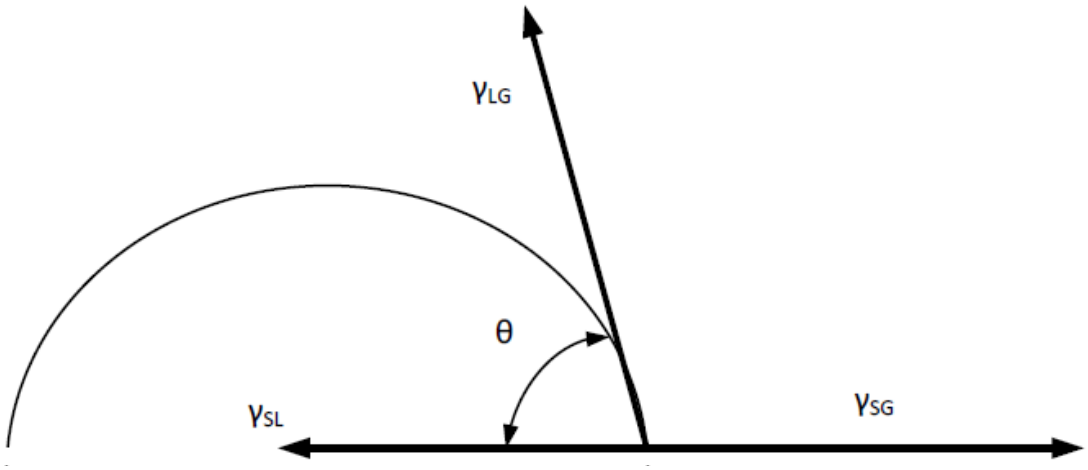


**Figure 2-2: Figure illustrating interfacial forces exerted on the interfaces during bubble-solid collision.**

Where $\gamma_{SG}$ is the solid-gas interfacial energy, $\gamma_{LG}$ is the liquid-gas interfacial energy and $\gamma_{SL}$ is the solid-liquid interfacial energy. Thermodynamically, for particles to be successfully attached to the bubbles the change in the free energy (ΔG) during the process should be negative (Laskowski, 1989).

$$\Delta G = \gamma_{SG} - (\gamma_{SL} + \gamma_{LG}) < 0 \qquad \textbf{Equation 2-1}$$

The presence of surfactants (collectors and frothers) which adsorb at all interfaces leads to a decrease of all surface tensions and renders an initially hydrophilic surface hydrophobic (Laskowski, 1989). An interpenetration theory has been proposed by Leja and Schulman (1954) detailing possible positive interactions between frothers and collectors during the attachment of solids to bubbles. They proposed that due to interactions between frothers and collectors the attachment of collector-frother covered solid particles to bubbles again coated by collectors and frothers is analogous to penetration of the solid-water and air-water interfaces respectively, resulting in the formation of a new solid-air interface (Yunkai, 2000).

The probability of collisions between solids and bubbles is a function of the bubble size. The existence of bubbles of small sizes is desirable as they present a greater surface area for collisions to occur. Recent studies (Laskowski et al., 2003b; Melo, 2001; Gupta et al., 2007) have shown that bubble size within the pulp phase is a function of frother type.

#### 2.2.2.1. Critical Coalescence Concentration (CCC)

Frothers reduce bubble size by ensuring a decrease in bubble coalescence (Cho & Laskowski, 2002; Laskowski et al., 2003a; Laskowski et al., 2003b) . Critical coalescence concentration (CCC) is defined as the concentration above which bubble coalescence is entirely prevented. At concentrations above the CCC the bubble size is not affected by frother concentration as shown in Figure 2-3,

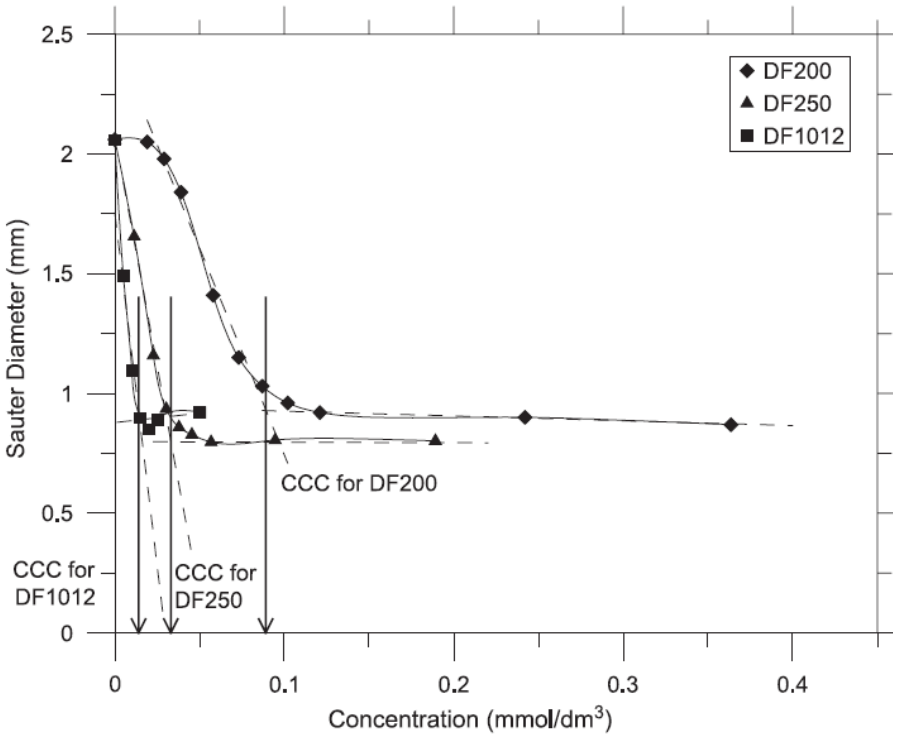


**Figure 2-3: Effect of addition of frothers on the Sauter mean diameter of bubbles; the critical coalescence concentration is denoted by the vertical lines (Laskowski, 2004).**

Comely et al. (2001) showed that the value of the CCC varied inversely with the molecular weight of the frother (Figure 2-4).

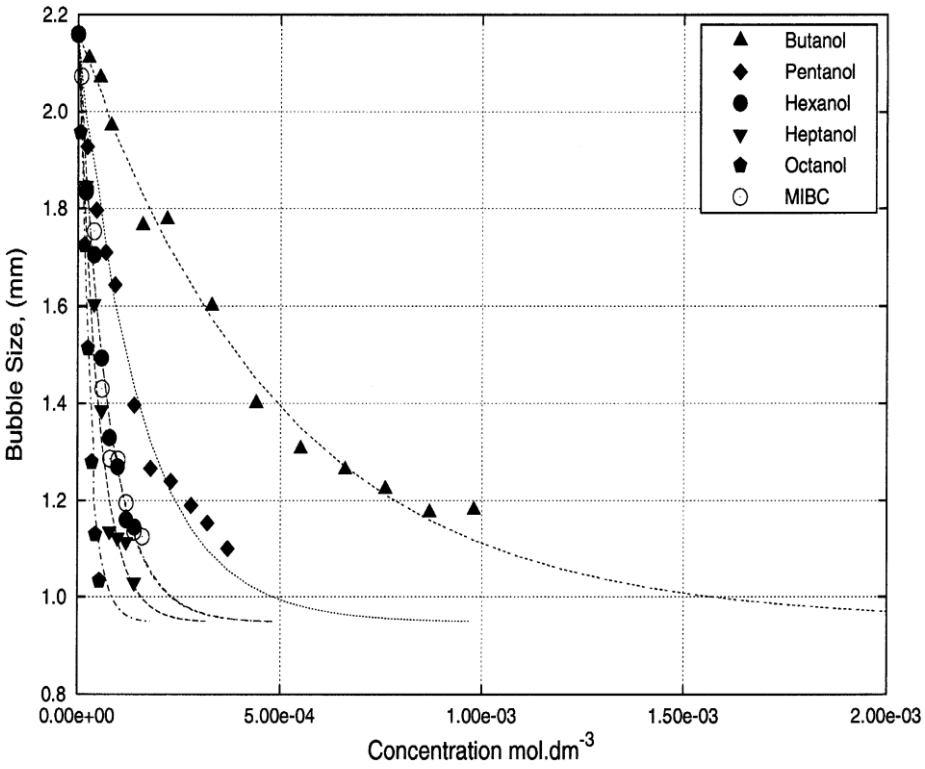


**Figure 2-4: Sauter mean diameter of bubbles as a function of frother type and concentration (Comley et al., 2001).**

Comley et al. (2001) proposed an exponential decay relationship which could be used to predict the bubble size as a function of frother concentration. This relationship is shown in relation to experimental data points for a number of alcohol frothers in Figure 2-4.

$$d_s = \left(d_s^0 - d_s^{min}\right) * e^{-\beta C_b} + d_s^{min} \qquad \textbf{Equation 2-2}$$

*Where $d_s$is Sauter mean bubble diameter (mm), $d_s^0 = d_s$ in the absence of a frother (mm), $d_s^{min}$is minimum $d_s$ produced by the system (mm); β is coalescence parameter (dm$^3$mol$^{-1}$) and $C_b$ is bulk concentration of frother (moldm$^{-3}$).*

Laskowski (2004) showed that frothers that are more efficient in reducing the bubble size also produce more stable foam. Cho and Laskowski (2002) investigated the effect of frothers on bubble size and of particular importance was their work involving the use of single-hole and multi-hole spargers. Figure 2-5 shows the results obtained using a single-hole sparger.

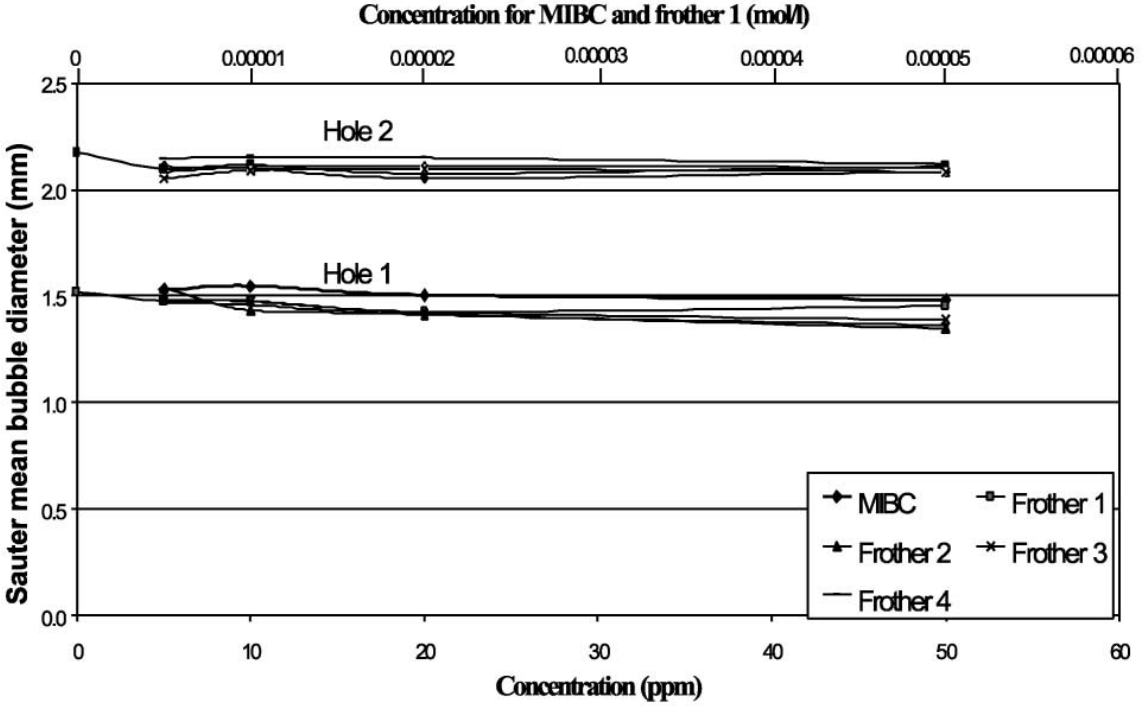


**Figure 2-5: Sauter mean bubble diameter as a function of frother concentration whilst using a 0.1 mm single-hole sparger (Cho & Laskowski, 2002).**

As indicated in Figure 2-5, frothers did not have any effect on bubble size when using single-hole spargers as can be seen from the uniform bubble size obtained despite changes in frother concentration. Figure 2-6 shows the results obtained using a three-hole sparger.

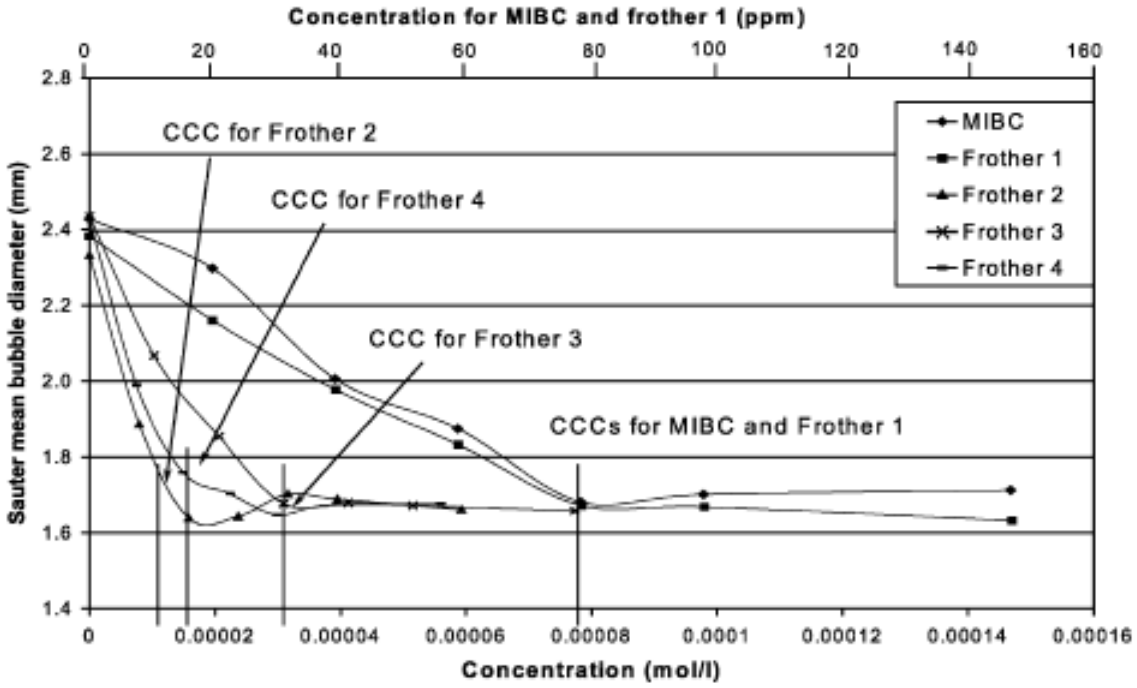


**Figure 2-6: Sauter mean bubble diameter as a function of frother concentration using a 0.1 mm diameter three-hole bronze sparger (Cho & Laskowski, 2002).**

This figure shows the existence of an exponential decay relationship between bubble size and frother concentration. Using these results Laskowski and Cho (2002) demonstrated that frother concentration controls bubble size only if the bubbles are able to collide (use of multi-hole sparger).

### 2.2.3. Role of the froth phase in flotation

In the discussion that follows, and in keeping with convention (Farrokhpay, 2011), the term 'foam' refers to a two-phase system comprising liquid and dispersed air while 'froth' is a three-phase structure compromising air bubbles, liquid and solids. The froth phase plays a significant role in the metallurgical performance of industrial flotation cells. The overall grade and recovery of valuable minerals in the concentrate launder are strongly dependent on the structure of the froth which is a function of frother type and concentration. The main roles of the froth phase according to (Heath, 2013) are:

1. Creating an environment for separation of valuable minerals attached to air bubbles from gangue minerals in the slurry.
2. Separating valuable minerals from entrained gangue materials.
3. Transporting mineral particles from the bulk slurry to the concentrate launder.

To ensure transportation of minerals from the bulk slurry to the concentrate it is essential to ensure a stable froth, as an unstable froth leads to minimum mineral transportation and hence a poor recovery from the flotation cell. On the other hand too stable a froth is undesirable as it is difficult to handle (Farrokhpay, 2011) particularly with regards to pumping the concentrate.

## 2.3. Froth stability

Froth stability is a measure of the ability of froth to withstand collapse when external forces are exerted on it (Farrokhpay, 2011). A number of theories have been proposed to explain the role frothers play on froth stability. Frothers, as surfactants, provide resistance to the thinning process of the bubble film. Frothers reduce the bubble film thinning rate by increasing the surface viscosity and surface elasticity of liquid films (Pugh, 1996). It is accepted that frothers aid in ensuring a stable froth phase (Laskowski, 1993; Gupta et al., 2007; Laskowski et al., 2003a; Laskowski, 2004) with several theories being proposed to explain the phenomenon.

### 2.3.1. Gibbs Marangoni Effect

Stability of foams depends on the elasticity of the liquid films surrounding the bubbles. If the films easily break when external pressure is exerted on them, the foam is unstable. Wang and Yoon (2008) considered the film elasticity as a "self-healing" capacity against external disturbances. The Gibbs elasticity of a thin film is defined as the ratio of the change in the film surface tension ($2d\gamma$) to the change in surface area ($dA$) per unit area ($A$) (Wang & Yoon, 2008). During dynamic conditions the change in surface tension is higher in comparison to equilibrium conditions, a phenomenon known as the Marangoni effect.

Frothers at the surface of bubbles counteract the local thinning of the bubble film which could ultimately result in the rupture of bubbles. The local thinning action results in a low concentration of the frother creating a surface-tension gradient at the surface. The surface-tension gradient results in a mass-transfer process at the interface ensuring the balancing of the thinning action and restoring the initial surface thickness. This theory is named the Gibbs-Marangoni effect (Koerner, 2008). Foam stability is a function of frother concentration (Koerner, 2008) as the Gibbs-Marangoni effect is only applicable within a limited frother concentration range as illustrated by Figure 2-7.

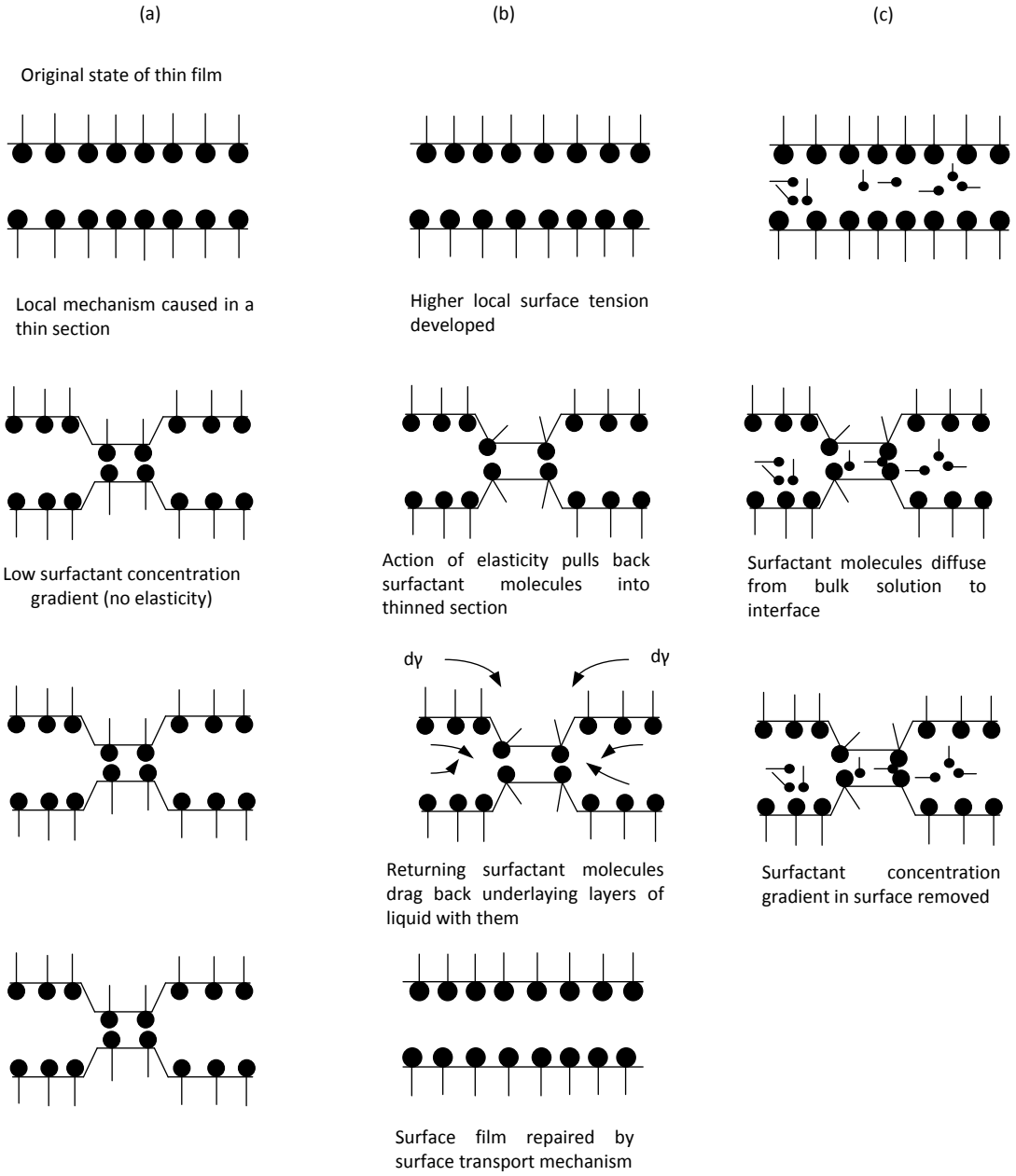


**Figure 2-7: Illustration of the reaction of liquid film to a surface disturbance at (a) low frother concentration (b) intermediate frother concentration and (c) high frother concentration (Pugh, 1996).**

At too high frother concentrations the local thinning action does not result in a frother concentration gradient, this is due to the rapid diffusion of the frother molecules from the bulk solution to the interface (Koerner, 2008). At too low concentrations the surface tension gradient is too low to result in sufficient force to balance the disturbances.

The importance of the film elasticity is corroborated by the work done by Wang and Yoon (2008) which showed that the lifetime of foam increases with increasing elasticity. Wang and Yoon (2008) also showed that elasticity is not the only factor affecting foam stability identifying disjoining pressure as another factor.

### 2.3.2. Hydration Layer Effect

Heteropolar molecules adsorb at the air-water interface with the polar groups directed toward the liquid phase. Interaction of the frother polar group (hydrophilic) and liquid phase surrounding the bubble (hydration layer) increases the mechanical strength of the layer hence a more stable bubble (Bulatovic, 2007). Frother chemistry determines the nature of the hydration layer hence having an effect on froth stability (Zhang, 2012). There exists an optimum frother concentration at which the most stable froth is obtained. Excess amounts of the frother leads to a decrease in the froth stability. This is due to the high frother concentration strongly lowering the surface tension of the solution which causes deterioration of the formation of the stable hydration layer (Bulatovic, 2007).

### 2.3.3. DLVO theory

At close proximities between bubble surfaces, surface forces of inter-molecular origin referred to as disjoining pressure determine the stability of bubble films (Tabakova & Danov, 2009). According to Derjaguin and Landau (1941) the sum of the attractive Van der Waals forces and repulsive double-layer forces determines the disjoining pressure. The disjoining pressure is the difference between pressure in the bulk liquid film and pressure at the air-water interface (Do, 2010).

The disjoining pressure characterises the state of the bubble film as a positive (repulsive) disjoining pressure leads to slowing of drainage hence a more stable foam whilst negative (attractive) pressure has the antagonistic effect (Wang & Yoon, 2004). To ensure the existence of stable foam the rate of drainage of the liquid forming the bubble film to the Plateau border should be slow. The drainage is due to capillary tension which is influenced by factors such as repulsive Coulombic forces, gravity and vapour velocity (Pauley et al., 1988). The repulsive forces oppose the formation of Plateau borders and hence retard liquid drainage.

Recent work (Wang & Yoon, 2004; Karakashev & Nguyen, 2007) has shown the failure of the classical DLVO theory to accurately predict foam stability at low surfactant concentrations and has suggested the existence of an additional attractive force (hydrophobic forces). Craig et al. (1993) observed a decrease in bubble coalescence as the electrolyte concentration increased suggesting a decrease in the hydrophobic force. Yoon and Aksoy (1999) also observed that the hydrophobic force increases as the surfactant concentration decreases. Addition of polymer frothers leads to their adsorption onto the bubble surface preventing surfaces from coming into contact (Steric Repulsion) and at those separation distances the Van der Waals forces are rendered weak and therefore cannot ensure coalescence of the bubbles.

### 2.3.4. Surface Viscosity

Surface elasticity among others is not enough alone to explain foam stability without taking into account surface viscosity (Fruhner et al., 1999). Surface viscosity also affects the stability of the foam phase by retarding the drainage of liquid from between the bubbles hence extending the life-time of the foam (Kitchener & Cooper, 1959). The rate of bubble coalescence decreases with increasing viscosity (Cho, 2001). The packing of a high concentration of surfactants at the surface of bubbles results in an increased inter-molecular cohesion leading to increased surface viscosity (Elmahdy, 2011).

## 2.4. Structure of foam and froth

A pure liquid does not foam, except in the presence of surfactants (Cho & Laskowski, 2002). Foam is a metastable disperse system of gas bubbles separated by liquid films (Exerowa & Kruglyakov, 1998). Foaming does not occur in pure liquids as no mechanism exists to retard film drainage (Kitchener & Cooper, 1959). Foams are a result of introducing any gas beneath the surface of a liquid which results in expansion of the liquid to enclose the gas inside a thin liquid film commonly referred to as a lamella. Foams show an extemporaneous nature to detach into two distinct bulk phases which are the liquid and gas phases (Bhakta & Ruckenstein, 1997). To efficiently use the froth generated during flotation it is critical that control of froth stability is ensured. As a result a comprehensive understanding of the mechanisms involved in foam and froth persistence and decay is important.

The Plateau borders form an interconnected system through which liquid flows in foam and hence contain virtually all the liquid in the foam (Cilliers, 2006). Figure 2-8 illustrates the structure of a Plateau border.

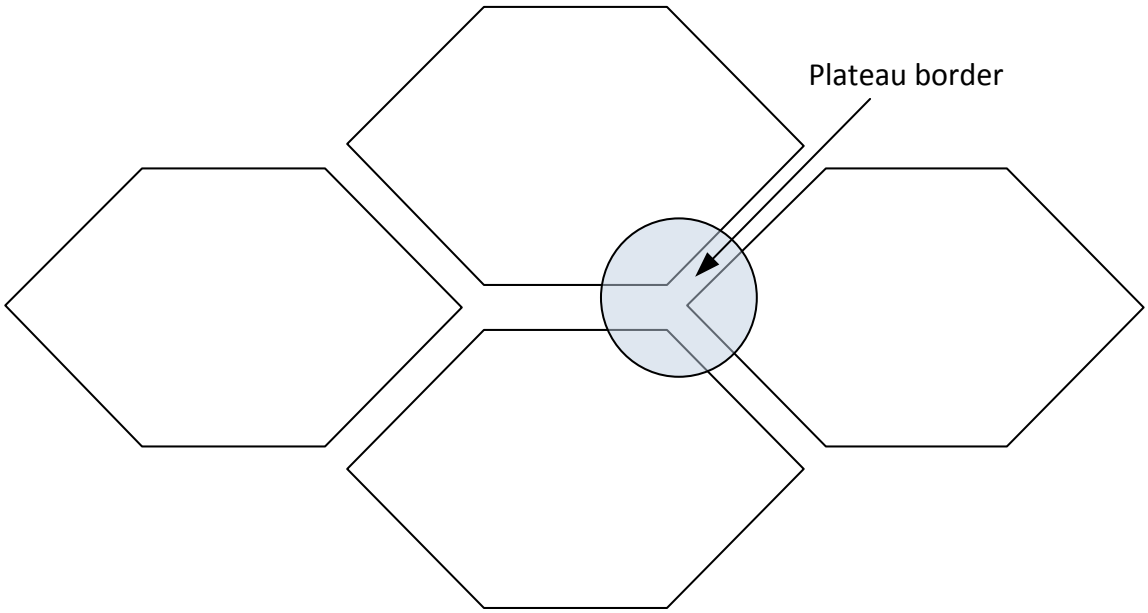


**Figure 2-8: Diagram illustrating the structure of foam and the Plateau border (Rajatanavin 2005).**

The curvature at the gas-liquid interface exerts a negative pressure on the film and draws liquid into the Plateau border (Cilliers, 2006). Standing foam becomes drier with time due to drainage (action of gravity) of liquid through the Plateau border channels. This leads to thinning of the bubble films and eventually to rupture of the films.

Film rupture has the following consequences: (a) rupture of the film at the top of the foam results in a decrease in the foam height (foam decay); and (b) rupture of the film shared by different bubbles within the foam causes the bubbles to coalesce forming larger bubbles. Coalescence results in a release of surfactant from the ruptured film leading to a local accumulation of surfactants and a more stable film due to the increase in surfactant concentration (Bhakta & Ruckenstein, 1997). The viscosity of the foaming solution has a significant effect on the rate of drainage of liquid films due to gravity. Increasing the viscosity of the solution slows down the rate of drainage of liquid thus increasing the lifetime of foams resulting in more stable foam.

Due to their high interfacial free energy, foams are thermodynamically unstable (Pugh, 1996). As a result two different types of foam have been identified: Unstable or transient foam and metastable foam.

### 2.4.1. Unstable or transient foam

This foam is characterised by spherical bubbles with thick liquid films (Melo, 2001). The lifetime of this foam is sensitive to the frother concentration showing a maximum at a critical concentration. The lifetime ranges from a few seconds to about 20 seconds (Pugh, 1996). Typical examples of frothers that produce this type of foam are short-chain aliphatic alcohols (ethyl, propyl, isobutyl) (Kitchener & Cooper, 1959). The lifetime of the foam can be significantly increased by addition of a viscous solute to the solution hence reducing the liquid drainage rate from the liquid films.

### 2.4.2. Metastable foams

This foam is characterised by polyhedral shaped bubbles separated by slightly curved liquid films (Melo, 2001). The liquid drainage from the foam eventually ceases and the bubble can persist for an indefinite time period even if no gas is pumped through the solution and as long as the bubbles are protected from disturbing influences (Kitchener & Cooper, 1959). Typical examples are solutions of soaps, modern synthetic detergents and even powerful frothers such as DF-1012 which can form metastable foams (Melo, 2001).

### 2.4.3. Three-phase froths

As mentioned in the preceding section the froth phase comprises of solid, liquid and air bubbles. Solid particles can have a stabilising effect on the froth by means of the following mechanisms:

1. Increasing the effective viscosity and hindrance to the drainage of water from the bubble film as the solid particles are trapped within the Plateau border and ensuring increased roughness of the lamellae respectively as shown in Figure 2-9.

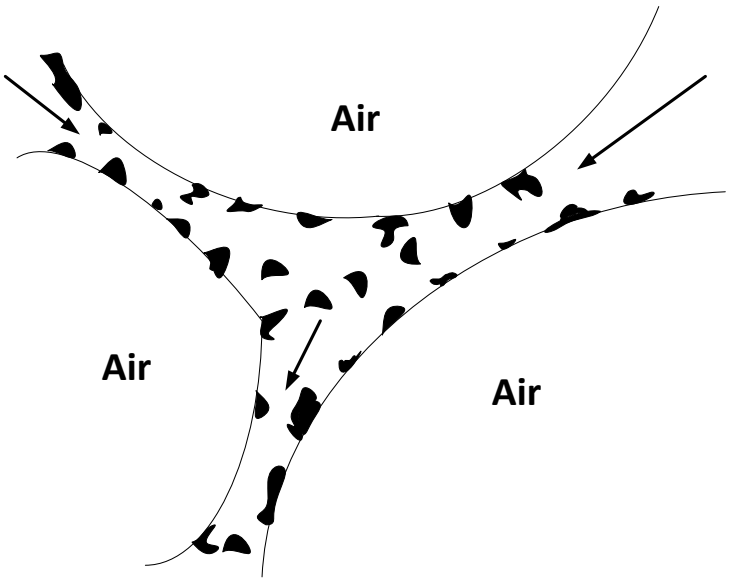


**Figure 2-9: Diagram showing the hindrance by particles attached to the bubble film and within the Plateau border to water drainage from the lamellae (Pugh, 2005).**

The hydrophobic nature of solid particles assists in aiding the solid particles to behave as frothing agents (Ata, 2012; Ata et al., 2003; Farrokhpay, 2011) with particles of intermediate hydrophobicity stabilising the froth (Pugh & Johansson, 1992). Operating conditions such as particle size, shape and pulp density have an effect on the stability of the froth phase (Pugh & Johansson, 1992).

## 2.5. Measures of froth stability

There is no generally accepted parameter that can be used to characterise foam or froth stability. Different methods have been devised as a measure of froth stability and can be categorised as dynamic and static tests. Dynamic tests involve dispersion of air through the solution or slurry eventually allowing for dynamic equilibrium to be reached between the rate of growth and decay of the foam or froth respectively. Static tests do not have air dispersed through the solution or slurry hence the rate of foam or froth growth is zero allowing the foam or froth to collapse.

Of the two tests, dynamic tests closely resemble the flotation process due to similar features such as continuous supply of air into the solution or pulp phase, formation of the froth phase at the bottom and its movement upwards (Barbian et al., 2003).

### 2.5.1. Dynamic tests

#### 2.5.1.1. Bikerman's Test

Bikerman (1973) determined a dynamic stability factor ($\Sigma$) of the foam phase as a ratio of the equilibrium volume of foam generated to the gas flowrate.

$$\sum = \frac{V_f}{Q} = \frac{H_{max} * A}{Q}$$ **Equation 2-3**

Where, $V_f$ is the volume of the foam, Q is the gas flowrate, $H_{max}$ is the maximum equilibrium height and A is the cross-sectional area of the column. The ratio physically translates to the average lifetime of bubbles in the foam. The test involves passing gas (air or nitrogen) at a given flowrate through a sinter into a column containing a known frother solution till an equilibrium foam height is reached. Bikerman (1973) observed that $\Sigma$ values are independent of the gas flowrate, shape and size of the column. A plot of foam volume versus gas flow rate gives a constant, known as the dynamic stability factor.

#### 2.5.1.2. Dynamic Foamability Index (DFI)

A parameter known as retention time (rt) is defined as the average residence time for a unit volume of gas within a system comprising of both the frother solution and foam within a frothing column (Malysa et al., 1978; Malysa et al., 1981). Graphically, rt corresponds to the slope of the linear segment of the dependence of the total gas volume in a system (solution + foam), Vg, as a function of the gas flow rate, $Q_g$. Mathematically, retention time is defined as shown in equation 2-4.

$$rt = \frac{\Delta V_g}{\Delta Q_g}$$ **Equation 2-4**

In further work (Czarnecki et al., 1982) observations of a dependency of rt to the solution concentration were made leading to the introduction of the "Dynamic Foamability Index" (DFI) as the limiting slope of the rt dependency on concentration curve as a "material constant" allowing for comparison of frothers.

$$DFI = (\frac{\partial rt}{\partial c})_{c=0}$$ **Equation 2-5**

Using DFI allows for the comparison of the action of frothers under conditions of identical frothability of their solutions. Larger DFI values indicate the existence of more stable foam, which does not easily coalesce (Laskowski, 2004). Laskowski (2003) highlighted that a DFI-CCC diagram as shown in Figure 2-10 can be used to classify frothers.

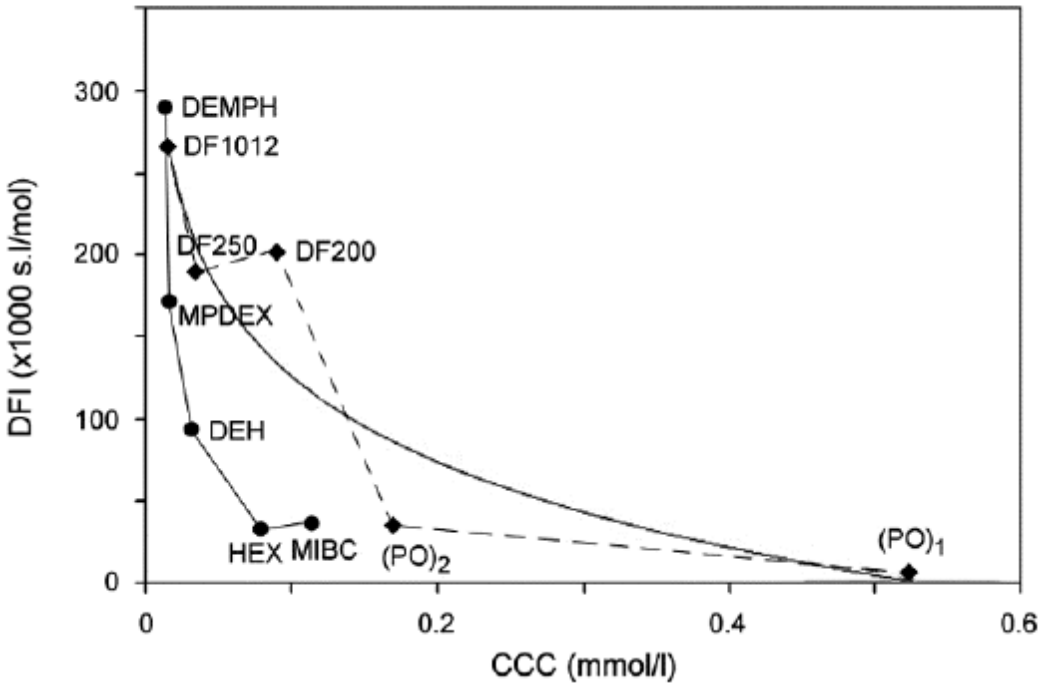


**Figure 2-10: Relationship between DFI and CCC values for tested frothers (Laskowski et al., 2003a).**

Frothers located at the upper-left corner of the diagram are powerful frothers, while the frothers situated in the bottom-right corner are selective frothers (Laskowski et al., 2003a).

#### 2.5.1.3. Froth rise velocity

More recently, in addition to the maximum equilibrium height as a measure of froth stability the froth growth rate has been used. This allows froth stability to be determined at both laboratory and industrial scale (Barbian et al., 2003; Barbian et al., 2005). Results from measuring the froth height as a function of time can be fitted to an exponential model (Barbian et al., 2003):

$$H = H_{max} * (1 - e^{-t/\tau}) \qquad \textbf{Equation 2-6}$$

where $H_{max}$ and $\tau$ are the maximum equilibrium height and average lifetime of bubbles in the froth phase respectively. The froth growth exponential model is fitted to the experimental data as shown in Figure 2-11.

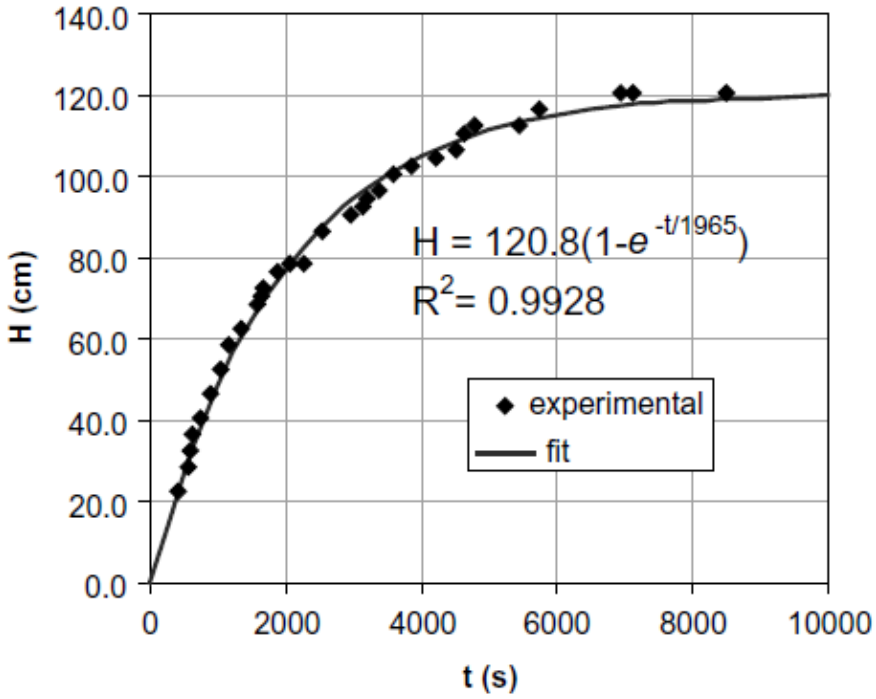


**Figure 2-11: Foam height as a function of time during growth of foam (Barbian et al 2005).**

Frothing columns of constant cross-sectional area translate to the froth volume and height being equivalent measures of the growth process.

#### 2.5.1.4. Bubble burst rate

Previously mentioned froth stability measurement techniques are intrusive to the flotation process and difficult to employ at an industrial level (Morar et al., 2012). Bubble burst rate has been proposed as a measure of froth stability (Morar et al., 2012) with unstable bubbles coalescing and bursting. The bursting event can also be quantified by a directly related parameter known as air recovery. Air recovery is defined as a fraction of air entering the froth phase that is recovered to the launder as unburst bubbles (Cilliers, 2006). This technique has been used in many studies as a proxy of froth stability (Ventura-Medina et al., 2003; Hadler & Cilliers, 2009; Ventura-Medina & Cilliers, 2002; Hadler et al., 2006; Hadler et al., 2010).

#### 2.5.1.5. Water recovery

Rupture of unstable bubbles causes fall back of both solid particles and water which once comprised the particle-bubble aggregate. As a result the amount of water recovered in the concentrate launder at a fixed froth height can be used as a proxy for froth stability (Wiese et al., 2011; Araya et al., 2011; Corin & Wiese, 2014).

### 2.5.2. Static tests

An efficient method to determine foam stability is observation of the decay in foam volume with time irrespective of the method of foam generation (Iglesias et al., 1995). Using a frothing column, Iglesias et al. (1995) allowed the foam dynamic equilibrium height to be

reached before cutting the supply of air to the column and monitoring the foam height decay versus time as shown in Figure 2-12.

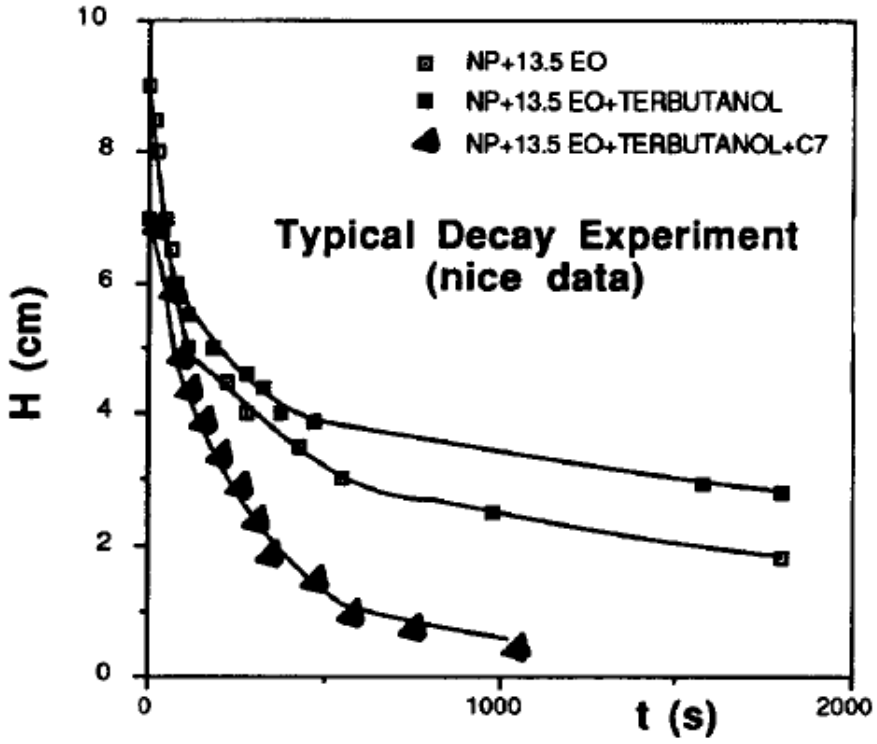


**Figure 2-12 : Typical observation of foam height decay vs time. The start time (t=0sec) corresponds to Bikerman's experimentally determined maximum equillibrium height. (Iglesias, 1995).**

From the observations the rate of change of foam height is given by,

$$\frac{\partial H_f}{\partial t} = -\frac{\propto}{t}$$ **Equation 2-7**

where α is an empirical constant. From integrating equation 2-7 the decay process can be expressed as the following form:

$$\frac{H_f}{H_{f_{max}}} = \frac{1}{2} - \propto \ln(\frac{t}{t_{1/2}})$$ **Equation 2-8**

where $t_{1/2}$ is a characteristic time (half-life) representing the time for the froth to decay to half of the initial froth height used as a measure of froth stability.

## 2.6. Effect of frother type on froth stability

Work by Tan et al. (2005) showed froth retention time previously defined by Equation 2-4 to be a function of frother type as shown in Figure 2-13.

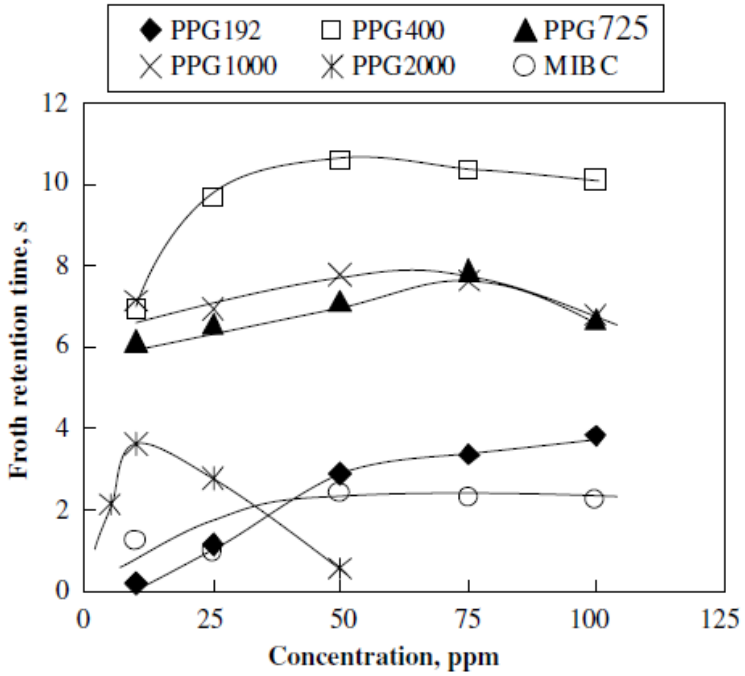


**Figure 2-13: Retention time as a function of frother type and concentration. (Tan et al., 2005)**

It is observed from Figure 2-13 that frothers of intermediate molecular weight (PPG 400 and PPG 725) gave a higher retention time in comparison to frothers of lower molecular weight (PPG 192 and MIBC) and frothers of higher molecular weight (PPG 1000). This earlier finding was corroborated by Wiese et al. (2012) whose work showed an increase in water recovery (froth stability) when DOW 250 was used in comparison to the use of DOW 200.

Gupta et al. (2007) whilst working with frothers of varying molecular weight concluded that the use of higher molecular weight frothers led to a more viscous hence stable froth. A comparison of the effect of frother structure of alcohol and polyglycol also demonstrated that the use of the latter resulted in a more stable froth. The observation was attributed to alcohol frothers having only one –OH group unlike polyglycol frothers which have multiple oxygenated units which interact with water molecules possibly increasing viscosity of the froth and hence, froth stability (Gupta et al., 2007; Khoshdast & Sam, 2011).

### 2.6.1. Frother blends

The use of dual frother blends is becoming common practice in flotation (Tan et al., 2005; Elmahdy, 2011). Studies by Tan et al. (2005) showed the existence of synergistic interactions on foam stability upon the use of frother blends confirming earlier work by Pugh (1996). Further work on the effect of frother blends on flotation performance of selected platinum group metals (PGM) ores showed that using PPG and alcohol frother blends at ratios of 4:1

and 1:4 gave the most stable froth (high water recovery) as shown in Figure 2-14 (Ngoroma et al., 2013).

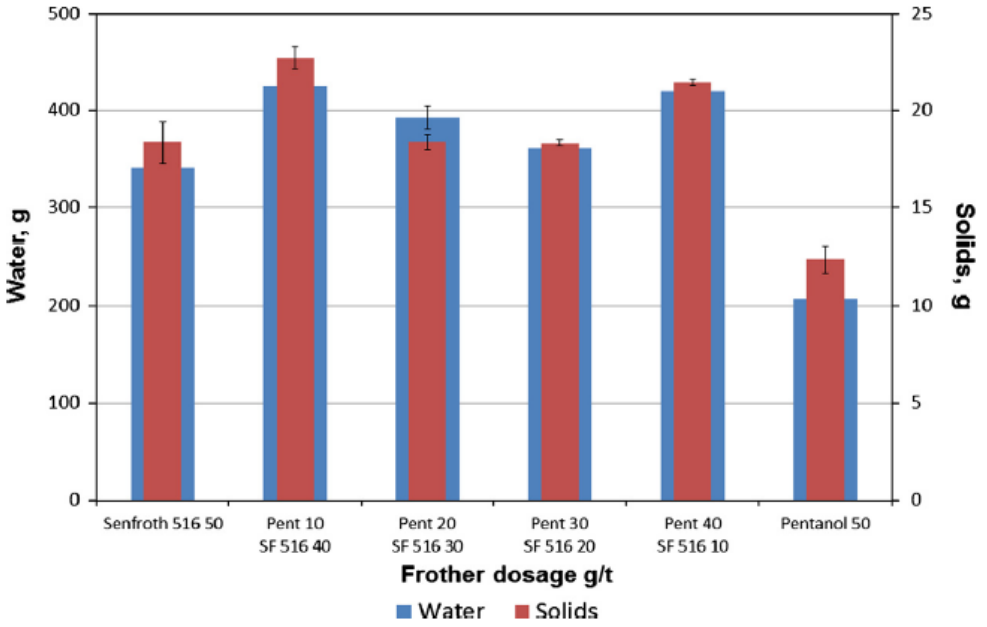


**Figure 2-14: Solids and water recovery as a function of frother blend ratio. (Ngoroma et al, 2013).**

This is an indication that adding small amounts of either frother to the other resulted in synergistic interactions. Similar findings were observed by other researchers (Elmahdy, 2011; Dey et al., 2014) where the use of blends significantly improved the froth stability compared to the stability attained by the use of single frothers.

## 2.7. Froth recovery

In the preceding sections it was mentioned that within the flotation cell there are two distinct phases: the pulp phase and the froth phase. Both phases have an effect on the performance of the flotation cell with the overall recovery being a function of the collection zone recovery and froth recovery as shown in equation 2-9 (Runge et al., 2010).

$$R = \frac{R_f R_c}{R_f R_c + 1 - R_c} \qquad \textbf{Equation 2-9}$$

*Where R is the overall recovery, $R_f$ is froth recovery and $R_c$ is collection zone recovery.*

During the flotation process not all the particles attached to the rising bubbles report to the concentrate launder, as a fraction of the particles detach from the bubbles and fall back into the pulp phase as shown in Figure 2-15. Froth recovery is defined as the fraction of particles that is recovered in the concentrate relative to the particles attached to bubbles entering the froth phase (Savassi et al., 1997) as shown in Equation 2-10.

$$R_f = \frac{Mass\ flow\ rate\ of\ particles\ reporting\ to\ the\ concentrate}{Mass\ flow\ rate\ of\ attached\ particles\ entering\ the\ froth\ phase} \qquad \textbf{Equation 2-10}$$

Low froth recoveries mean attached particles entering the froth phase are likely to drop back into the pulp phase resulting in a decrease in the overall recovery. Vera et al. (2002) noted that the collection zone recovery can vary between 60% and 99% whilst the froth recovery can vary from 10% to 90%.

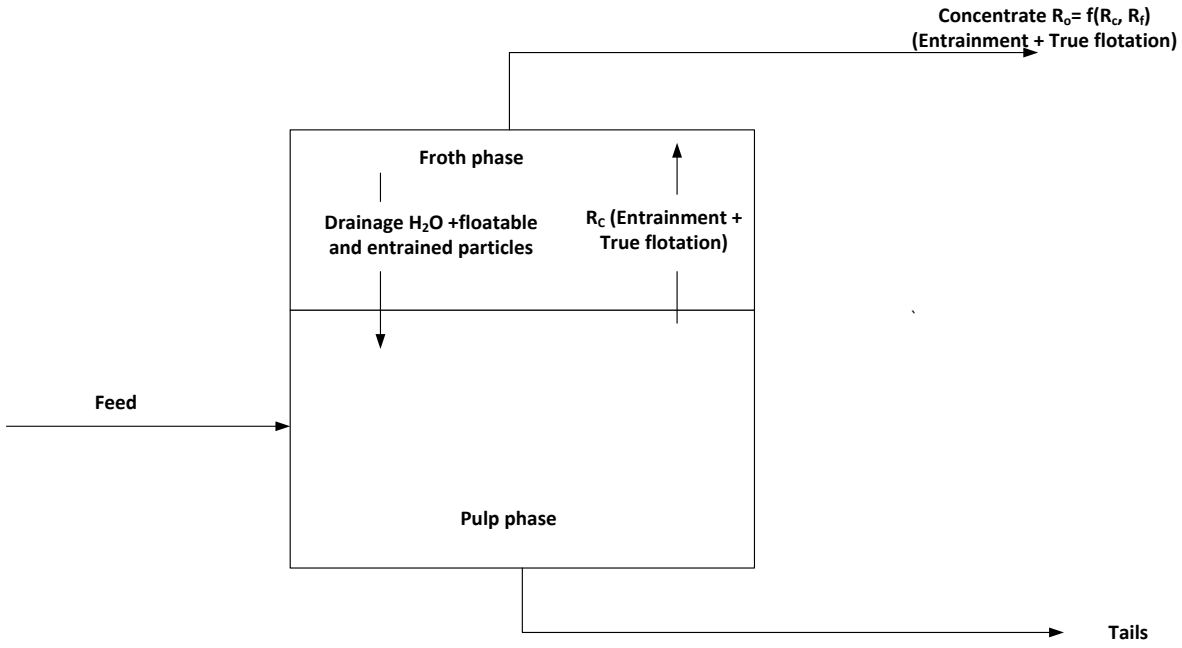


**Figure 2-15: Diagram illustrating the two-phase nature of the flotation process. (Arbiter & Harris, 1962).**

This is due to bubble coalescence, collapse of the froth and bursting of bubbles (Runge et al., 2010). A number of factors affect froth recovery and these include frother type and concentration, operational design of flotation cells and froth depth. Various techniques can be used to measure froth recovery. The following section gives a brief overview of techniques that can be used to measure froth recovery.

### 2.7.1. Froth recovery measurement techniques

Different techniques can be used to determine froth recovery (Runge et al., 2010):

1. Changing froth depth method.
2. Direct measurement of bubble load.
3. Mass balance estimation of bubble load.

#### 2.7.1.1. Changing froth depth method

In line with earlier work done by Feteris et al. (1987), Vera et al. (1999a, 1999b) determined froth recovery based on a technique which involves sampling of the concentrate at different froth depths whilst keeping a constant volume of the pulp phase. Key assumptions for the method are (Vera et al., 2002):

1. Mass transfer of particles from the bulk pulp phase to the pulp-froth interface is dependent on processes occurring in the pulp phase.
2. Mass transfer of particles from the froth phase to the concentrate is dependent on processes occurring in the froth phase.

In trying to account for processes in the froth phase Finch and Dobby (1990) mathematically defined froth recovery as a ratio of rate of mass transfer from the pulp to the concentrate (k) to the rate of mass transfer from the pulp to the froth phase ($k_c$):

$$R_f = \frac{k}{k_c}$$ **Equation 2-11**

The overall first-order rate constant (k) is a function of the overall flotation recovery and residence time. The rate constant in a perfectly mixed environment is given by Equation 2-12 (Mathe et al., 1998; Vera et al., 1999b; Tsatouhas et al., 2006),

$$k = \frac{R_0}{\tau(1 - R_0)}$$ **Equation 2-12**

*where τ is the mean residence time within the collection zone and $R_0$ is the overall recovery.* Assuming a plug flow model within the collection zone (continuous flow but with no longitudinal mixing in the flow direction) the overall rate constant is given by Equation 2-13 (Mathe et al., 1998).

$$k = -\frac{1}{\tau}\ln(1 - R_0)$$ **Equation 2-13**

From the observed linear relationship (Feteris et al., 1987) between flotation rate constant and froth depth the collection zone rate constant is obtained by extrapolation of the relationship as shown in Figure 2-16.

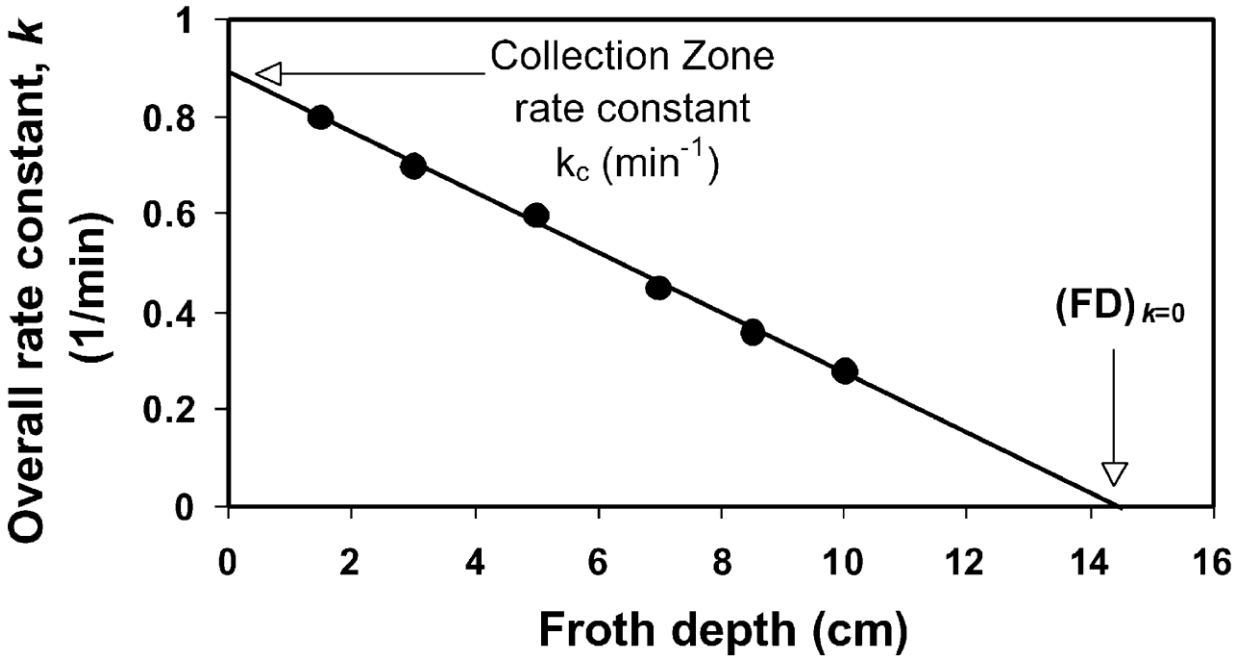


**Figure 2-16: The relationship between the flotation rate constant and froth depth (FD). (Vera et al, 2002).**

At zero froth depth there is no solid particle loss in the froth phase hence the rate constant at this depth is equal to the collection zone flotation rate constant.

#### 2.7.1.2. Direct measurement of bubble load

As mentioned in the preceding section froth recovery is a ratio of the mass flow rate of particles reporting to the concentrate to the mass flow rate of attached particles entering the froth phase (Equation 2-10). The mass flow rate of particles reporting to the concentrate can easily be determined, but difficulties lie in determining the mass flow rate of attached particles entering the froth phase. Work has been conducted (Falatsu & Dobby, 1992; Dyer, 1995; Moys et al., 2010; Seaman et al., 2004) in developing devices that can measure the mass flow rate of particles from the pulp to the froth phase. The devices measure the loading of particles onto bubbles (bubble load) just below the pulp-froth interface and do not take into account particle attachment or detachment that can occur at the interface (Moys et al., 2010). During use of these devices froth recoveries of greater than 100 % have been observed which has prompted the need for improved designs of the measuring devices (Moys et al., 2010).

#### 2.7.1.3. Mass balance estimation of bubble load.

Savassi et al. (1997) suggested an alternative to direct measurement of bubble load which was an estimation method for the bubble load. The technique, however, proved not to be accurate in low bubble load environments such as in scavenger, cleaner and recleaner banks and was difficult to use as the measuring equipment was not robust (Savassi et al., 1997).

### 2.7.2. Effect of frothers on froth recovery

Froth recovery is a function of froth stability. Froth stability has a significant effect on froth recovery because the bursting of bubbles within the froth phase leads to particle drop back into the pulp phase hence reducing the froth recovery (Zanin et al., 2009). As mentioned previously froth stability is a function of frother type thus frother type has an effect on froth recovery

## 2.8. Entrainment during froth flotation

Ideal separation of valuable minerals and gangue materials during flotation is impossible as hydrophilic gangue minerals are also recovered in the concentrate. The deportment of hydrophilic minerals to the concentrate occurs by means of different mechanisms such as entrainment, entrapment and slime coating (Melo, 2001).

The entrapment mechanism entails hydrophilic gangue material being trapped between particles attached to the air bubbles. Probability of particle entrainment is relatively high in flocculated or coagulated and highly mineralized froths (Kirjavainen, 1996).

Flotation of minerals is dependent on the particle size of minerals. Slime coating is a result of excessive grinding leading to low rates of flotation and the recovery of unwanted material (Melo, 2001). Entrainment is the main transport mechanism in the recovery of hydrophilic gangue material in the concentrate. This occurs via the unselective transport of material between rising bubbles from the pulp phase to the froth phase.

### 2.8.1. Entrainment mechanisms

Different mechanisms have been proposed to explain the transport of hydrophilic gangue material by entrainment:

- The hydrophilic material is transported into the froth phase as a result of mechanical carryover in the water layers surrounding bubbles (Kirjavainen, 1996; Savassi et al., 1997).
- Gangue material is transported in the wake of ascending bubbles (Savassi et al., 1997).
- Mechanical transportation of gangue material entrained in voids that exist between rising bubbles (Savassi et al., 1997; Moyo, 2005).

### 2.8.2. Effect of frothers on entrainment

A strong correlation exists between water recovery and the degree of entrainment of gangue minerals (Smith & Warren, 1989; Savassi et al., 1997; Melo, 2001). Frothers by virtue of their ability to change the froth structure i.e. water recovery have an effect on the degree of entrainment. On investigating the effect of frothers on entrainment Ekmekci et al. (2003) observed the results shown in Figure 2-17,

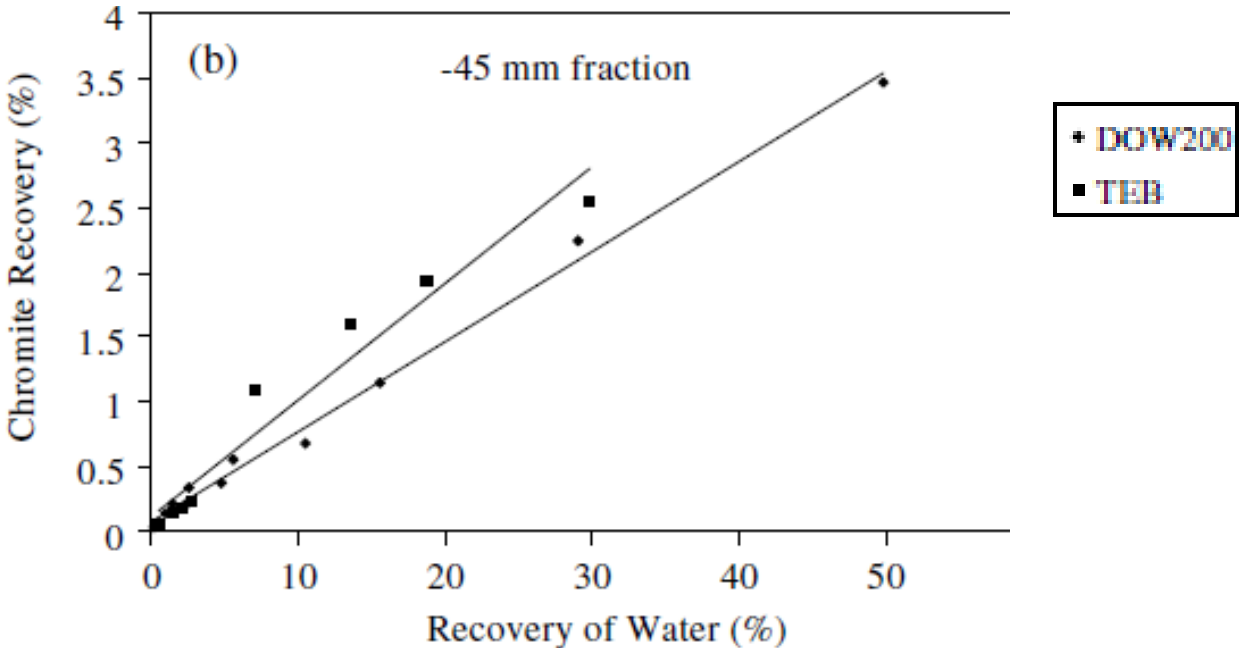


**Figure 2-17: Chromite recovery as a function of water recovery for tests with DOW200 and TEB performed at various froth heights (Ekmekci et al., 2003).**

The results are based on the use of Upper Group 2 (UG2) ore which contains substantial amounts of chromite which is a naturally hydrophilic gangue mineral which is recovered to the concentrate via entrainment. The difference in chromite recovery per unit of water (entrainability) is as a result of the existence of different froth structures (Ekmekci et al., 2003). A more stable froth phase allows for greater entrainment of gangue material due to a low rate of water drainage (Neethling & Cilliers, 2002). Wiese et al. (2010) whilst investigating the effect of increased frother dosage on froth stability obtained results shown in Figure 2-18.

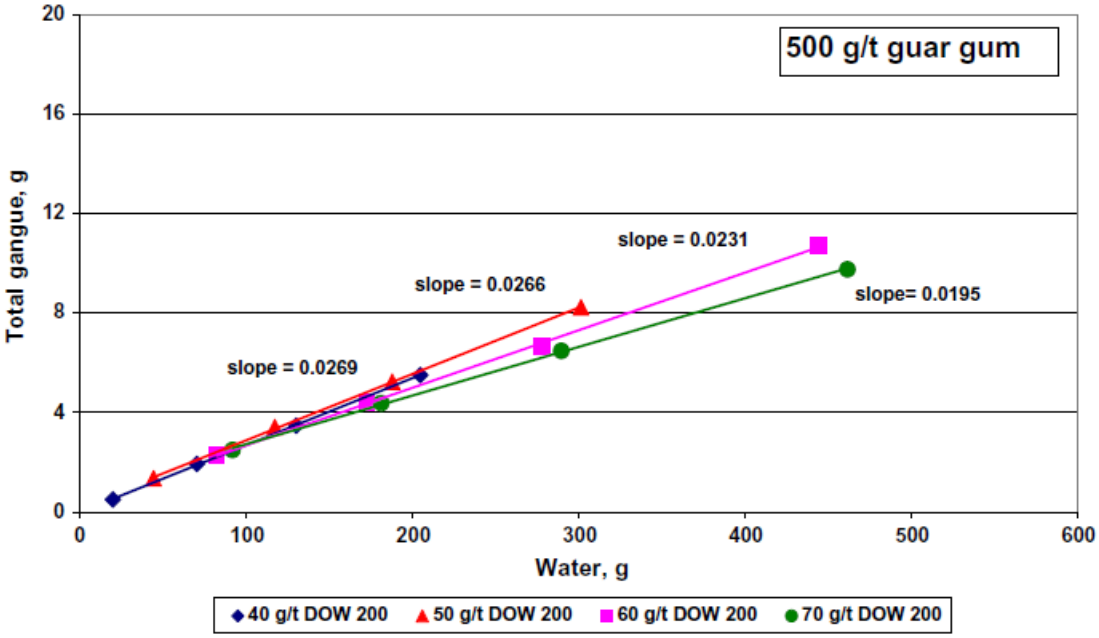


**Figure 2-18: Entrainability factor as a function of frother (DOW200) concentration (Wiese et al, 2010).**

Figure 2-18 illustrates a decrease in the entrainment factor (slope of line) of gangue material as the frother concentration was decreased.

## 2.9. Surface tension

Surface tension is a measure of surface energy per unit area (Masutani & Stenstrom, 2001; Comley et al., 2001). The net force of bulk liquid molecules is zero, but for surface liquid molecules the net force is a non-zero quantity in the direction of the bulk liquid due to an uneven distribution of intermolecular forces. To expand the area of the liquid surface, work is done against the existing cohesive forces at the surface; the energy required for the process is called surface energy.

$$\gamma = \left(\frac{dG}{dA}\right)_{T,P}$$ **Equation 2-14**

Frothers due to their hetero-polar nature migrate to the liquid surface disrupting intermolecular forces between surface molecules. The hydrophobic portion of the frother interacts with air or gas inside a bubble and the hydrophilic portion remains in contact with water. As there is less attraction between the hydrophobic groups than there is between water molecules which the frothers have interspersed, the surface tension is lower than that of pure water (Bamforth, 1985). Thus even in small amounts, frothers change the surface properties in liquids. The migration of the frother molecules to the surface is time dependent and over long periods of time the frother concentration at the surface approaches an equilibrium value and hence an equilibrium surface tension value (Eastoe & Dalton, 2000). The transient time frame within which the frother molecules migrate to the surface until equilibrium is attained is a basis of dynamic surface tension (Masutani & Stenstrom, 2001).

### 2.9.1. Equilibrium adsorption isotherm

The surface tension of solutions is dependent on surfactant concentration as illustrated in Figure 2-19.

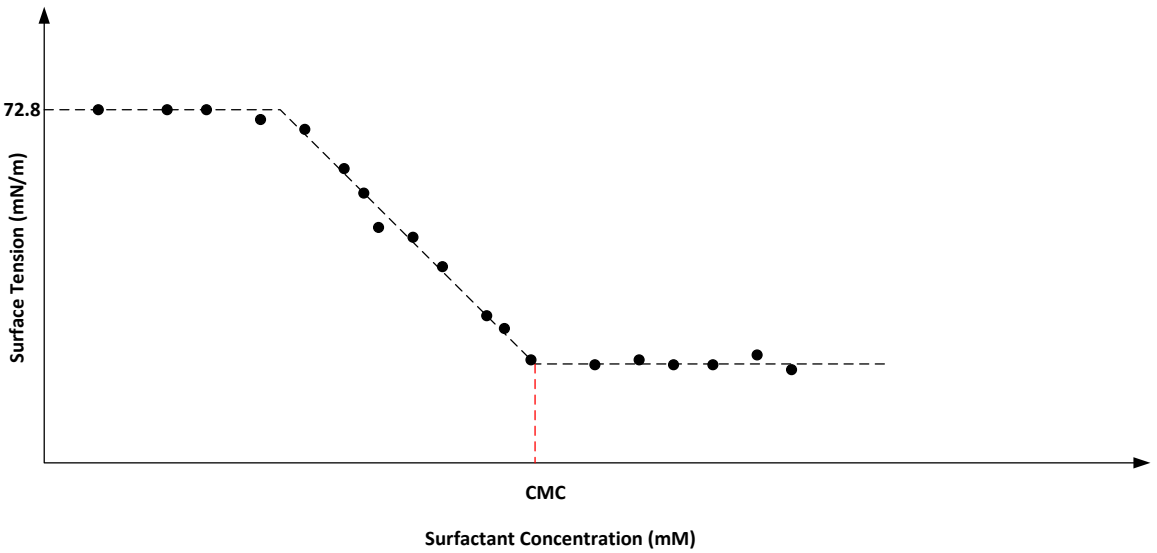


**Figure 2-19: General trend of the effect of frother concentration on equilibrium surface tension.**

At concentrations above the critical micelle concentration (CMC), the equilibrium surface tension is not a function of surfactant concentration as only surfactants in the monomeric form contribute to the surfactant activity and hence to tension reduction (Chang & Franses, 1995). For surfactant concentrations below CMC a decrease in the equilibrium surface tension results from an increase in the bulk surfactant concentration. A measure of the amount of adsorbed surfactant at the interface is usually determined indirectly using interfacial tension measurements, the Gibbs equation can be used to determine the surfactant concentration at the interface. The amount of adsorbed surfactant is usually determined in terms of surface excess, $\boldsymbol{\Gamma}$. Surface tension measurements which are an indication of the amount  to can be used to determine the amount of a solute adsorbed using the Gibbs equation.

The simplest form of the Gibbs equation is written as (Gibbs, 1928):

$$-d\gamma = RT\sum_i \Gamma_i d\ln a_i \qquad \textbf{Equation 2-15}$$

where γ is the surface tension, and $a_i$ and $\boldsymbol{\Gamma}_i$ are the activities and surface concentration (surface excess) of all components respectively. For non-ionic surfactants the Gibbs equation reduces to Equation 2-16

$$-\frac{1}{RT}\left(\frac{d\gamma}{d\ln a}\right)_T = \boldsymbol{\Gamma} \qquad \textbf{Equation 2-16}$$

Surface tension at the interface is dependent on surfactant concentration at the interface whose measure is termed surface excess. Equation 2-16 demonstrates the relationship between surface tension and surface excess as the slope of the plot of frother concentration versus surface tension. The usual practice with non-ionic surfactants is the use of surfactant concentration instead of activities (Rosen, 2004)

$$-\frac{1}{RT}\left(\frac{d\gamma}{d\ln c}\right)_T = \boldsymbol{\Gamma} \qquad \textbf{Equation 2-17}$$

As a result, the plot of equilibrium surface tension as a function of surfactant concentration can be used to determine the amount of surfactant adsorbed per unit area of interface (Rosen, 2004). Knowing the surface excess of surfactants it is possible to determine important parameters such as the degree of packing, orientation of molecules at the interface and the area occupied by surfactant molecules at the interface (Schwartz, 2004). The migratory movement of surfactant molecules to the interface occurs in two stages (Eastoe & Dalton, 2000):

1. Adsorption of surfactant onto interface from the subsurface layer.
2. Diffusion of surfactant from the bulk liquid to the subsurface layer.

Adsorption is often studied by means of graphs/equations of state known as Adsorption isotherms. Adsorption isotherms relate the amount of surfactant on the interface as a function of bulk concentration at a constant temperature.

#### 2.9.1.1. Henry isotherm

This is the simplest isotherm which states that the amount of surfactant at the interface is proportional to the surfactant bulk concentration as stated in Equation 2-18.

$$\Gamma = K_H c \qquad \textbf{Equation 2-18}$$

The Henry adsorption constant, $K_H$, is a measure of the surface activity of the surfactant and the thickness of the bulk solution which contains a similar amount of surfactant as in a monolayer of surface monolayer of concentration (Chang et al., 1991; Chang & Franses, 1995). Due to the assumption that there is no intermolecular interaction between adsorbed molecules the isotherm is only valid at low surface concentrations (Eastoe & Dalton, 2000).

#### 2.9.1.2. Langmuir isotherm

This is a commonly used non-linear adsorption isotherm. The isotherm was developed by Irving Langmuir in 1916 as a description that relates surface coverage of adsorbents to the concentration of adsorbents and vacant sites available at the contact surface. The isotherm assumes that the probability of occupying a site is independent of the occupancy of neighbouring sites and there is no interaction between adsorbed surfactants hence every adsorption site is equivalent (Colegate, 2009). The equation is stated as shown in Equation 2-19:

$$\Gamma = \Gamma_m \frac{K_L c}{1 + K_L c} \qquad \textbf{Equation 2-19}$$

Where $K_L$ is a constant (Langmuir equilibrium adsorption constant) and $\boldsymbol{\Gamma}_m$ is the maximum surface concentration (Chang & Franses, 1995; Eastoe & Dalton, 2000).

## 2.10. Summary of Literature

In the light of the literature reviewed here it is evident that extensive research has been conducted with regards to the effect of frothers on the flotation process. However, most of the research has been focused on the pulp phase and only recently has attention shifted to the froth phase (Seaman et al., 2006; Nagaraj & Ravishankar, 2007). Recently work has been done investigating the effect of polyglycol frother structure on foam and froth stability (Tan et al., 2005; Schwartz, 2004) extending work done which investigated the effect of alcohol frother type (Cho, 2001; Comley et al., 2001). However, little research has been conducted on the effect of frother type on froth recovery and entrainment.

The work on frother blends (Ngoroma et al., 2013; Tan et al., 2005; Elmahdy, 2011) has highlighted the need for more attention on understanding the effect of frothers on the

flotation process. From the literature reviewed the author proposes the following hypotheses:

1. An increase in the molecular weight of the frothers results in a more stable froth phase. This is because a frother of higher molecular weight leads to a more viscous bubble film hence retarding the drainage rate and ultimately leads to a more stable froth phase.
2. An increase in froth stability is associated with a decrease in the grade of the valuable minerals recovered in the concentrate. This is because a high water recovery is an indication of a stable froth phase and is associated with an increase in the amount of entrained material in the froth.
3. A mixture of a high molecular weight, less hydrophilic frother with a low molecular weight, highly hydrophilic frother will result in a more stable froth. The less hydrophilic frother is less soluble in water and the mixture of the molecules will result in a closer packing at the air-water interface. This results in a higher dynamic surface tension gradient and a more stable froth.

# Chapter 3

# Experimental Methodology

The purpose of this chapter is to describe the experimental approach that was taken to test the proposed hypotheses. To ensure a better understanding of the effect of frothers on the flotation process, the experimental approach was split into two-phase and three-phase tests. The tests were based on the use of polypropylene glycol and alcohol frothers. Polypropylene frothers were characterised on the basis of their molecular weights which were 192, 425, 725 and 1000 g/mol and are referred to throughout the text as PPG192, PPG425, PPG725 and PPG1000 respectively.

The chapter begins with a description of the test rigs used for the test work investigating the effect of frother structure on foam and froth stability and surface activity of surfactants. A froth stability column provided different measures of froth stability such as foam or froth retention time, maximum foam or froth height and froth stability factors. A laboratory scale column flotation cell in closed loop continuous operation provided solids and water recovery data which could be used to determine the effect of frother type on froth stability, froth recovery and entrainment. This is followed by a detailed experimental procedure including the measurements that were taken and an outline of analysis of the data obtained.

## 3.1. Sample Preparation Equipment and material

### 3.1.1. Ore Preparation

The ore that was used in the study was a sample of UG2 ore obtained from the mill feed of a LONMIN operated concentrator within the Bushveld Igneous Complex in Rustenburg (South Africa). The ore comprised of PGMs (3.15 g/t) and chromite (24.9 %) among other constituents. The bulk ore sample had a particle size distribution of 13.8 % passing 75 µm and weighed approximately 400 kg. It was prepared for testwork at the CMR laboratory (UCT). The ore was thoroughly blended and continuously split using a rotary splitter manufactured by Dickie and Stockler until approximately 1.35 kg representative portions were obtained. This method aimed to ensure a homogenous composition and particle size distribution for the different sample portions (Allen, 1997).

### 3.1.2. Synthetic Plant Water Preparation

All tests, unless stated otherwise, were performed using synthetic plant water, which was a modification of distilled water by means of addition of ionic salts. This was to ensure that the water attained a specific ionic strength typically found at PGM flotation plants (Wiese et al., 2005). Synthetic water was prepared in 40 $\ell$ batches, the composition of which is shown

Table 3-1. This is the standard salts addition based upon historical data from a single concentrator (Wiese et al, 2005).

**Table 3-1: Summary of ingredients of synthetic plant water (Wiese et al., 2005).**

| Chemical salt | Chemical Formula | Mass (g) / 40ℓ Distilled Water |
|---|---|---|
| Magnesium Sulphate Heptahydrate | $MgSO_4.7H_2O$ | 24.60 |
| Magnesium Nitrate Hexahydrate | $Mg(NO_3)_2.6H_2O$ | 4.28 |
| Calcium Nitrate Tetrahydrate | $Ca(NO_3)_2.4H_2O$ | 9.44 |
| Calcium Chloride Dihydrate | $CaCl_2.2H_2O$ | 5.88 |
| Sodium Chloride | NaCl | 14.24 |
| Sodium Carbonate | $Na_2CO_3$ | 1.20 |

### 3.1.3. Milling Equipment

The ore was milled to the required particle size distribution of 60 % passing 75 µm which is similar to the particle size distribution of the primary rougher feeds of concentrating plants for similar ore (Wiese, 2009). The milling was done using a 3 kg SALA stainless steel rod mill shown in Figure 3-1.

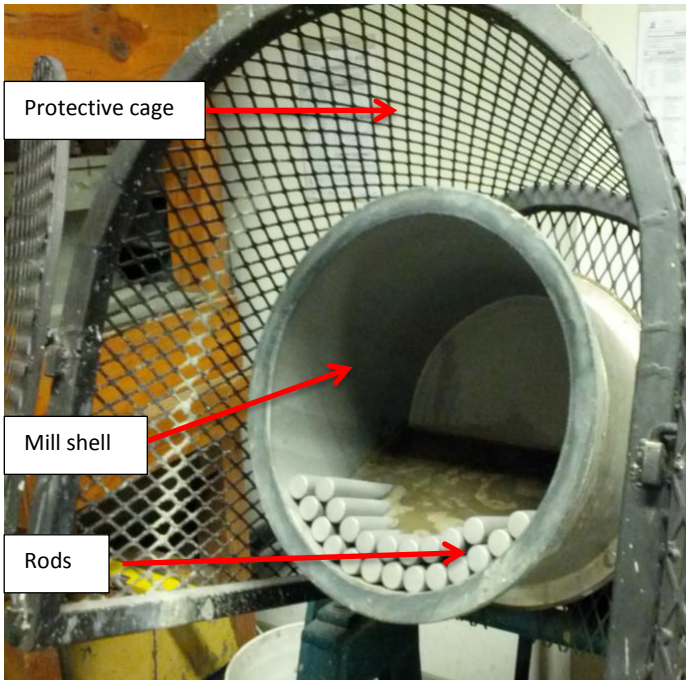


**Figure 3-1: A 3 kg SALA stainless steel rod mill used during the ore preparation process.**

The mill had an internal diameter of 30 cm and a length of 29 cm. The mill was charged with 22 stainless steel rods each with a diameter of 25 mm and a length 285 mm. The mill was operated at a speed of 77.1 rpm corresponding to 95 % critical speed. No reagents were added into the mill.

### 3.1.4. Milling Curve

A 2.7 kg portion of the prepared ore was milled at 66 % solids using synthetic plant water for different durations to determine the milling time required to obtain a required size distribution of 60 % passing 75 µm as shown in Figure 3-2.

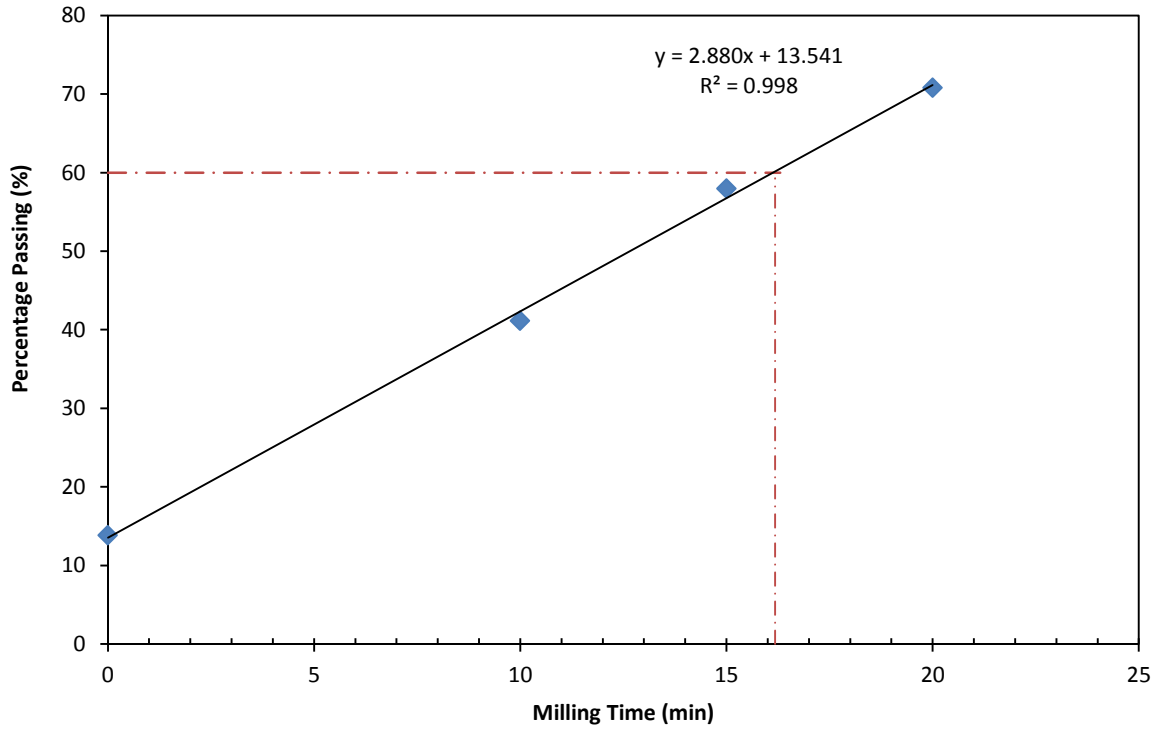


**Figure 3-2: Milling curve of the feed ore.**

The milling time required to obtain a grind of 60 % passing 75 µm was determined to be 16 minutes 18 seconds. The milling curve was confirmed by milling a portion of the ore for the predetermined duration with results showing that milling for the predetermined duration yielded an ore with a size 60 % passing 75 µm as shown in Figure 3-3.

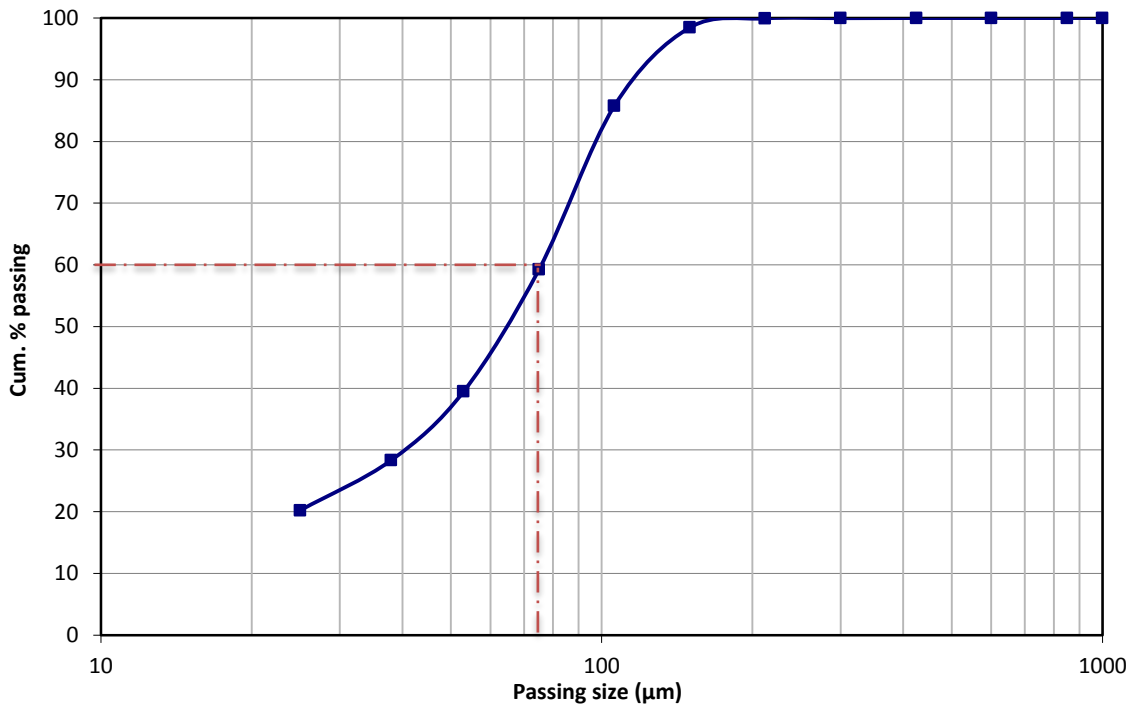


**Figure 3-3: Particle size distribution of ore milled for the duration determined from the milling curve.**

## 3.2. Flotation Reagents and Equipment

### 3.2.1. Frother

A list of frothers that were used in the experiments is shown in Table 3-2. The frothers were supplied by Sigma Aldrich at purities (see Tables 3-3 and 3-4) determined by SENMIN using gas chromatography analyses. The molecular composition of the higher molecular weight frothers PPG725 and PPG1000 could not be confirmed by gas chromatography with the equipment at hand.

**Table 3-2: List of frothers and their respective chemical structure used in the research.**

| Frother Name | Chemical Structure |
|---|---|
| Pentanol | 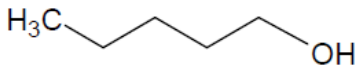 |
| Methyl Isobutyl Carbinol (MIBC) | 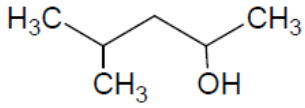 |
| Hexanol | 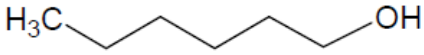 |
| Octanol | 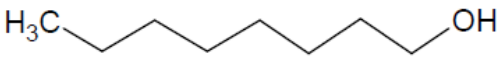 |
| PPG192 | 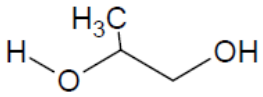 |
| PPG425 | 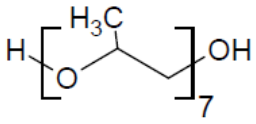 |
| PPG725 | 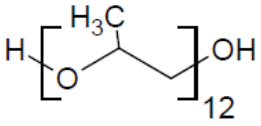 |
| PPG1000 | 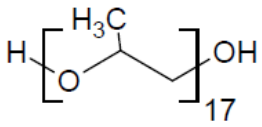 |

**Table 3-3: Summary of the molar composition of alcohol frothers.**

| Frother | Molar Composition (%) |
|---|---|
| 1-Pentanol | 100 |
| 1-Hexanol | 99.2 |
| MIBC | 99.9 |
| 1-Octanol | 99.8 |

**Table 3-4: Summary of the molar composition of PPG192 and PPG425.**

| Component, mol.wt | PPG192 | PPG425 |
|---|---|---|
| Di-PG, 134 | 0.3 | - |
| Tri-PG, 192 | 99.7 | 0.4 |
| Tetra-PG, 250 | - | 5.6 |
| Penta-PG, 308 | - | 10.8 |
| Hexa-PG, 366 | - | 18.8 |
| Hepta-PG, 424 | - | 28.7 |
| Octa-PG, 482 | - | 20.9 |
| Nona-PG, 540 | - | 10.7 |
| Deca-PG, 598 | - | 4.0 |
| **Average mol. Wt.** | **191.8** | **421** |

### 3.2.2. Collector

The collector of choice was Sodium Isobutyl Xanthate (SIBX) which was supplied by SENMIN in powder form at a purity of 90 %. Flotation tests were carried out using a collector dosage of 100 g/t which was added to the slurry in solution form. The collector solutions were prepared by weighing the required amount of collector to ensure a dosage of 100 g/t and mixing it with 100 ml distilled water. The predetermined amount of collector was added to the feed tank and allowed to condition for 10 min before addition of the frother.

### 3.2.3. Column flotation cell

Flotation tests were carried out using a modified conventional column flotation cell shown in Figure 3-4. The column had a diameter of 3 cm and variable height due to the different heights (4, 8 and 11 cm) required for the froth phase section of measurements.

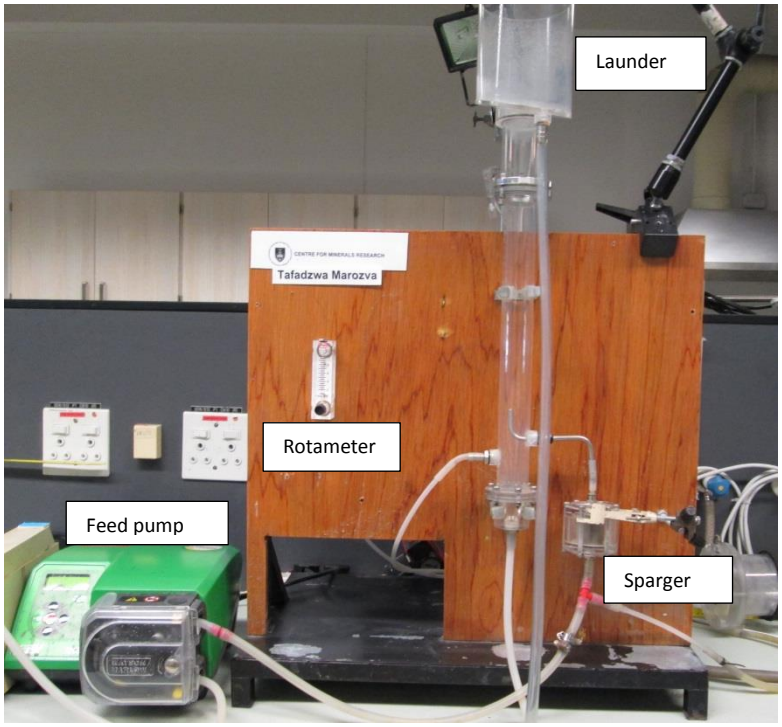


**Figure 3-4: Picture of flotation column.**

The pulp and froth section of the column were constructed from Perspex and glass respectively allowing for easy viewing of the froth phase. Attached to the column was an external sparger and three peristaltic pumps used to ensure continuous flow of the feed, recycle and tails streams. A rotameter was connected to the air supply of the column to ensure an air supply in the range of 0-1 $\ell$pm measured at 0.1 $\ell$pm intervals.

### 3.2.4. Flotation Procedure

A 2.7 kg ore sample was wet milled at conditions described in the preceding section for a duration of 16.18 min. The slurry was then transferred to a feed tank with additional synthetic plant water added to attain the required pulp density of 30 % percentage solids. The slurry was then stirred in the feed tank ensuring the creation of a homogenous solid particle suspension. The collector and frother were then added sequentially into the feed tank according to the dosages shown in Tables 3-5, 3-6 and 3-8.

**Table 3-5: Reagent dosage for flotation tests investigating the use of polyglycol frothers in single component frother suites.**

| Reagent | Dosage |
|---|---|
| SIBX (g/t) | 100 |
| Polyglycol frother (mM) | 0.314 |

**Table 3-6: Reagent dosage for flotation tests investigating the use of alcohol frothers in single component frother suites.**

| Reagent | Dosage |
|---|---|
| SIBX (g/t) | 100 |
| Alcohol frother (mM) | 11.3 |

The frother dosages were all at a concentration above the CCC values (shown in Table 3-7) ensuring generation of bubbles of the same size in the pulp zone.

**Table 3-7: CCC92 (mM) versus molecular weight (Zhang et al., 2012)**

| Frother type | CCC95/(mM) |
|---|---|
| Pentanol | 3.92 |
| Hexanol | 0.11 |
| PPG192 | 0.17 |
| PPG425 | 0.014 |
| PPG725 | 0.0091 |

Tests investigating the use of dual component frother suites were carried out at a similar total frother concentration as the concentration of polyglycols in single component frother tests (0.314 mM). Polyglycol frothers were blended with MIBC to form dual frother blends. MIBC is the most commonly used frother due to it being relatively inexpensive and giving good performance with different ores (Jiang et al., 2006; Pugh, 2007; Kawatra, 2011) hence investigations into the use of frother blends focused on mixing MIBC with other frothers. A PPG: MIBC molar ratio of 4:1 was investigated as shown in Table 3-8. The 4:1 ratio followed earlier work by Ngoroma et al (2013) which showed the greatest amount of solids and water recoveries were obtained when using the blends at ratios 4:1 and 1:4. The frothers were added separately into the feed tank from different frother stock solutions.

**Table 3-8: Reagent dosages for flotation tests investigating the use of dual component frother suites.**

| **Reagent** | **Dosage** |
|---|---|
| SIBX (g/t) | 100 |
| Polyglycol frother (mM) | 0.251 |
| MIBC (mM) | 0.0628 |

Upon addition of the reagents into the slurry a conditioning time of 15 min followed after which the slurry was pumped into the column at a volumetric flow rate of 0.49 $\ell$pm. A continuous air supply at a superficial velocity of 1.70 cm/sec was co-fed into the column. The recycle stream was pumped into the sparger at a volumetric flow rate of 0.24 $\ell$pm. Initially the concentrate and tails were recycled into the feed tank creating a closed circuit until the column operation attained steady state with the pulp-froth interface at the required height within the column. Thereafter the column was operated in open circuit. Manipulation of the interface was done manually with the tails flow rate as the control variable. The flotation tests were carried out at froth heights 4, 8 and 11 cm.

Concentrate and tailings sample were collected simultaneously for duration of three minutes. To determine the solids and water recoveries, the samples were weighted before and after drying overnight in an oven at a temperature of 70 ℃. The tests were performed

in duplicate to ensure that the experimentally determined recoveries were within the acceptable relative standard deviation range (0- 15 %).

The dried concentrate and tails samples were sent to a LONMIN operated laboratory for PGM and chromite assays. Analysis of the concentrate particle size distribution was done at the Analytical laboratory at UCT using a Laser Malvern Mastersizer 2000 manufactured by Micromeritrics.

### 3.2.5. Data Processing

Froth recovery was determined as shown in Equations 3-1 to 3-3:

$$R_i = \frac{F_C x_{i,conc}}{F_C x_{i,conc} + F_T x_{i,tails}} * 100$$ **Equation 3-1**

$$k_{O,i} = \frac{R_i}{\tau(1 - R_i)}$$ **Equation 3-2**

*Where: $R_i$ is Overall flotation recovery of constituent i (%), $F_C$ is solids mass recovery in the concentrate (g/min), $F_T$ is solids mass recovery in the tails (g/min), $x_{i,conc}$ is mass composition of constituent i in the concentrate stream (-), $x_{i,tails}$ is mass composition of constituent i in the tails stream, $k_{O,i}$ is overall flotation rate constant of constituent i ($min^{-1}$) and τ is froth residence time (min).*

Extrapolation of the froth rate constant – froth depth relationship enables the evaluation of the pulp rate constant, $k_c$ which is used to determine the froth recovery as shown in Equation 3-3:

$$R_f = \frac{k_{O,i}}{k_c} * 100$$ **Equation 3-3**

*Where: $R_f$ is froth recovery (%) and $k_C$ is pulp rate constant ($min^{-1}$).*

**Demonstration**

From flotation tests performed using PPG192 at a height of 8 cm the following experimental data was obtained,

**Table 3- 9: Experimental flotation results obtained on use of PPG192.**

| | |
|---|---|
| Solids mass recovery in the concentrate (g/min) | 6.02 |
| Solids mass recovery in the tails (g/min) | 151.9 |
| Mass composition of constituent PGM in the concentrate stream (g/t) | 39.4 |
| Mass composition of constituent PGM in the tails stream (g/t) | 1.75 |
| Water mass recovery in the concentrate (g/min) | 34.4 |

$$R_{PGM} = \frac{\frac{6.02}{10^6} * 39.4}{\frac{1.75}{10^6} * 151.9 + \frac{6.02}{10^6} * 39.4} * 100 = 47.2\%$$

$$k_{O,PGM} = \frac{0.472}{2.91 * (1 - 0.472)} = 0.3077$$

Following similar calculations for tests performed at different froth heights Figure 3-5 is obtained which allows for the determination of the collection rate constant, $k_c = 0.513$

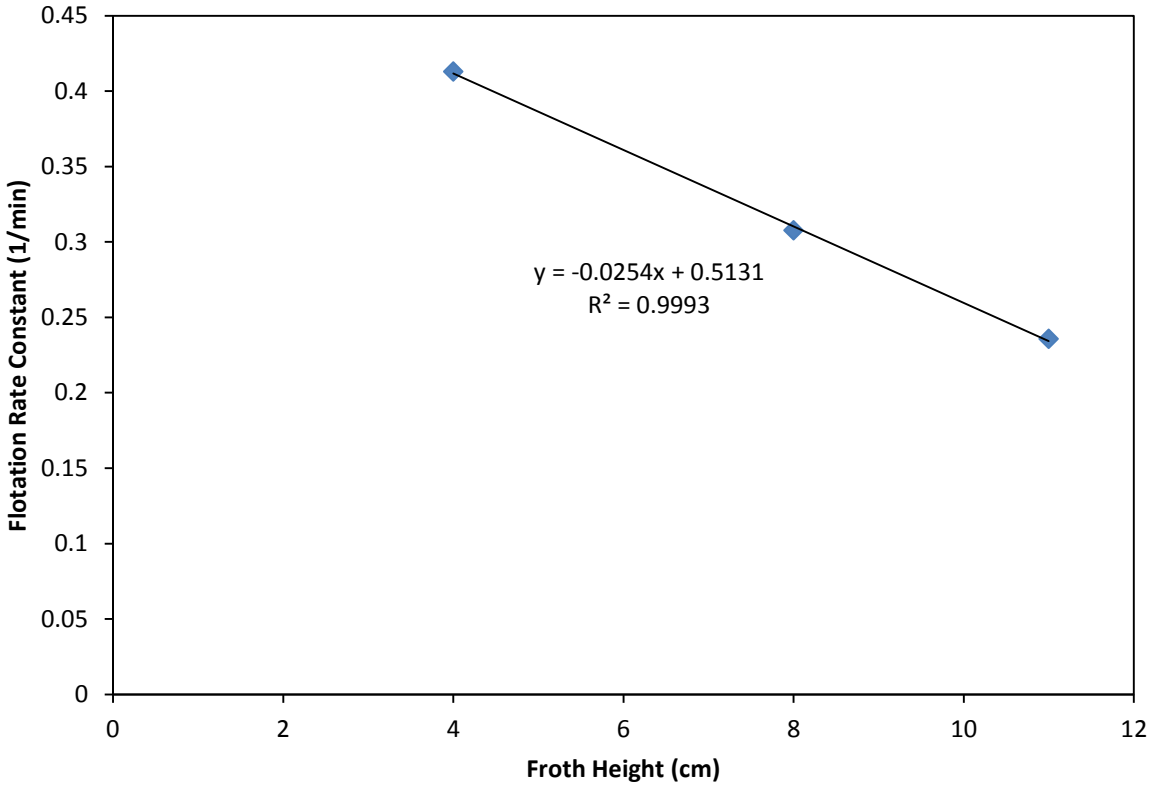


**Figure 3-5: Relationship between flotation rate constant and froth depth on tests performed using PPG192.**

$$Froth\ recovery, R_f = \frac{0.3077}{0.513} * 100 = 60.0\%$$

The entrainment factor for chromite was determined as shown in Equations 3-4 and 3-5:

$$F_{Cr_2O_3,conc} = F_C x_{Cr_2O_3,conc}$$ **Equation 3-4**

$$Entrainment\ factor = \frac{F_{Cr_2O_3,conc}}{F_{H2O,conc}}$$ **Equation 3-5**

*Where: $F_{Cr2O3,conc}$ is mass recovery of chromite in the concentrate (g/min) and $F_{H2O,conc}$ is mass recovery of water in the concentrate (g/min).*

Defining the entrainment factor as mass of gangue material recovered per unit mass of water eliminates the effect of the different water recoveries obtained under different experimental conditions which is necessary due to the effect of water recovery on entrainment. The results obtained from the chemical assays were also used to determine the grade and recovery of valuable minerals from the flotation process.

### 3.2.6. Froth Stability Column

The effect of frother type on two-phase and three-phase systems was investigated using a froth stability column shown in Figure 3-6. The column was made of Perspex and had a diameter of 10 cm and a height of 1 m and was fitted with a 40- 100 µm sized pore frit to ensure even gas distribution within the rig. For the three-phase work, an axial flow agitator was put inside the column to avoid settling of solids in the column.

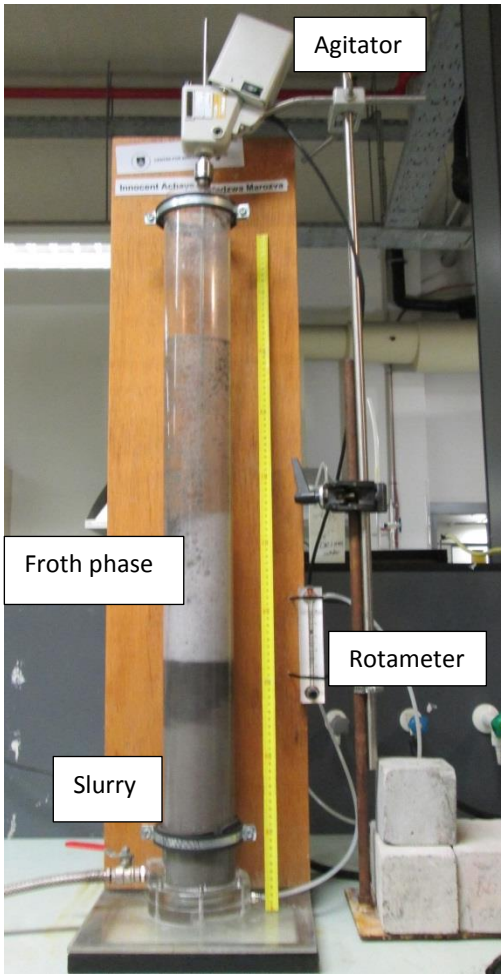


**Figure 3-6: Picture showing setup of the frothing column.**

### 3.2.7. Foam Rise Rate Experimental Procedure

A 2 $\ell$ aqueous frother solution of concentration 500 ppm was prepared using synthetic plant water. For tests focused on dual frother suites at PPG: alcohol ratio of 4:1 was investigated. The frothers were added to the synthetic plant water from different stock solutions. The frother solution (mixture of frother and water) was stirred and poured into the column and air at a superficial velocity of 1.70 cm/sec was passed through the column. The superficial air velocity was determined as a ratio of the air volumetric flow rate to the cross sectional area of the column. Changes in the foam height as a function of time were observed till the maximum stable equilibrium height was reached (approximately 2 min) and were recorded.

The experiments were carried out in duplicate to ensure reproducibility. The uncertainty associated with the equilibrium height measurement was about $\pm$ 0.4 cm.

The experiments were intended to be carried out at the same frother molar concentration to allow for an accurate comparison of the results. However, due to the large differences in the molecular weight and frothing abilities between the alcohol and polyglycols this was not feasible.

### 3.2.8. Froth Rise Rate Experimental Procedure

The tests were performed using the froth stability column and a slurry with a pulp density of 30 % prepared as outlined in the preceding sections. The tests were done to investigate the use of single and dual component frother suites. Single component frother tests were done at concentrations of 0.314 and 11.3 mM for polyglycol and alcohol frothers respectively. Dual component frother suite tests were performed at a polyglycol: MIBC ratio of 4:1 at a total concentration of 0.314 mM. All tests were conducted at a SIBX dosage of 100 g/t. After allowing the conditioning time of 15 min where the slurry was agitated in the feed tank, 2.35 $\ell$ of the slurry was pumped into the column. The column had an agitator operating at a speed of approximately 300 rpm to avoid settling of solids in the column. Air was then passed into the column at a superficial velocity of 1.06 cm/sec and froth height changes were noted till the maximum equilibrium froth height was attained. These tests were repeated at different superficial air velocities to determine the froth stability factor, $\Sigma$. All experiments were carried out in duplicates to ensure generation of data within an acceptable experimental error range.

### 3.2.9. Data Processing

Foam/froth height – time experimental data was fit to Equation 3-6 by a regression tool (Excel Solver) making use of the principle of least squares to determine a proxy for foam/froth stability, τ.

$$H = H_{max}(1 - e^{t/\tau}) \quad \textbf{Equation 3-6}$$

A plot of $H_{max}$ versus superficial velocity allows for the evaluation of $\Sigma$ as it is the slope of the curve following from its definition as shown in Equation 3-7(Bikerman, 1973):

$$\sum = \frac{H_f}{J_g} \quad \textbf{Equation 3-7}$$

*Where: $H_f$ is foam/froth maximum equilibrium height (cm) and $J_g$ is superficial air velocity (cm/sec).*

Due to the linear relationship that exists between frother dosage and froth stability (Wiese et al., 2010; Tan et al., 2005; Wiese et al., 2011; Corin & Wiese, 2014) the author proposed the use of a new parameter termed molar foam stability factor, $\bar{\Sigma}$ as a more accurate method of comparing the foam stability results of experiments carried out at different frother molar concentration. Molar foam stability factor is defined as shown in Equation 3-8.

$$\bar{\Sigma} = \frac{\Sigma}{n_{frother}} \quad \textbf{Equation 3-8}$$

*Where $n_{frother}$ is the number of moles of frother present in the experiment.*

## 3.3. Surface Tension Measurements

Surface tension studies were performed to further the understanding of the effect of frother structure on the action of frothers at a molecular level. The surface tension measurements were carried out using a BP2 Kruss bubble pressure tensiometer shown in Figure 3-7 on solutions of different frother type and concentration.


**Figure 3-7: Picture showing Tensiometer used in determining surface tension.**

The tensiometer comprised of a movable platform with a height control mechanism and a salinized glass capillary attached to a clamping spring which was connected to a sensitive pressure measuring device. The platform, upon which a petri dish containing a sample solution was placed, was connected to a temperature control system allowing for all measurements to be carried out at a temperature of 25.6 ± 0.2 ℃. The tensiometer was also connected to a gas line containing dry nitrogen which was released at a pressure of 0.45 MPa and passed through the glass capillary for the continuous generation of bubbles. Connecting the tensiometer to a computer interface allowed for easy control of the measuring process.

### 3.3.1. Experimental Procedure

Aqueous solutions of different frother concentrations were carefully prepared using distilled water purified by a Milli Q system and were poured into a petri dish placed on the movable platform. The surface tension of the distilled water was 72.1 mN/m with a standard deviation of 0.02 mN/m. The platform was lifted towards the tip of the glass capillary by means of a height control mechanism to a height that allowed for the capillary to be dipped into the solution. The components were enclosed in a working area to prevent possible contamination of the samples. The surface tension of the most dilute solution was measured first with all tests performed over a surface age of 10-2000 msec. The surface tension- surface age experimental data was the saved as an Excel files for further analysis.

Equilibrium surface tension was considered to be achieved when the surface tension became constant with increasing surface age.

### 3.3.2. Data Processing

Using the equilibrium surface tension versus bulk frother concentration data, the relative surface excess of single and dual component frother mixtures were determined using the Gibbs adsorption isotherm and Hutchinson method respectively. The equations are shown as Equation 3-9 and 3-10 respectively,

$$\boldsymbol{\Gamma} = -\frac{1}{RT}\left(\frac{d\gamma}{d\ln c}\right)_T \qquad \textbf{Equation 3-9}$$

*Where: $\boldsymbol{\Gamma}$ is frother surface excess (mol/m2), R is gas constant ($m^3\,Pa\,K^{-1}\,mol^{-1}$), γ is equilibrium surface tension (mN/m), C is bulk frother concentration (mol/ℓ) and T is temperature (K).*

$$\Gamma_{PPG} = -\frac{1}{RT}\left(\frac{d\gamma}{d\ln c_{PPG}}\right)_{MIBC,T} \qquad \textbf{Equation 3-10}$$

**Demonstration**

A plot of the equilibrium surface tension of PPG192 frother solutions at different concentrations is shown in Figure 3-8. Determining the slope of the surface tension – frother concentration relationship allows for the determination of the surface excess using equation 3-10. For example, in the case of PPG192 the surface excess is obtained as follows;

$$\Gamma_{PPG} = -\frac{1}{RT}\left(\frac{d\gamma}{d\ln c_{PPG192}}\right)_T$$

$$= \frac{1}{8.314\ Jmol^{-1}K^{-1} * 298.15\ K} * -0.0042\ Jm^{-2}$$
$$= 1.70\ \mathrm{mol}/m^2$$

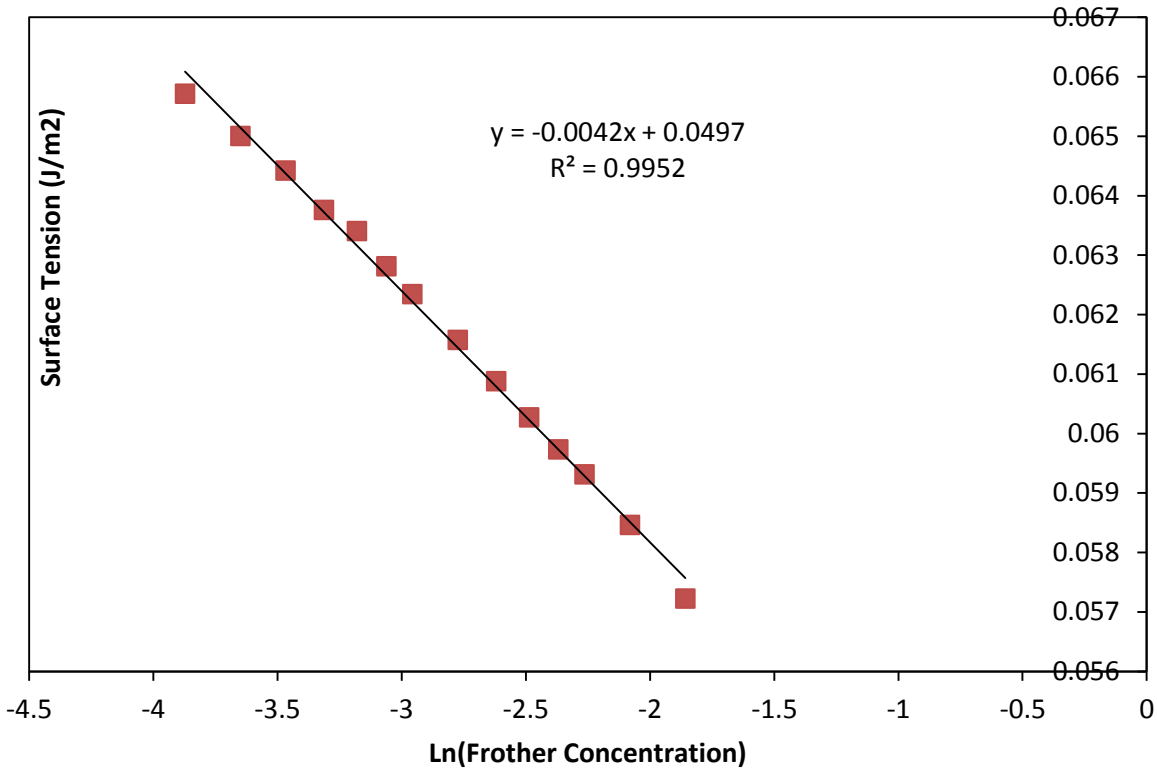


**Figure 3-8: Equilibrium surface tension measurements for known concentrations of PP192 solutions measured using a BP2 Kruss tensiometer.**

The surface area occupied by a frother molecule at the interface was determined as shown in Equation 3-11:

$$A_{exp} = \frac{1}{N_A \Gamma}$$ **Equation 3-11**

*Where: $N_A$ is the Avogadro number ($mol^{-1}$)*

In the case of PPG192, using Equation 3-11 and the earlier determined surface excess of 1.70 mol/$m^2$ translates to an experimentally determined surface area, $A_{exp}$ = 97.4 $Å^2$/molecule.

Using the experimentally determined $A_{exp}$ and the Stokes- Einstein equation, the diffusion coefficient of the different frothers were determined as shown in Equation 3-12:

$$D_{frother} = \frac{k_B T}{3\pi\eta A_{exp}}$$ **Equation 3-12**

*Where: $k_B$ is Boltzmann constant ($m^2$ kg $s^{-2}$ $K^{-1}$) and $\eta$ is the bulk viscosity (Pa. s).*

As a result of the very low frother concentrations typical of flotation processes used during the experiments the diffusion coefficient was assumed to be independent of concentration.

This is a valid assumption when the diffusion gradient is negligible (Murthy et al., 2005; Taylor & Krishna, 1993).

The Langmuir adsorption constant was evaluated by fitting the experimental data to the Szyszkowski model and using the principles of least squares (Chang & Franses, 1995). For convenience the model is given in Equation 3-13:

$$\gamma_0 - \gamma = RT\Gamma_m \ln(1 + K_L c) \qquad \textbf{Equation 3-13}$$

An analysis of the coiled nature of polyglycol frothers at the interface was carried out by comparing the experimentally determined surface area ($A_{exp}$) of frothers to theoretically evaluated surface areas representing the area occupied by a fully extended and parallel aligned molecule at the interface ($A_{cal}$). The general structural formula of polyglycols is shown in Figure 3-9.

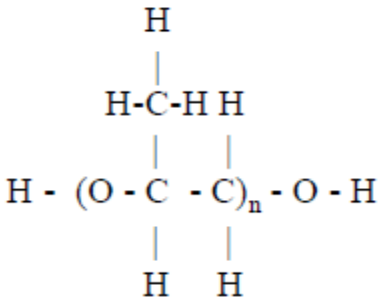


**Figure 3-9: General structural formulae of a polyglycol molecule**

Determining $A_{cal}$ was done based on the Schwartz (2004) method which assumes an average bond length of 1.54 Å (for C-O, C-H and C-C) and is based on the general structure of polyglycols of Equation 3-14 to 3-16:

$$Length = (3n + 2) * 1.54\text{Å} \qquad \textbf{Equation 3-14}$$

$$Width = 3 * 1.54\text{Å} \qquad \textbf{Equation 3-15}$$

$$A_{calc} = Length * Width \qquad \textbf{Equation 3-16}$$

**Demonstration**

Again using PPG192 as an example, and based on a molecular weight of 192 g/mol, it was determined that n=3 in Figure 3-9. Using Equation 3-14 and 3-15, the length and width of PPG192 are 16.9 and 4.62A, respectively. The calculated area occupied by a PPG192 molecule was determined to be 78.3 $A^2$ using Equation 3-16.

The ratio of $A_{exp}$:$A_{calc}$ gives an indication of the coiling nature of the frother at the interface. When $A_{calc}$ is equivalent to $A_{calc}$ this is interpreted as an indication that the molecule is aligned flat at the interface without any coiled nature. If $A_{calc}$ is greater than $A_{exp}$ this is interpreted as the frother molecule being coiled at the interface as it is the only explanation of the observation.

**Demonstration**

The Langmuir adsorption constants were determined by fitting the Szyszkowski equation to the experimental data as shown in Figure 3-10 using PPG192 as an example.

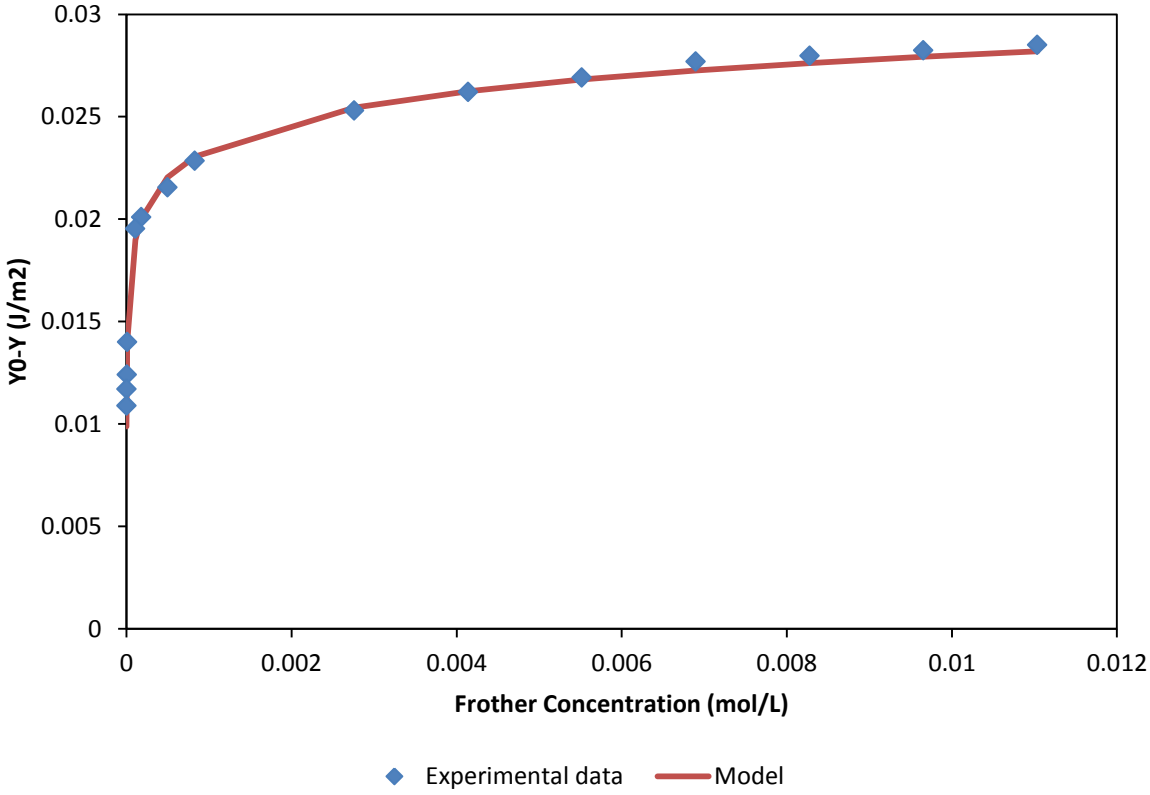


**Figure 3-10: Fitting of the Szyszkowski model to the experimental data to determine the adsorption constant of PPG192 molecules at the interface.**

## 3.4. Frother Characterisation

O'Connor et al (2013) proposed the use of thermodynamics as a robust method of quantifying the polar nature of molecules such as excess Gibbs free energy which in turn is obtained from the activity coefficients of such molecules. Prediction of the activity coefficients in a mixture using the UNIFAC group contribution activity coefficient model was done using a computer programme developed by Sandler.

### 3.4.1. Programme parameters

The UNIFAC model sub-divides molecules into atomic functional groups and determines the activity coefficient by utilising interactions between functional groups (Fredenslund et al.,

1977). As a result a detailed count of the structural functional groups that comprised of the frothers was necessary to determine the activity coefficient of the different frothers as summarised in Table 3-9.

**Table 3-9: Summary of a count of atomic functional groups in the different frother types.**

| | Frother type | | | | | | |
|---|---|---|---|---|---|---|---|
| Functional group description | Pentanol | Hexanol | MIBC | PPG192 | PPG425 | PPG725 | PPG1000 |
| CH3 | 1 | 1 | 3 | 3 | 7 | 12 | 16 |
| CH2 | 4 | 5 | 1 | 1 | 1 | 1 | 1 |
| OH (P) | 1 | 1 | | 1 | 1 | 1 | 1 |
| CH | | | 2 | 3 | 7 | 12 | 16 |
| OH (S) | | | 1 | 1 | 1 | 1 | 1 |
| CH2O | | | | 2 | 6 | 11 | 15 |

Figure 3-11 illustrates a screen-shot of the setting up of the programme calculations showing a full description of the functional groups associated with, in this case pentanol. All calculations were made for a frother solution at a mole fraction of 0.01 and a temperature of 298 K. For the characterisation of dual component frother blends all calculations were based on a polyglycol:alcohol ratio of 4:1.

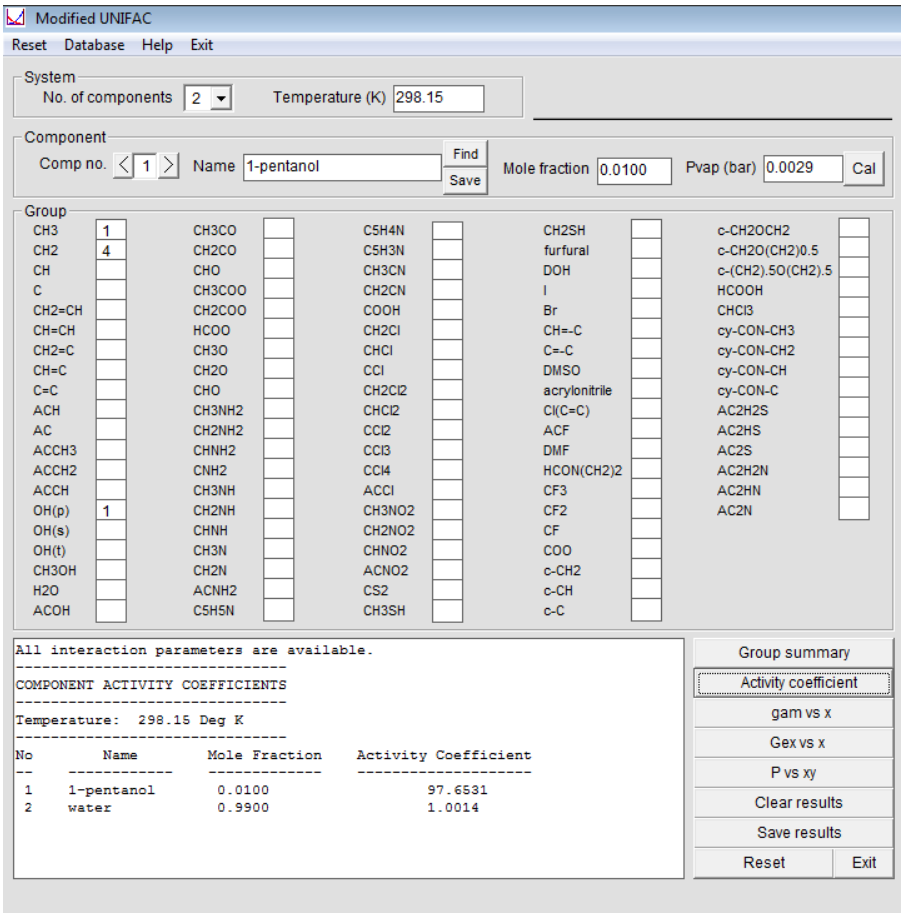


**Figure 3-11: Screen-shot showing setting up of activity coefficient calculations using Sandler programme.**

### 3.4.2. Data processing

The partial molar excess Gibbs energy, $\bar{G}_i^{ex}$ was calculated using the activity coefficients ($\gamma_i$) of the components of the frother solution using the relationship as shown in Equation 3-17 (Sandler, 2006):

$$\bar{G}_i^{ex} = R * T * \ln \gamma_i(T, P, x) \qquad \textbf{Equation 3-17}$$

The total molar excess Gibbs energy, $\bar{G}^{ex}$ was evaluated as shown in Equation 3-18:

$$\bar{G}^{ex} = \sum_{i=1}^{N} x_i * \bar{G}_i^{ex} \qquad \textbf{Equation 3-18}$$

## 3.5. Reproducibility of Experimental Data

### 3.5.1. Statistical Analysis Tools

All experiments were carried out in duplicates to ensure reproducibility and reliability of the results. The repeat experiments allow for an accurate evaluation of the observed parameter by use of the arithmetic mean value,$\bar{x}$, defined as shown in Equation 3-19:

$$\bar{x} = \frac{1}{N}\sum_{x=i}^{N} x_i$$ **Equation 3-19**

Relative standard deviation (RSD) was used as an indicator of the precision of experimental data about the mean. For the purposes of this study it was deemed that only a RSD less than 15 % was acceptable. RSD was calculated as shown in Equation 3-20:

$$RSD = \frac{100}{\bar{x}}\sqrt{\sum_{x=i}^{N}\frac{(x_i - \bar{x})^2}{N-1}}$$ **Equation 3-20**

A graphical depiction of the error associated with the mean values in this study will be represented by error bars obtained from standard error calculations. Standard error is defined as shown in Equation 3-21:

$$Standard\ Error = \frac{1}{\sqrt{N}}\sqrt{\sum_{x=i}^{N}\frac{(x_i - \bar{x})^2}{N-1}}$$ **Equation 3-21**

### 3.5.2. Reproducibility Experimental Tests

Figure 3-12 illustrates repeat foam growth rate experiments that were carried out at the same conditions using solutions that were prepared separately. The figure shows that the different runs and models were closely grouped.

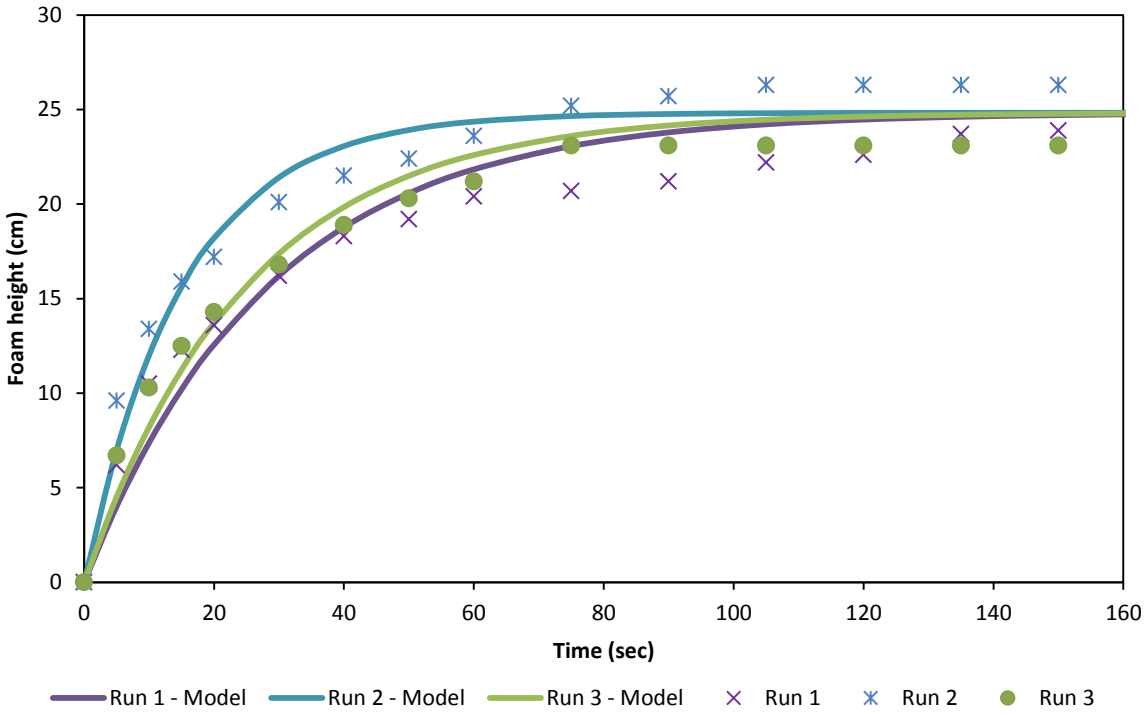


**Figure 3-12: A comparison showing the reproducibility of the foam growth rate experiments performed using MIBC at a concentration of 500 ppm.**

Residual plots were used to determine where the model was a fit to the experimental results, Figure 3-13 shows a residual plot in comparison to the Barbian model and experimental data during the use of pentanol. The residual plot shows a random dispersion of points along the x-axis a similar trend was also observed at different experiment conditions.

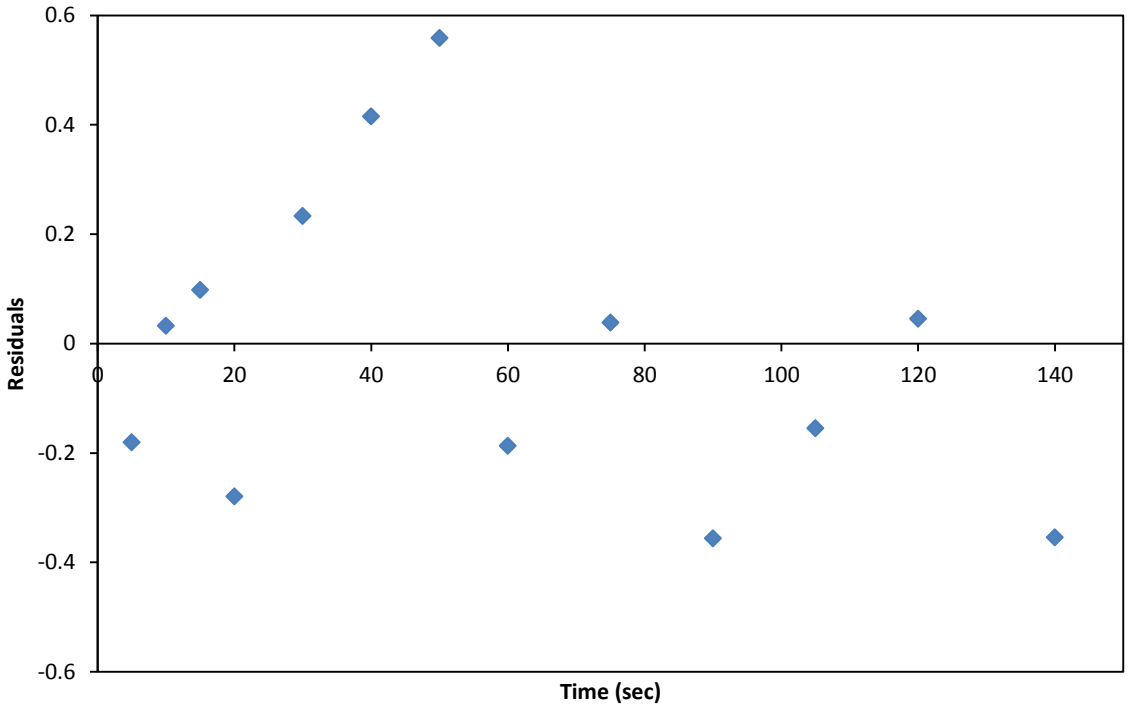


**Figure 3-13: Residual plot comparing Barbian model to experimental data during the use of pentanol.**

Results from repeat froth growth rate experiments carried out using the PPG725 and MIBC frother blend are shown in Figure 3-14. The repeated experiments made use of freshly prepared slurry samples specifically for the purpose of testing reproducibility. It can be seen that the experiments were reproducible.

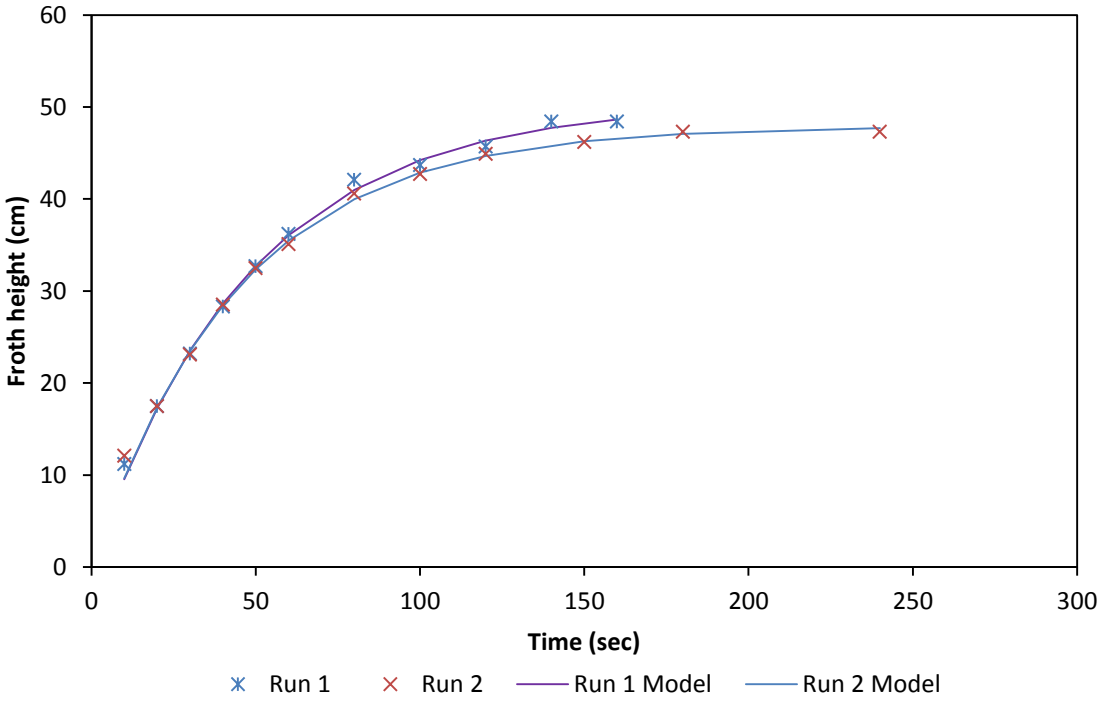


**Figure 3-14: A comparison showing the reproducibility of the froth growth rate experiments performed using PPG725 and MIBC frother blend at a concentration of 0.314 mM.**

Figure 3-15 presents results of the reproducibility tests carried out on the surface tension measurements. The results showed a good agreement between the two experimental runs.

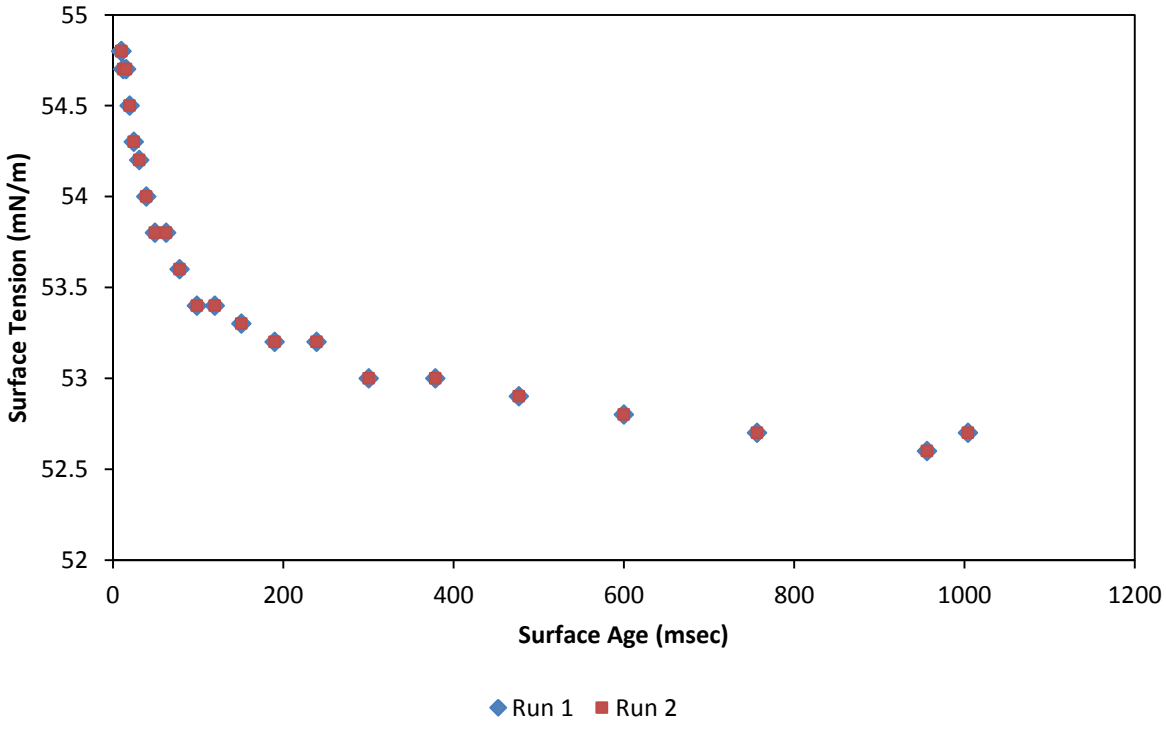


**Figure 3-15: A comparison showing the reproducibility nature of the surface tension experiments performed using PPG425 at a concentration of 0.00706 mM**

# Chapter 4

# Results

This chapter presents results of the tests that were performed to meet the objectives of the project. The initial section of the chapter focuses on two phase experiments with the rest of the chapter focusing on three phase work.

The aim of the two phase work was three-fold: firstly, to characterise the frothers with respect to one another, secondly to determine the effect of frothers on the stability of the foam and froth and, thirdly, to fundamentally understand the mechanism of action of single and dual component frothers. Two phase experiments avoid the complications associated with the ore and fluid dynamics of the slurry. The aim of the three phase work was to determine the effect of frother type at an operational level on froth recovery, entrainment and froth stability. Results from the froth growth rate and the Bikerman's tests performed to determine the stability of the foam/froth phase are included in the chapter. Also included in this chapter is the particle size distribution, PGM and chromite grade of the solid samples collected during the flotation tests.

## Two phase Results

### 4.1. Frother characterisation

The frothers were characterised on the basis of the total excess Gibbs energy ($G_i^{ex}$) of solutions with the same frother concentration based on the use of the UNIFAC model.

Figures 4-1 and 4-2 are an illustration of the changes in the $G_i^{ex}$ of 1 M solutions of polyglycol and alcohol frothers respectively at a frother mole fraction of 0.01 at 298 K. The figures show an increase in $G_i^{ex}$ as the frother molecular weight is increased. It is also observed in Figure 4-2 that the isomers, hexanol and MIBC showed a slight difference of the $G_i^{ex}$ values with the former yielding a greater value. Also evident is that alcohol frothers had low values of $G_i^{ex}$ compared to the polyglycols. The $G_i^{ex}$ values were obtained from activity coefficient ($\gamma_i$) values shown in Table 4-1 and 4-2 based on the UNIFAC model as shown in Equation 3-17.

**Table 4-1: $G_i^{ex}$ values as a function of various alcohol frother aqueous mixtures at a frother mole fraction of 0.01 and temperature of 298 K.**

| 2 Component system | Mole fraction | $\gamma_i$ | Partial Molar Gibbs Excess (J/mol) | Total Gibbs Excess (J/mol) |
|---|---|---|---|---|
| Pentanol | 0.01 | 97.9 | $1.14 \times 10^4$ | 116.0 |
| Water | 0.99 | 0.990 | 3.47 | |
| Hexanol | 0.01 | 274.0 | $1.39 \times 10^4$ | 142.0 |
| Water | 0.99 | 1.00 | 4.7 | |
| MIBC | 0.01 | 243.0 | $1.36 \times 10^4$ | 139.0 |
| Water | 0.99 | 1.00 | 4.5 | |
| Octanol | 0.01 | 2120 | $1.90 \times 10^4$ | 196.0 |
| Water | 0.99 | 1.00 | 7.9 | |

**Table 4-2: $G_i^{ex}$ values as a function of various polyglycol frother aqueous mixtures at a frother mole fraction of 0.01 and temperature of 298 K.**

| 2 Component system | Mole fraction | $\gamma_i$ | Partial Molar Gibbs Excess (J/mol) | Total Gibbs Excess (J/mol) |
|---|---|---|---|---|
| PPG192 | 0.01 | 126 | $1.20 \times 10^4$ | 127.0 |
| Water | 0.99 | 1.00 | 8.17 | |
| PPG425 | 0.01 | $3.22 \times 10^4$ | $2.57 \times 10^4$ | 292.0 |
| Water | 0.99 | 1.02 | 37.6 | |
| PPG725 | 0.01 | $7.96 \times 10^6$ | $3.94 \times 10^4$ | 484.0 |
| Water | 0.99 | 1.04 | 93.9 | |
| PPG1000 | 0.01 | $1.57 \times 10^8$ | $4.68 \times 10^4$ | 615.0 |
| Water | 0.99 | 151 | 151 | |

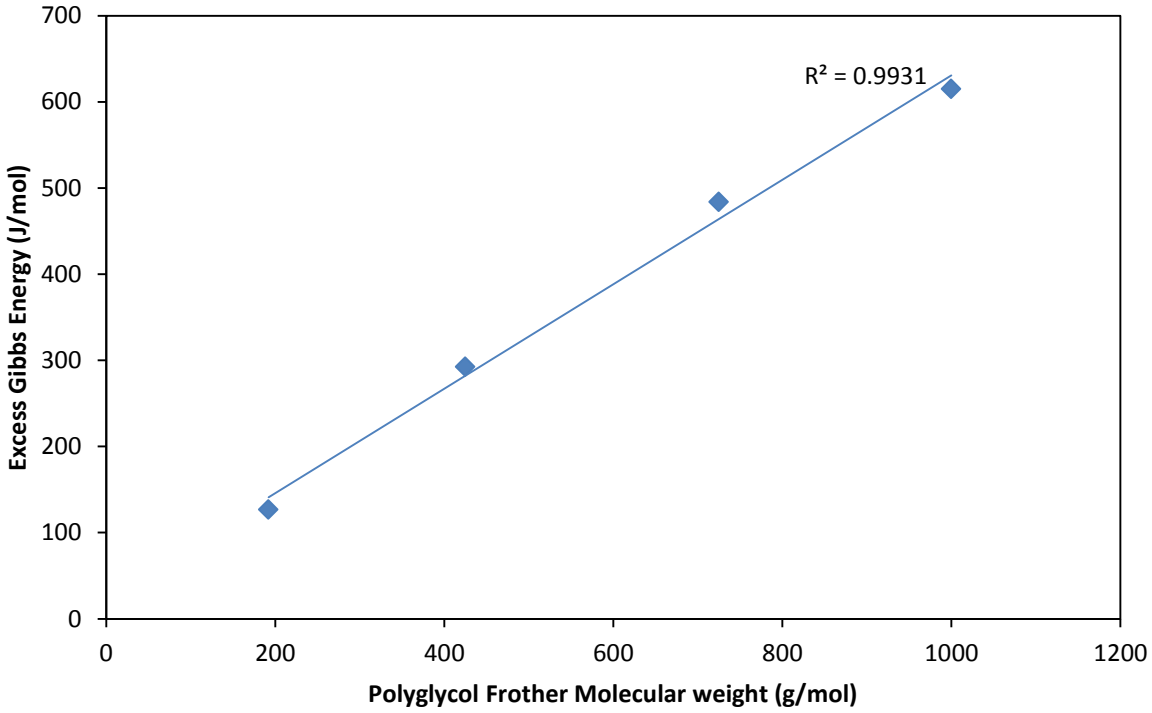


**Figure 4-1: Variation of Excess Gibbs energies of polyglycol frother solutions at a mole fraction of 0.01 with respect to changing molecular weight at 298 K.**

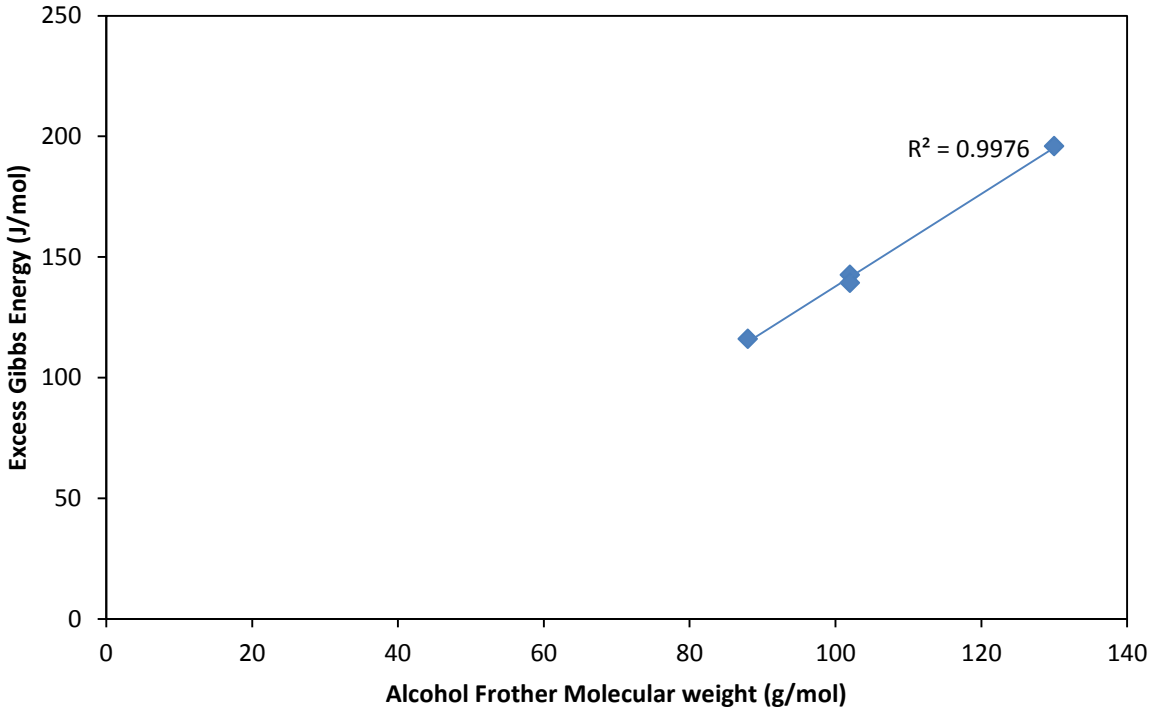


**Figure 4-2: Variation of Excess Gibbs energies of alcohol frother solutions at a mole fraction of 0.01 with respect to changing molecular weight.**

Of increasing importance in froth flotation is the use of frother blends. Figure 4-3 shows $G_i^{ex}$ as a function of frother type for dual-frother solutions comprising of polyglycol and alcohol frothers at a mole ratio of 4:1 and a total mole fraction of 0.01. Figure 4-3 shows that

frother blends generally have lower $G_i^{ex}$ values in comparison to single polyglycol component frothers and that this difference increases as the molecular weight of the polyglycol frother increases. There is little difference in the $G_i^{ex}$ between the frother blends. However, pentanol and octanol blends had slightly lower and higher $G_i^{ex}$ values respectively with hexanol and MIBC blends showing a similar measure of excess Gibbs energy.

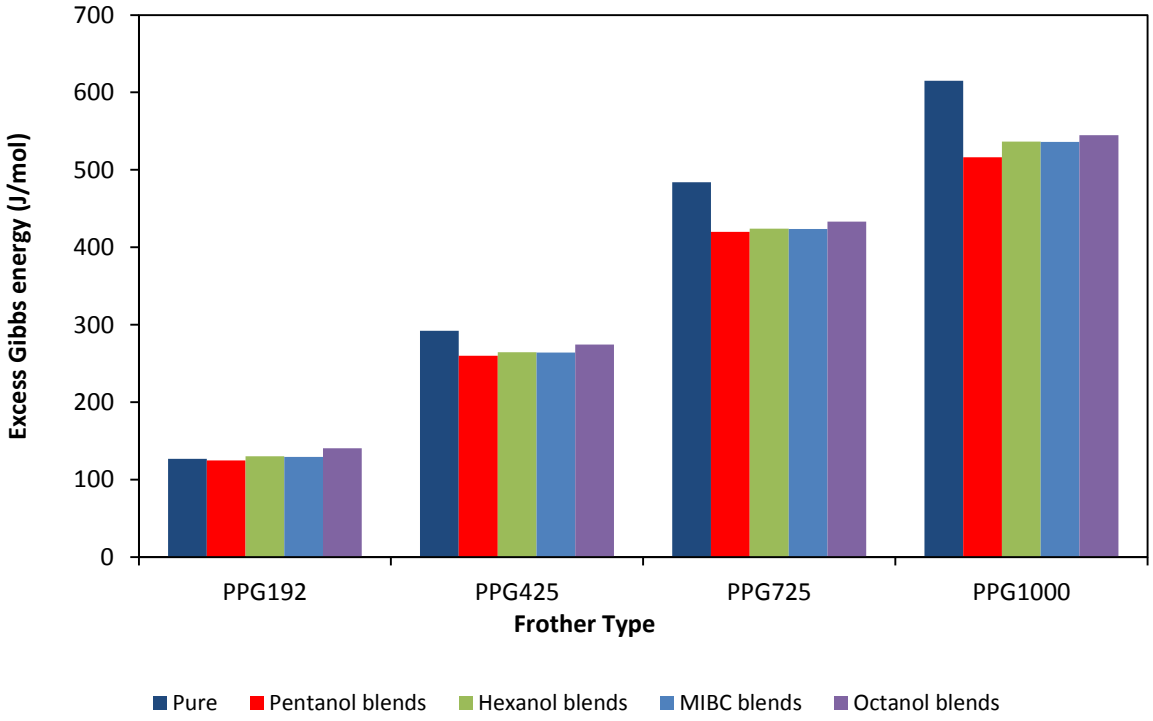


**Figure 4-3: Excess Gibbs energy for single and dual-frother blends. Frother blends were mixed in a polyglycol: alcohol ratio of 4:1 at a total concentration of1 M, which is equivalent to a mole fraction of 0.01.**

## 4.2. Effect of frother type on surface tension

### 4.2.1. Equilibrium surface tension

Stability of the foam/froth phase is significantly influenced by the surface activity of frothers. Changes in equilibrium surface tension as a function of frother type and concentration were investigated using the maximum bubble pressure method and the results are shown in Figures 4-4 and 4-5. It is observed that with increasing frother concentration the surface tension of the solutions was lowered. Analysis of the polyglycol frother series shows that the ability of frothers to lower surface tension increases with the molecular weight of the frothers. A similar finding is observed with regards to the alcohol frother series which shows the isomers (MIBC and hexanol) of higher molecular weight lowering the surface tension to a greater extent compared to pentanol. It is also observed from Figure 4-5 that the equilibrium surface tension achieved by the linear isomer, hexanol, is lower than that achieved by the branched isomer, MIBC, at similar concentrations. It is also evident that a high alcohol frother concentration is required to achieve similar surface tension values obtained at lower concentrations of polyglycol frothers.

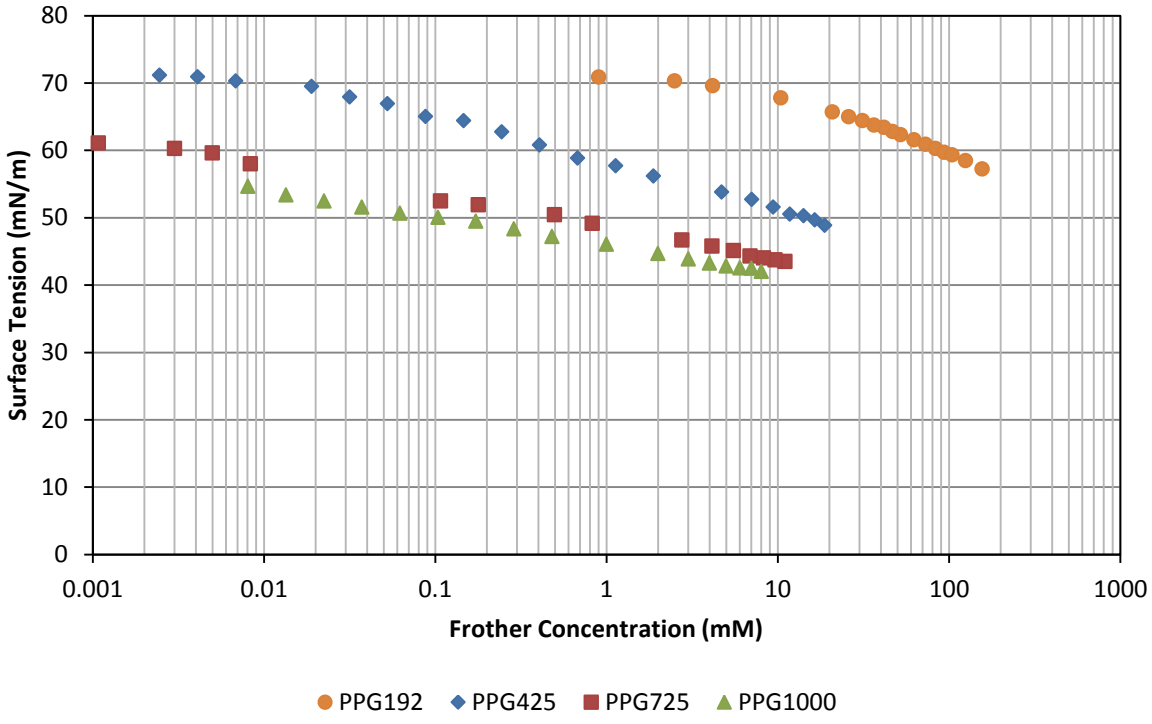


**Figure 4-4: Effect of the different polyglycol frother type and concentration on equilibrium surface tension.**

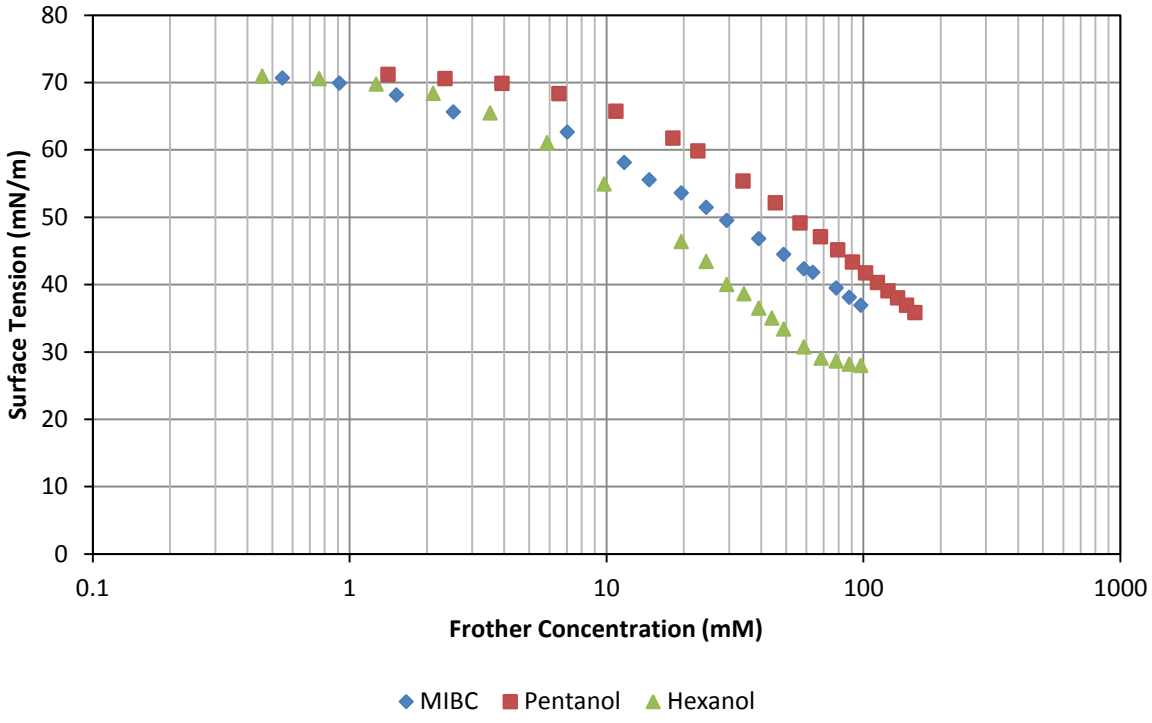


**Figure 4-5: Effect of the different alcohol frother type and concentration on equilibrium surface tension.**

Results comparing the effect of single and dual component frothers at a PPG : MIBC molar concentration ratio of 4:1 on equilibrium surface tension are shown in Figures 4-6 to 4-8. The PPG192-MIBC blend lowered the surface tension to values intermediate between the

two pure frothers. There was no significant surface tension difference between the single component frothers of PPG425 and PPG725 and their blends at similar concentration.

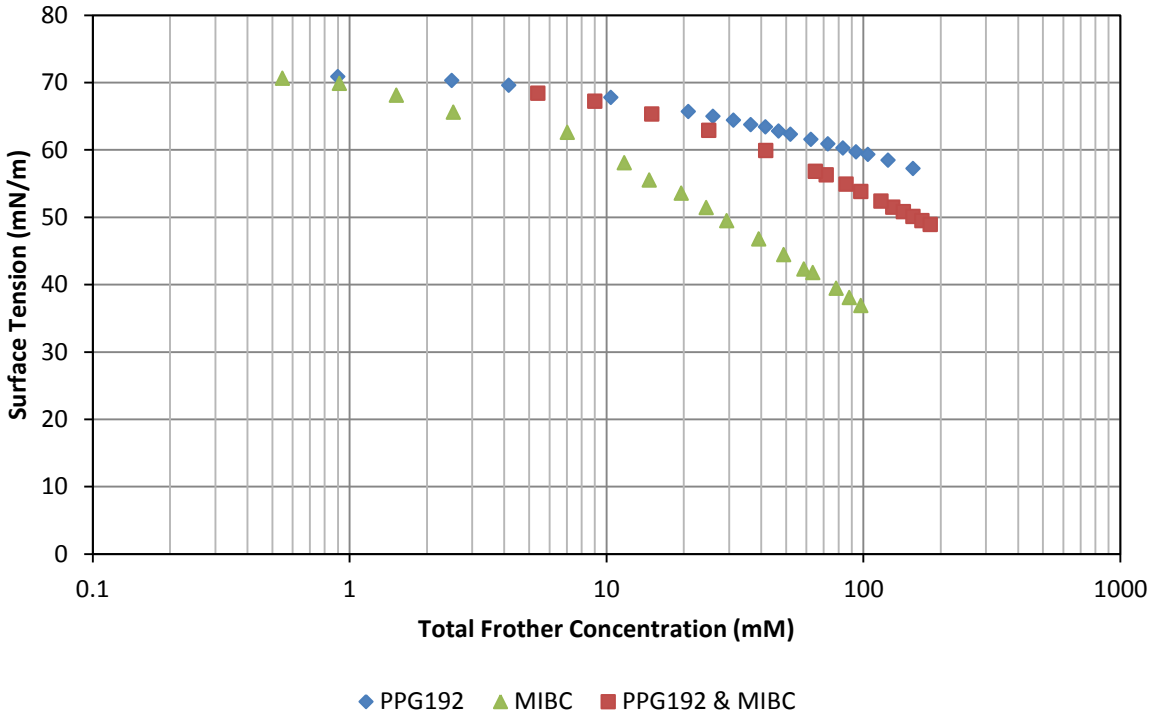


**Figure 4-6: Comparison of the effect of PPG192 single and dual component frother mixture on equilibrium surface tension.**

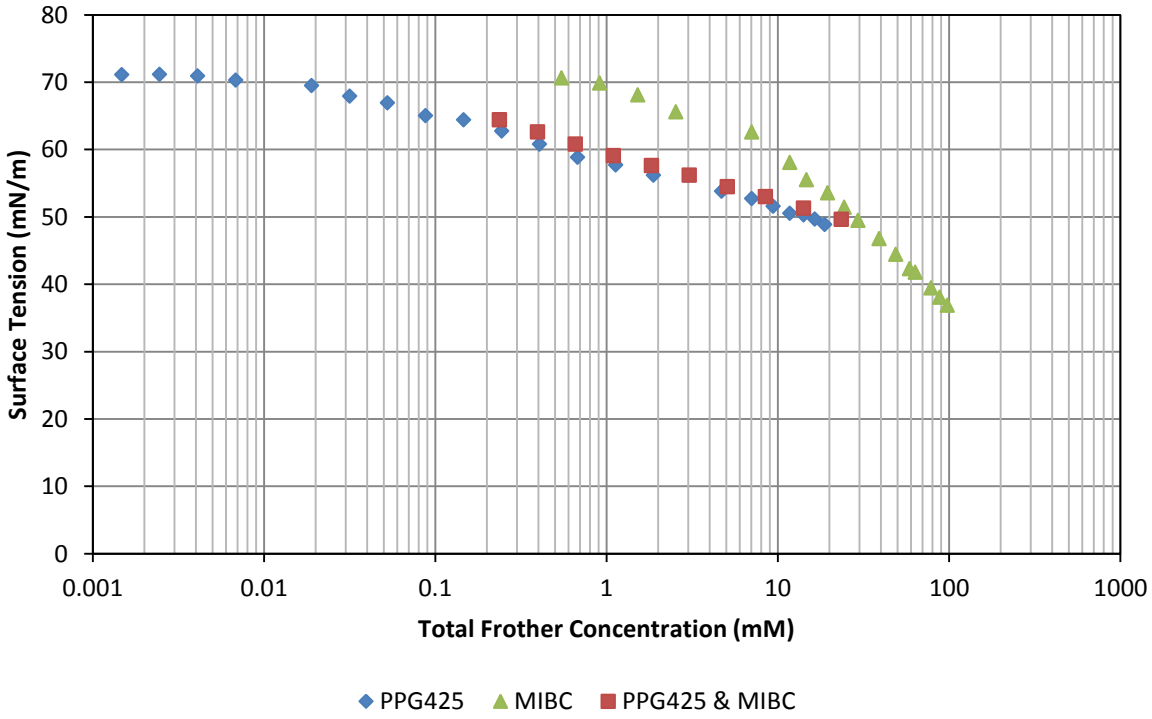


**Figure 4-7: Comparison of the effect of PPG425 single and dual component frother mixture on equilibrium surface tension.**

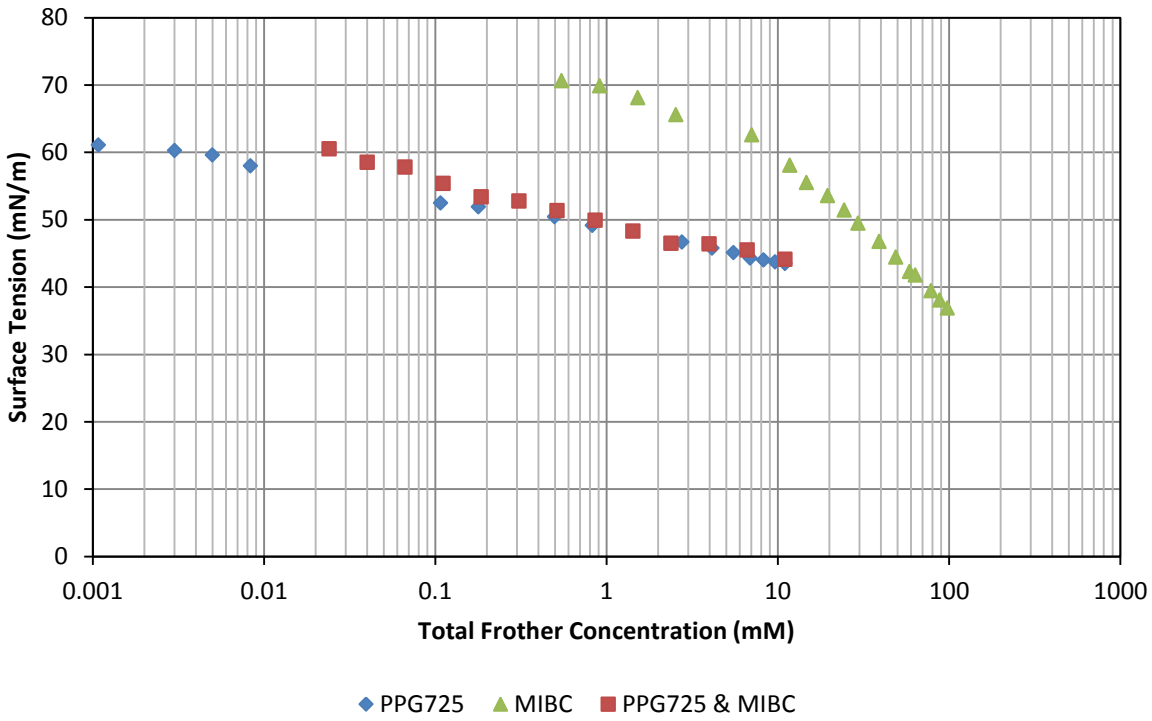


**Figure 4-8: Comparison of the effect of PPG725 single and dual component frother mixture on equilibrium surface tension.**

Application of the Gibbs Adsorption isotherm (Equation 2-16) as mentioned in the preceding chapter can be used to determine the surface excess of surfactants as shown in Figure 4-9. The figure shows that for the polyglycol frother series, the surface excess of the frothers at the interface (defined as the measure of the amount of adsorbed surfactant at the interface) increased as the frother molecular weight decreased. However, the alcohol frother type series does not show a similar trend as MIBC had a surface excess value of 3.94 x $10^{-6}$ mol/$m^2$ and pentanol a value of 5.02 x $10^{-6}$ mol/$m^2$. Hexanol exhibited a higher surface excess in comparison to MIBC. Surface excess values of pentanol and hexanol showed a negligible difference with hexanol having a slightly higher value.

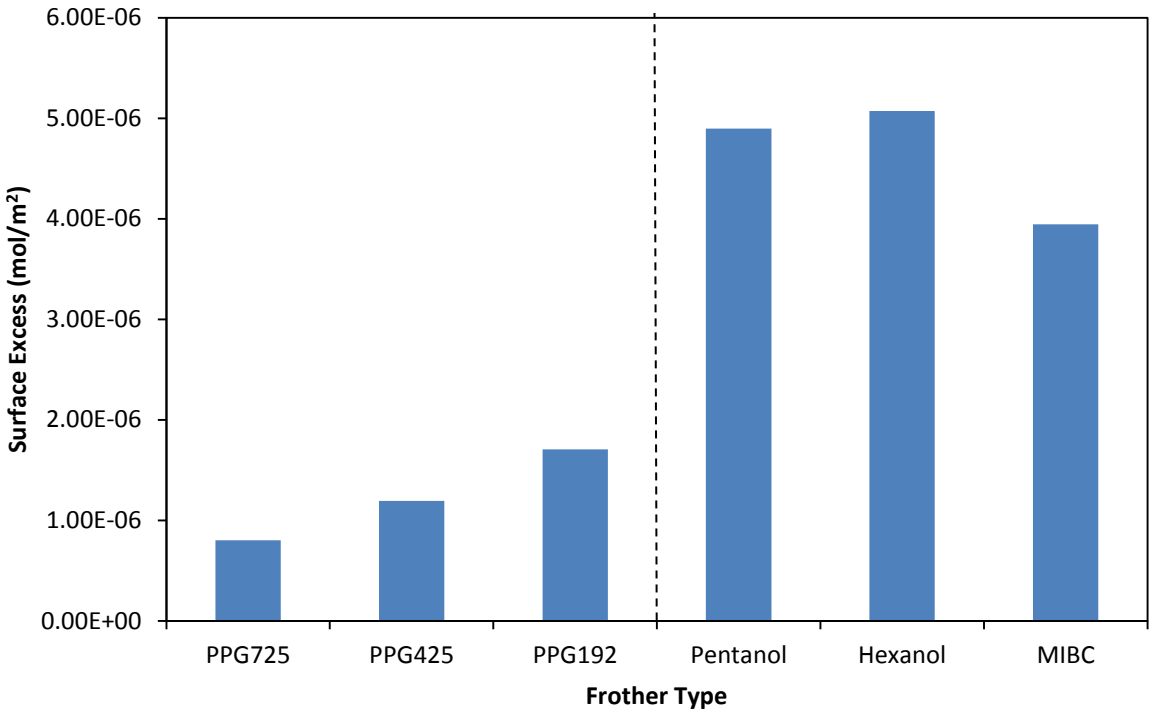


**Figure 4-9: Comparison of surface excess values for polyglycol and alcohol frothers.**

Figure 4-10 shows the comparison of the surface excess for pure polyglycol frothers and those blended with MIBC in a 4:1 ratio. The figure shows that PPG425 and PPG725 blended frother solutions had a greater surface excess compared to the single component polyglycol frother solutions. This shows that during the use of the blended PPG425 and PPG725 frother solutions there is a greater number of the surfactants at the interface. Single and dual blended mixtures of PPG192 showed no difference in the surface excess values.

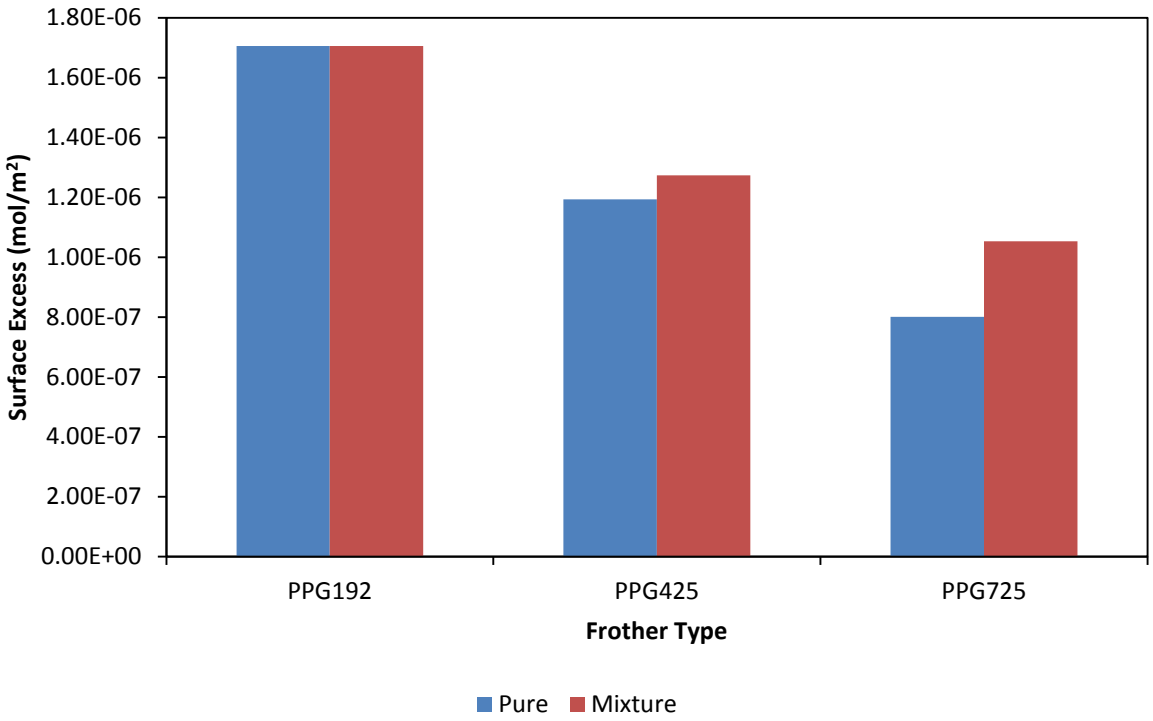


**Figure 4-10: Comparison of surface excess obtained on use of single and polyglycol-MIBC blended frothers.**

Table 4-3 and Figure 4-11 gives a summary of the surface area occupied by a frother molecule and coiling nature ($A_{Exp}$:$A_{Cal}$) of surfactants of each frother type. The polyglycol frother series shows an increase in surface area occupied by the frother at the interface as the frother molecular weight increases as expected. $A_{Cal}$ is the calculated theoretical surface area of a fully extended frother molecule as shown in Chapter 3 and the ratio of the experimentally calculated surface area to the theoretical surface area ($A_{Exp}$:$A_{Cal}$), therefore gives an indication of the extent of coiling. The polyglycol frother series shows an increase in the surface area occupied by the frother molecule at the interface as the frother weight increases, as expected. As the frother molecular weight increases it is also observed that the ratio $A_{Exp}$:$A_{Cal}$ decreases indicating a more coiled nature. This analysis was not conducted on the alcohol frother series due to their perpendicular alignment at the interface as a result of the position of the polar group within the frother molecule. Anomalies such as $A_{Exp}/A_{Cal}$ values greater than unity were obtained possibly due to errors associated with the experiments.

**Table 4-3: Summary of inter-phase properties of the frothers.**

| Frother type | $\Gamma$ (mol/m$^2$) | $A_{Exp}$ (A$^2$/molecule) | $A_{Cal}$(A$^2$/molecule) | $A_{Exp}/A_{Cal}$ (-) |
|---|---|---|---|---|
| PPG192 | 1.70 e -6 | 97.4 | 78.3 | 1.24 |
| PPG425 | 1.19 e -6 | 139 | 166 | 0.84 |
| PPG725 | 8.01 e -7 | 207 | 294 | 0.70 |
| PPG1000 | 7.23 e -7 | 230 | 364 | 0.63 |
| Pentanol | 5.02 e -6 | 34.3 | - | - |
| Hexanol | 5.08 e -6 | 32.7 | - | - |
| MIBC | 3.94 e -6 | 42.1 | - | - |

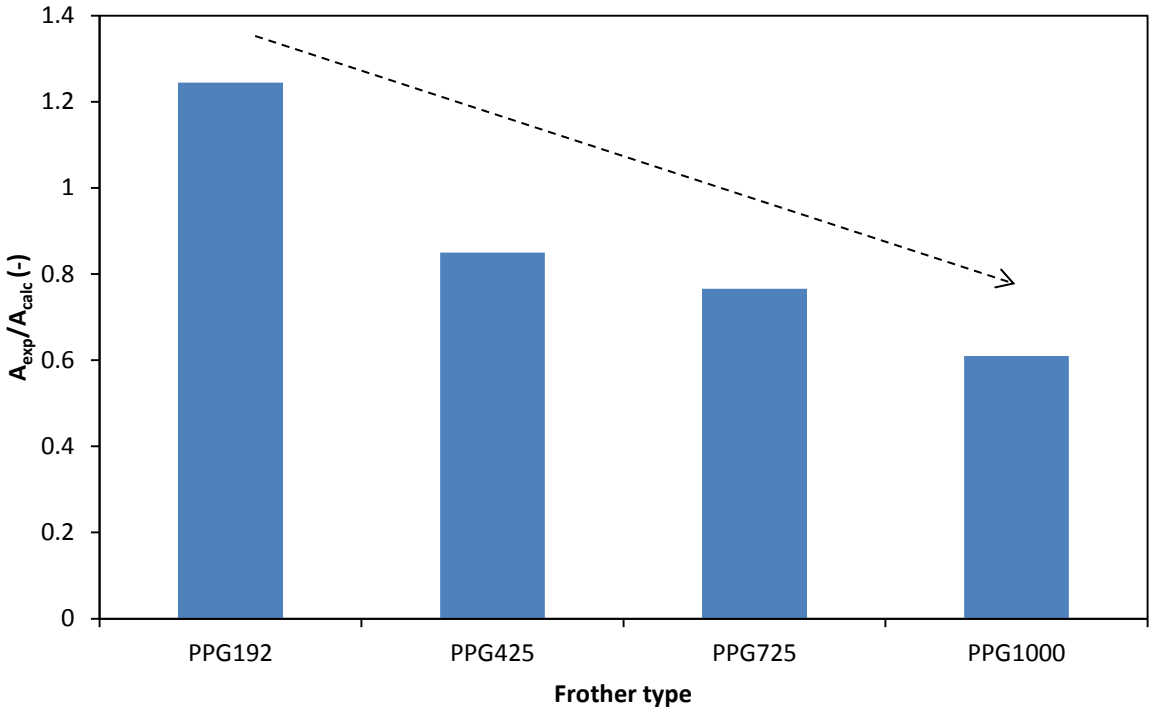


**Figure 4-11: Comparison of the coiling nature of frothers as a function of frother type.**

Using the Langmuir adsorption isotherm equation (Equation 2-18) allows for the characterisation of the frothers on the basis of the Langmuir equilibrium adsorption constant, $K_L$ which is an indication of measure of the energy of adsorption at the interface. Table 4-4 shows the values of the parameters obtained. Generally values of $K_L$ for both frother series type show an increase as the molecular weight increases. However, the branched-chain MIBC showed lower values of the parameter in comparison to hexanol.

**Table 4-4: Summary of numerical values of Langmuir adsorption constant used as a measure of the active nature of frothers at the surface.**

| Frother Type | $K_L$ ($m^3$/L) |
|---|---|
| PPG1000 | 2.08E+06 |
| PPG725 | 1.33E+05 |
| PPG425 | 1.03E+02 |
| PPG192 | 1.70E-01 |
| Pentanol | 1.04E-01 |
| Hexanol | 3.79E-01 |
| MIBC | 3.33E-01 |

Similar investigations on the use of dual frother blends yielded results shown in Figure 4-12 which show a decrease in the $K_L$ values on the use of dual blends compared to the use of single component frothers. Differences between single and dual component adsorption

values decreased as the polyglycol frother molecular weight decreased with little differences observed on use of PPG192.

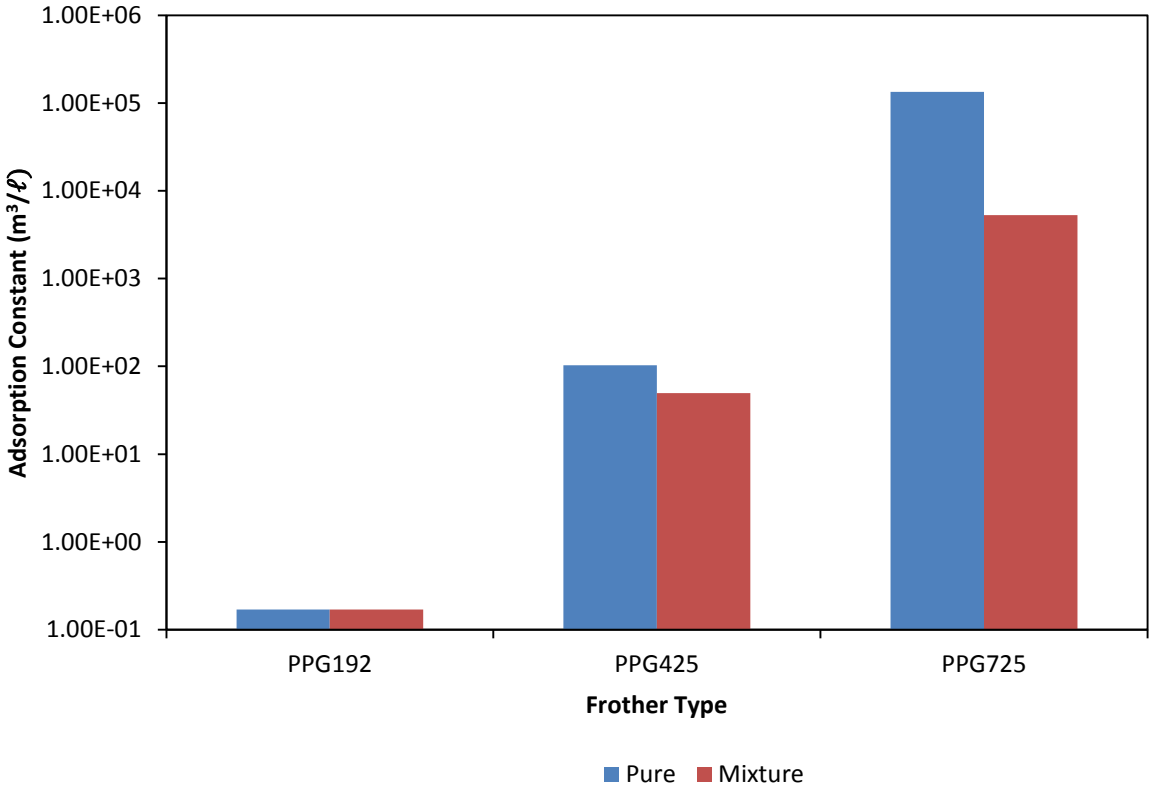


**Figure 4-12: Langmuir adsorption constant value comparison on use of pure polyglycol and polyglycol-MIBC frother mixture.**

A plot of the $G_i^{ex}$ versus the adsorption constants of the various frothers is shown in Figure 4-13 which shows a linear relationship between the Langmuir adsorption constant and $G_i^{ex}$.

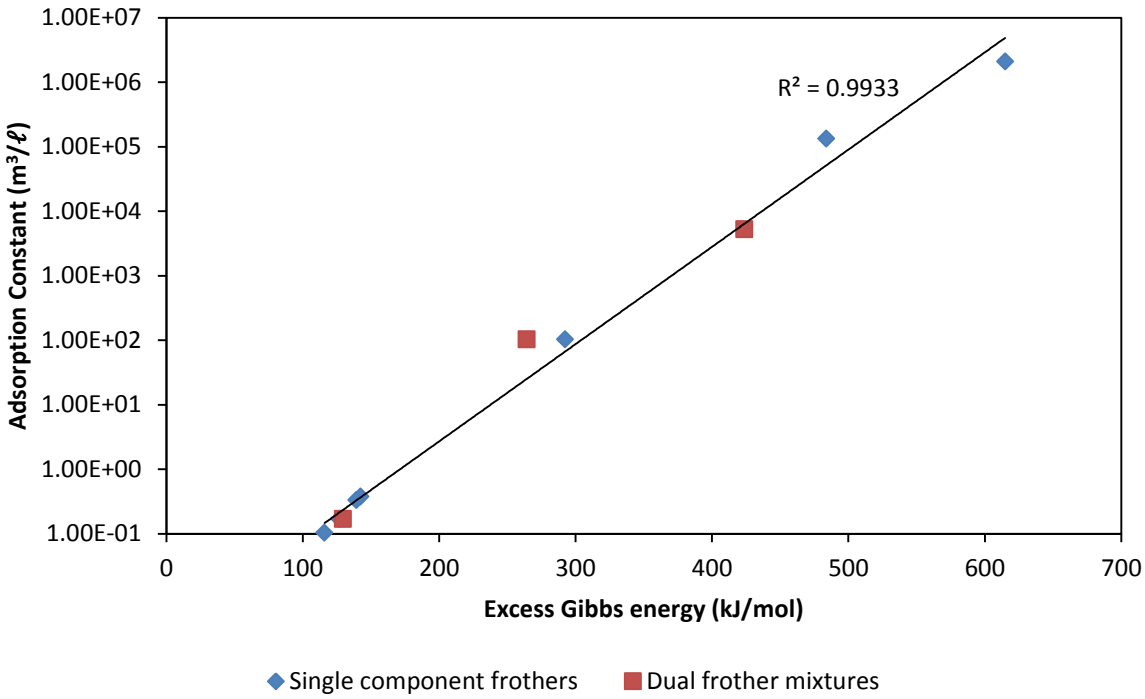


**Figure 4-13: Adsorption constant as a function of $G_i^{ex}$.**

The Stokes-Einstein model (Equation 3-12) as mentioned in preceding chapters can be used to predict the diffusion coefficients of the frother molecules as shown in Figure 4-14. For the polyglycol series it is evident from Figure 4-14 that PPG192 has the greatest diffusion coefficient of 3.92E-10 $m^2$/sec compared to PPG1000 whose value is 2.55E-10 $m^2$/sec showing the effect of molecular weight on the diffusion coefficient. For the alcohol series, MIBC has the least diffusion coefficient value of 5.96E-10 $m^2$/sec and hexanol has the greatest coefficient value of 6.77E-10 $m^2$/sec.

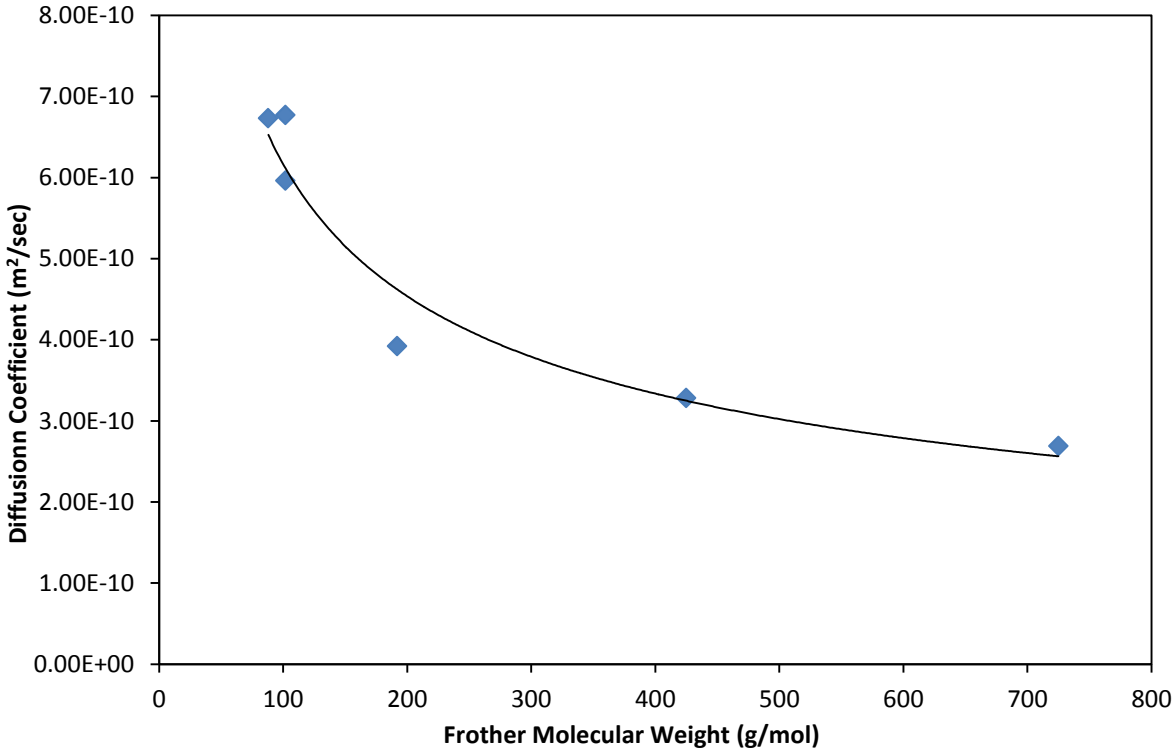


**Figure 4-14: Diffusion Coefficient as frother molecular weight.**

## 4.3. Foam Stability Analysis

As mentioned in the preceding chapters foam stability has a significant effect with regards to the flotation process. Figures 4-15 and 4-16 show the foam growth rates as a function of time for polyglycol and alcohol frother types respectively. By means of regression analysis a model (Equation 2-3) represented by lines in the figures was fit to the experimentally determined growth curves. The regression analysis gives values of the parameters, $\tau$ and $H_{max}$ corresponding to the characteristic average bubble lifetime and equilibrium height respectively which can be used as proxies of foam stability (Barbian et al., 2003).

The figures show that as the molecular weight of frothers increased from 192 to 425 the maximum foam equilibrium height increases, but thereafter an increase in the molecular weight results in a decrease in the maximum equilibrium height. Though hexanol and MIBC are of the same molecular weight the latter gave a foam of greater equilibrium height. On comparison of the two frother types generally the polyglycol frothers resulted in a foam of greater height than alcohol frothers. Other foam growth rate curves obtained under different experimental conditions which could be used to infer a measure of stability are shown in Appendix A.

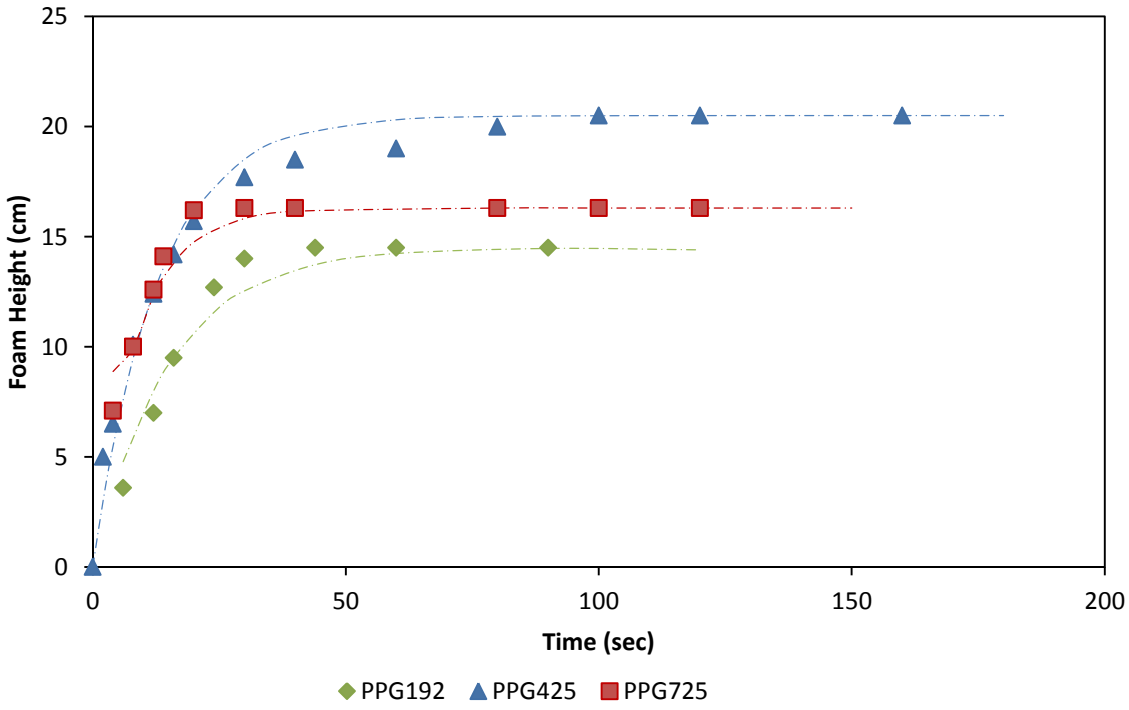


**Figure 4-15: Foam height as a function of time using polyglycol frothers at a concentration of 500 ppm. The dotted lines represent an exponential model fitted to the experimental data.**

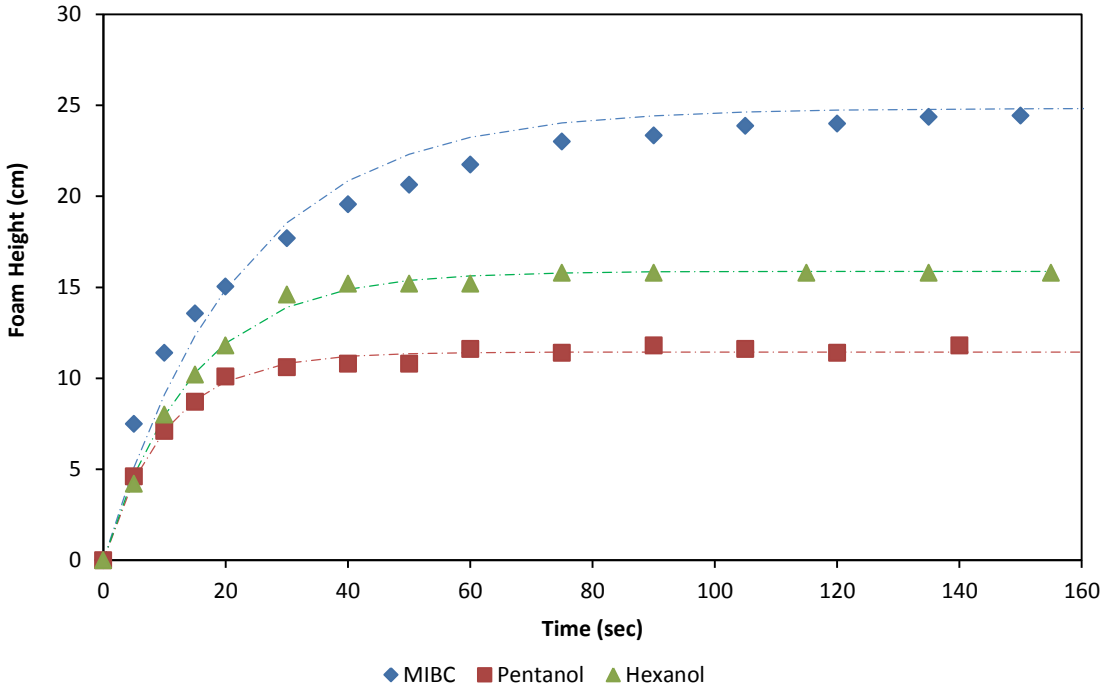


**Figure 4-16: Foam height as a function of time using alcohol frothers at a concentration of 500 ppm. The dotted lines represent an exponential model fitted to the experimental data.**

Table 4-5 gives a summary of the average bubble lifetime which can be used as a measure of stability. Also shown is the measure of error that was associated with the experiments which were carried out in duplicates. A similar trend to Figures 4-15 and 4-16 is observed in Table 4-5. Other values of τ values obtained under different experimental conditions are shown in Appendix A.

**Table 4-5 : Comparison of retention time for different frothers.**

| Frother type | τ (sec) | Percentage error (%) |
|---|---|---|
| Pentanol | 10.3 | 11.2 |
| Hexanol | 14.4 | 10.1 |
| MIBC | 26.7 | 6.51 |
| PPG192 | 5.19 | 7.40 |
| PPG425 | 12.8 | 5.32 |
| PPG725 | 8.48 | 1.07 |

Using the growth rate experimental data, the foam stability factors ($\Sigma$) associated with the use of the different frother types were determined as shown in Figure 4-17. It is evident that PPG425 gave the greatest foam stability factor in comparison to PPG192 and PPG725. With regards to the alcohol frothers it is shown that use of MIBC and pentanol resulted in foams of the highest and least foam stability factor respectively. Although the use of both polyglycols and alcohols resulted in relatively similar values, it should be noted that the frothers were added on a mass basis. This resulted in a far larger molar concentration of the

alcohols than the polyglycols and highlighted the fact that alcohols are much weaker frothers.

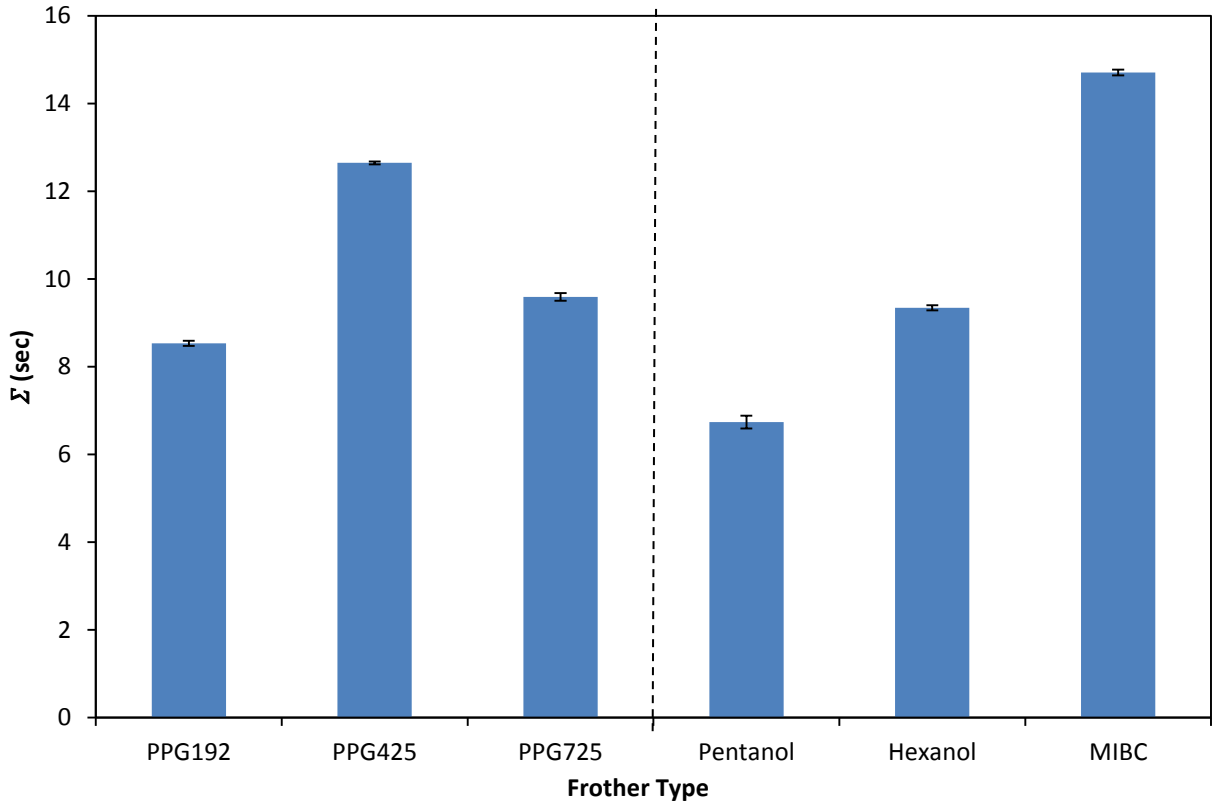


**Figure 4-17: Comparison of foam stability factor values obtained on use of polyglycol and alcohol frothers at a dosage of 500 ppm**

A more accurate comparative method between the different frother types taking into account the number of moles of the frothers is a parameter termed the partial molar foam stability factor ($\overline{\sum}$) as shown in Figure 4-18. In this figure, the foam stability factor was normalised with respect to the number of moles of frother present. With respect to alcohol frothers it is shown that MIBC and pentanol had the highest and least values respectively. The figure shows that as the polyglycol frother molecular weight increases, the $\overline{\sum}$ values increase. It is evident that use of polyglycol frothers results in much higher $\overline{\sum}$ values compared to the use of alcohol frothers.

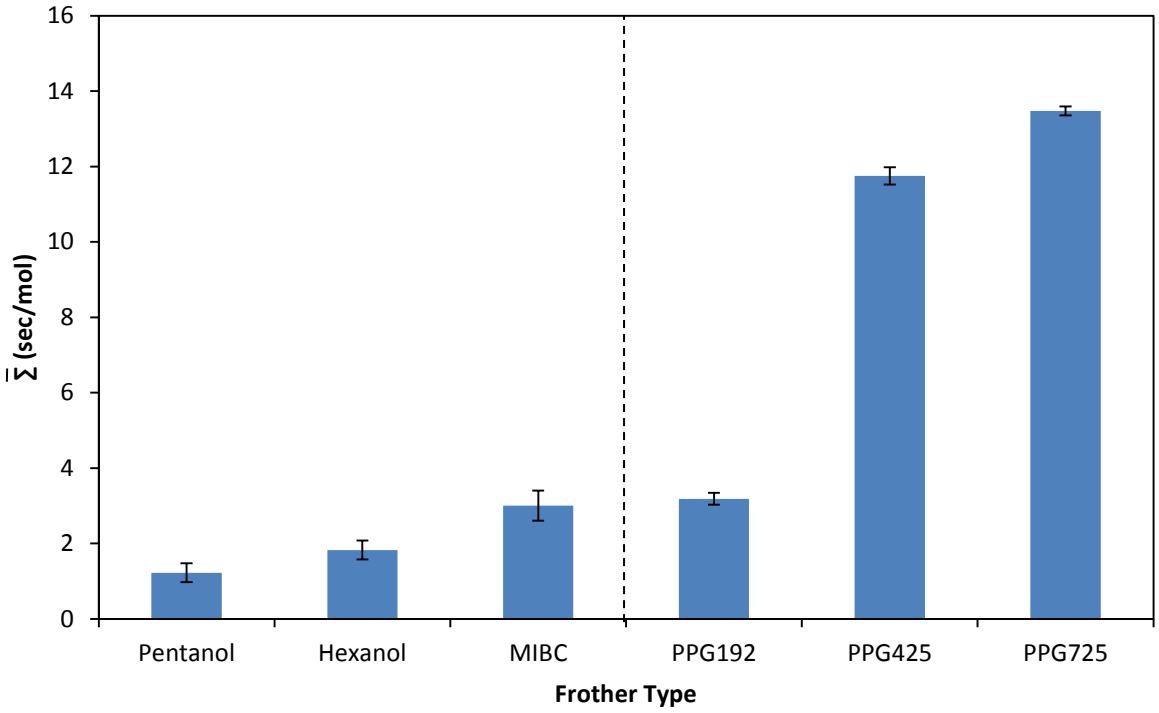


**Figure 4-18: Comparison of $\bar{\sum}$ values on use of alcohol and polyglycol frothers.**

On tests carried out investigating the effect frother dual blends, an example of results obtained is shown in Figure 4-19 with all tests carried out at a similar total frother mass concentration (500 ppm). The ratio of the polyglycol and alcohol frothers in the dual component blends was 4:1. Figure 4-19 shows that the dual component frothers gave rise to a foam of greater height in comparison to single component frothers.

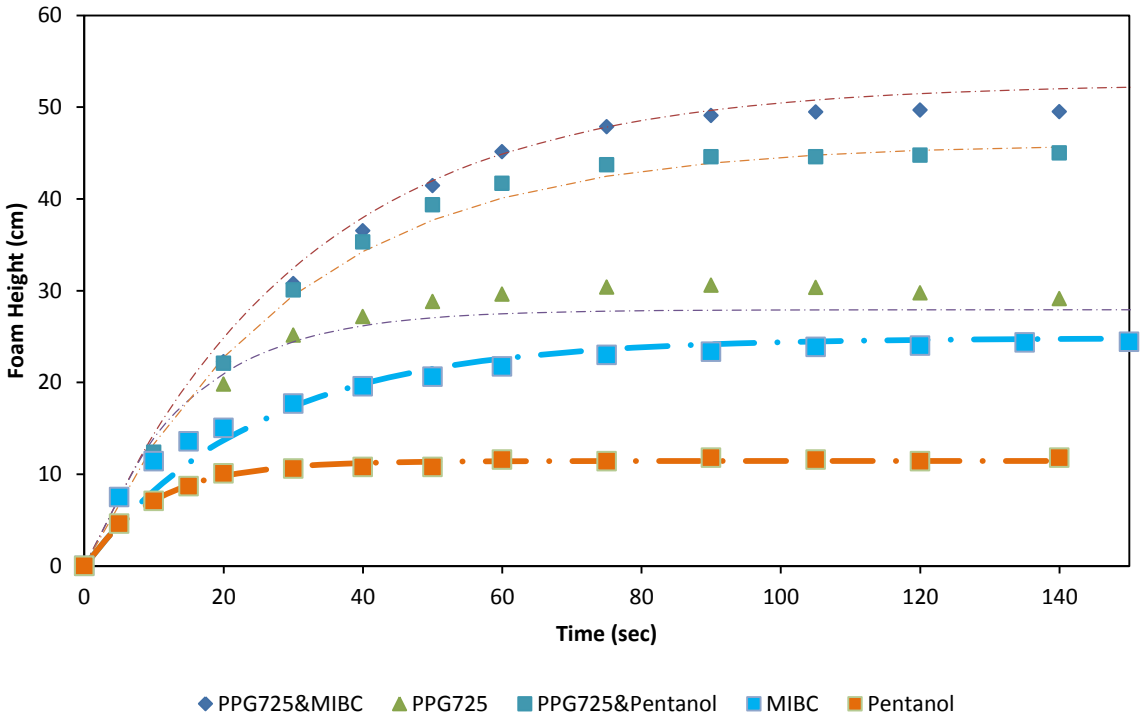


**Figure 4-19: Comparison of the effect of single and dual component frothers on foam growth rate curve.**

Comparison of the use of frother single and dual component blends using $\bar{\Sigma}$ as an indicator of the stability of the foam results observed are shown in Figure 4-20. The figure shows the dual component frother blends having a distinctly higher foam stability factor compared to the single component frothers. However, the pentanol and MIBC blends illustrate similar foam stability factor.

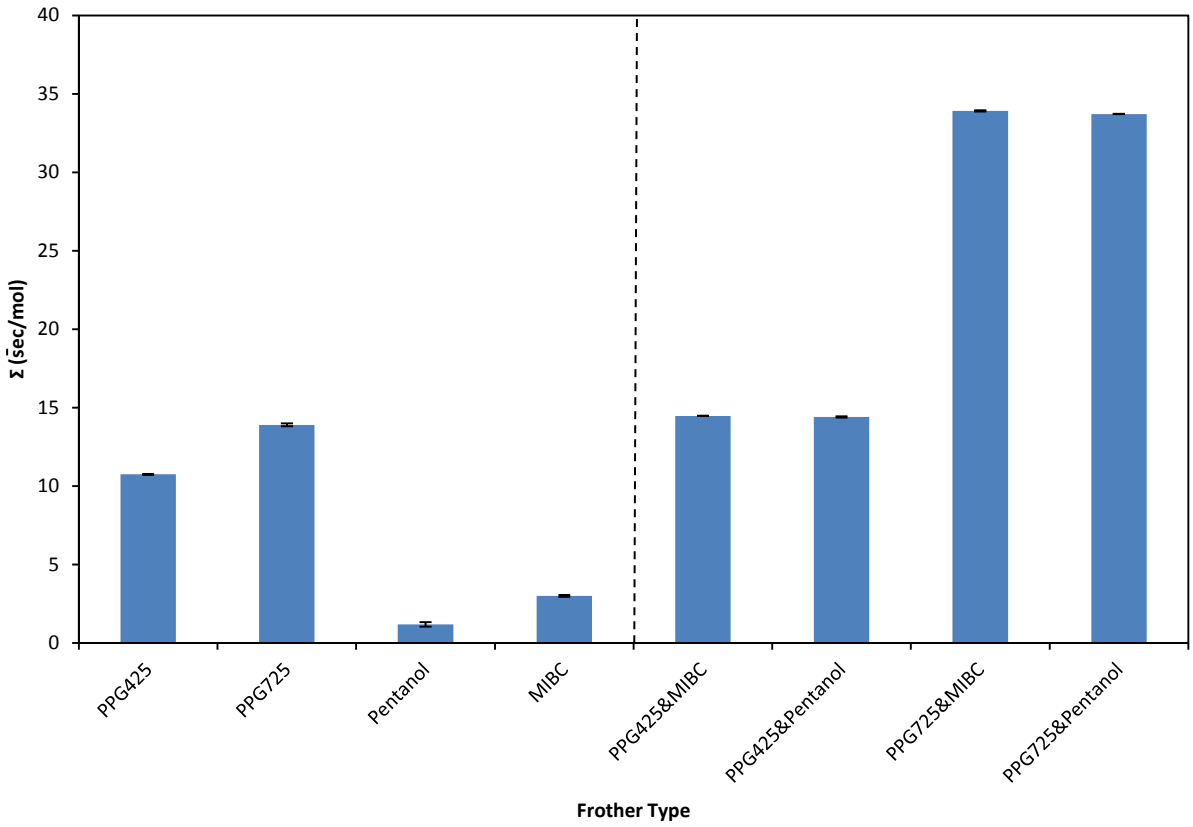


**Figure 4-20: Illustration of the effect of dual and single component frothers on foam stability factor.**

# Three Phase Results

## 4.4. Froth stability

To investigate the effect of frother type on the stability of a three-phase froth comprising UG2 ore, froth growth rate tests were measured at experimental conditions described in the preceding chapter. Results from the Bikerman's tests carried out on alcohol frothers on UG2 ore are shown in Figure 4-21. The figure shows that a positive linear correlation is observed between the froth height produced and superficial air velocity. The froth stability factor, $\Sigma$, represented by the slope of the line on use of different frother types is shown in Figure 4-21. It is shown that pentanol achieved a stability factor of 16.0 sec which was greater than the stability factor on use of hexanol ($\Sigma$= 6.95 sec) and MIBC ($\Sigma$= 8.30 sec).

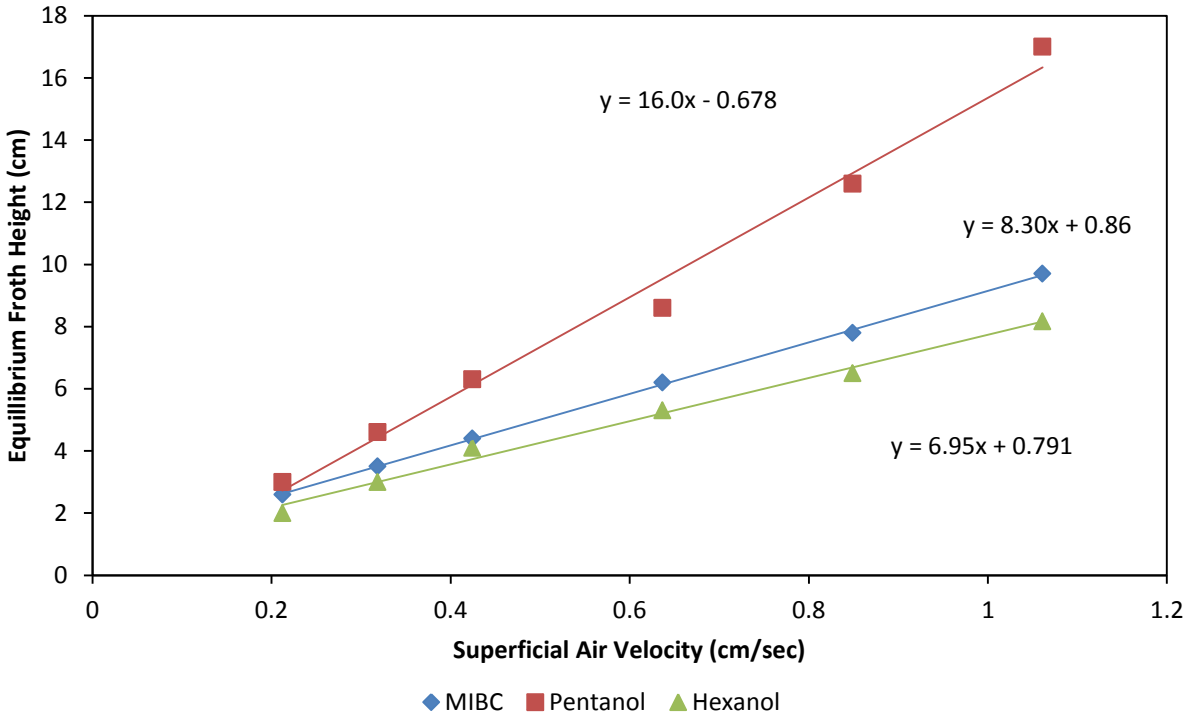


**Figure 4-21: Relationship between superficial air velocity and height of froth produced using alcohol frothers at a total molar concentration of 11.3 mM in the absence of a depressant.**

Figure 4-22 shows examples of the raw data that gave rise to Figure 4-21. Figure 4-22 shows the froth rise rate at the highest air flow rate shown in Figure 4-21, 1.06 cm/sec. As shown in Figure 4-22 pentanol achieved an equilibrium froth height of 17.1 cm which was greater than the 8.17 cm achieved when using hexanol frother and 9.7 cm on use of MIBC. Other froth growth rate curves obtained under different experimental conditions together with the τ and $H_{max}$ values obtained from fitting the Barbian model are shown in Appendix A.

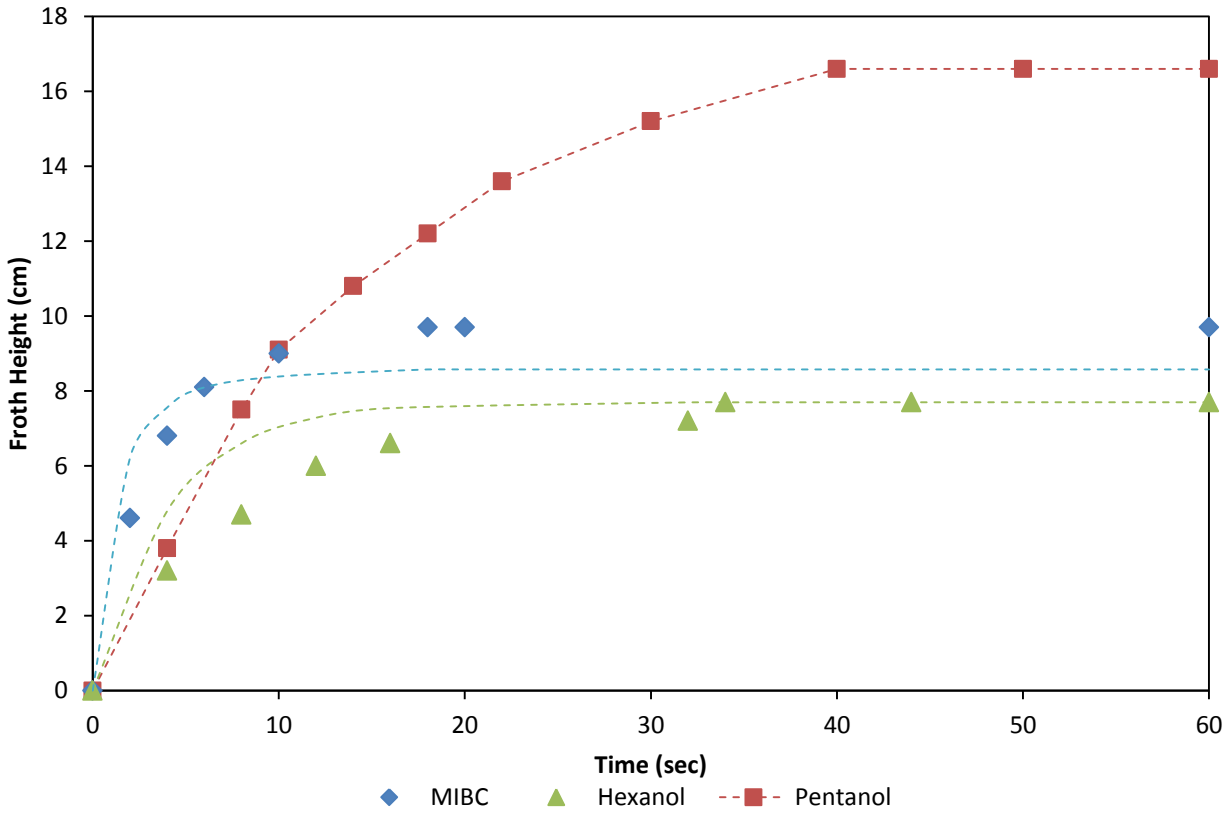


**Figure 4-22: Froth height as a function of time on use of different alcohol frothers at a total molar concentration of 11.3 mM in the absence of a depressent at Jg of 1.06 cm/s.**

Figure 4-23 shows the molar stability factor on use of alcohol frothers. It is interesting to note that the molar stability factor ranges 20 – 50 sec/mol unlike the two-phase experiments which ranged 1-3 sec/mol.

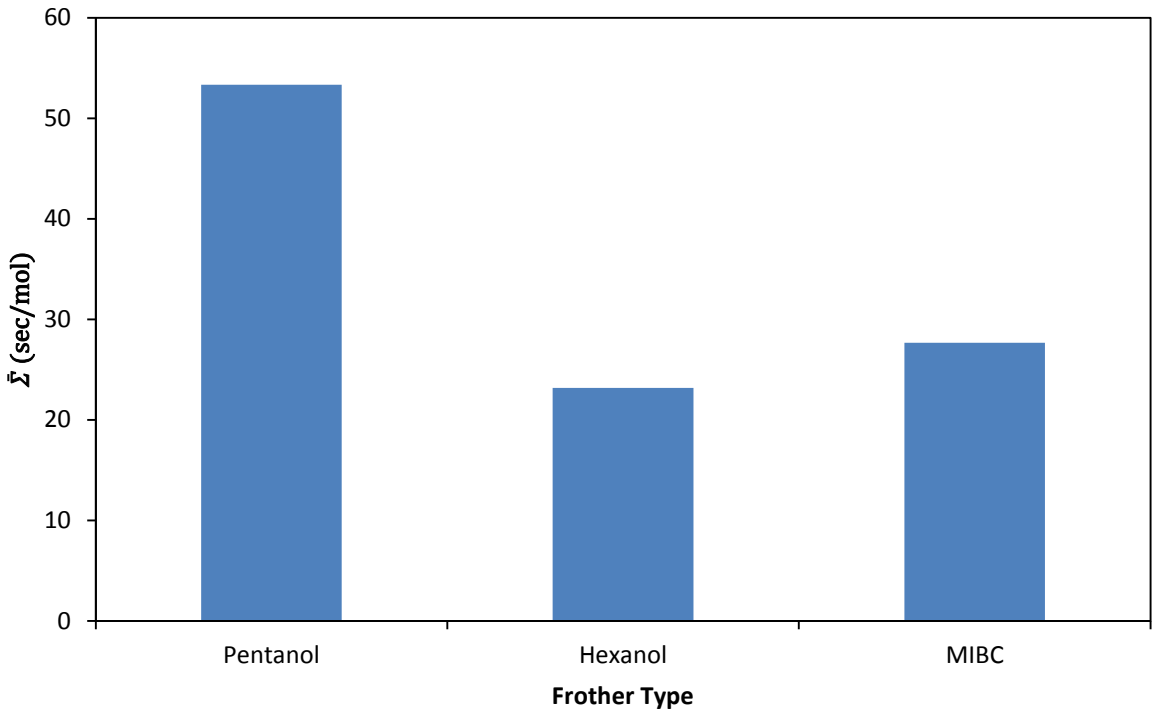


**Figure 4-23: Comparison of the molar froth stability factors on use of alcohol frothers.**

Results from similar experiments performed on polyglycol frothers are illustrated in Figure 4-24 with a summary of the fitted Barbian model parameters shown in Appendix A. Figure 4-24 demonstrates that PPG425 and PPG192 have the highest and least $\Sigma$ values respectively of 43.7 and 13.0 sec. Results focused on the use of frother blends are also shown in Figure 4-24. The use of polyglycol-MIBC frother blend resulted in higher $\Sigma$ values compared to the use of single component frothers. Other froth stability proxy measures as shown in Appendix A corroborate these findings as evidenced by the similar trend of use of dual component frothers resulting in a more stable froth in comparison to use of single component frothers.

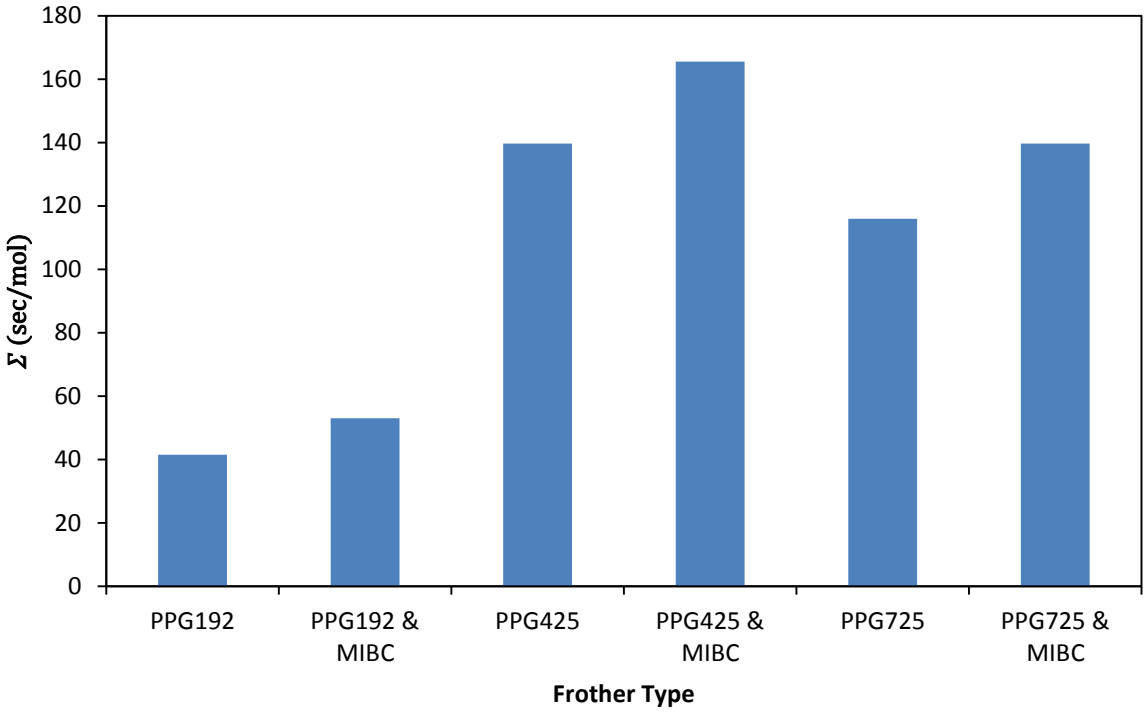


**Figure 4-24: Relationship between froth stability and frother type using polyglycol frothers at a total molar concentration of 0.314 mM in the absence of a depressant.**

## 4.5. Flotation test results

To investigate the effect of frother type on the flotation process, flotation tests were conducted using the different types of frothers. To determine the effect of frother type on froth recovery the tests were performed at different froth heights. Figures 4-25 and 4-26 illustrates the effect of frother type namely alcohol and polyglycol frothers respectively on solid and water recoveries at experimental conditions described in Chapter Three. Figure 4-25 shows that using pentanol gave the highest solids and water recoveries in comparison to the other alcohol frothers, contrary to expectations. Hexanol yielded the lowest solids and water recoveries. As expected, the solids and water recoveries decreased with an increase in froth height. Figure 4-26 illustrates that PPG425 gave the highest solids and water recoveries compared to use of PPG725 and PPG192 which gave the lower recoveries with use of PPG192 resulting in the lowest recoveries. Differences observed in solid and water recoveries on use of PPG425 and PPG725 were more pronounced at a froth height of 4 cm.

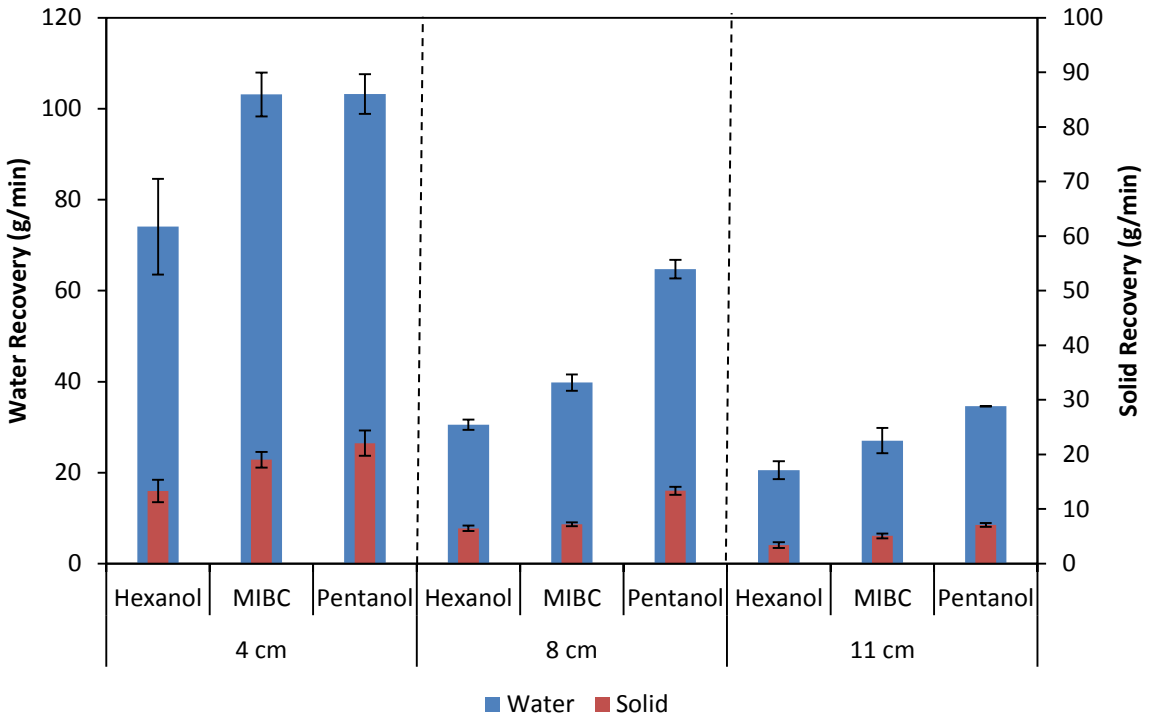


**Figure 4-25: Final solids and water recoveries from alcohol frother flotation tests at froth heights 4, 8 and 11 cm in the absence of a depressant at Jg of 1.70 cm/s and a total frother concentration of 11.3 mM.**

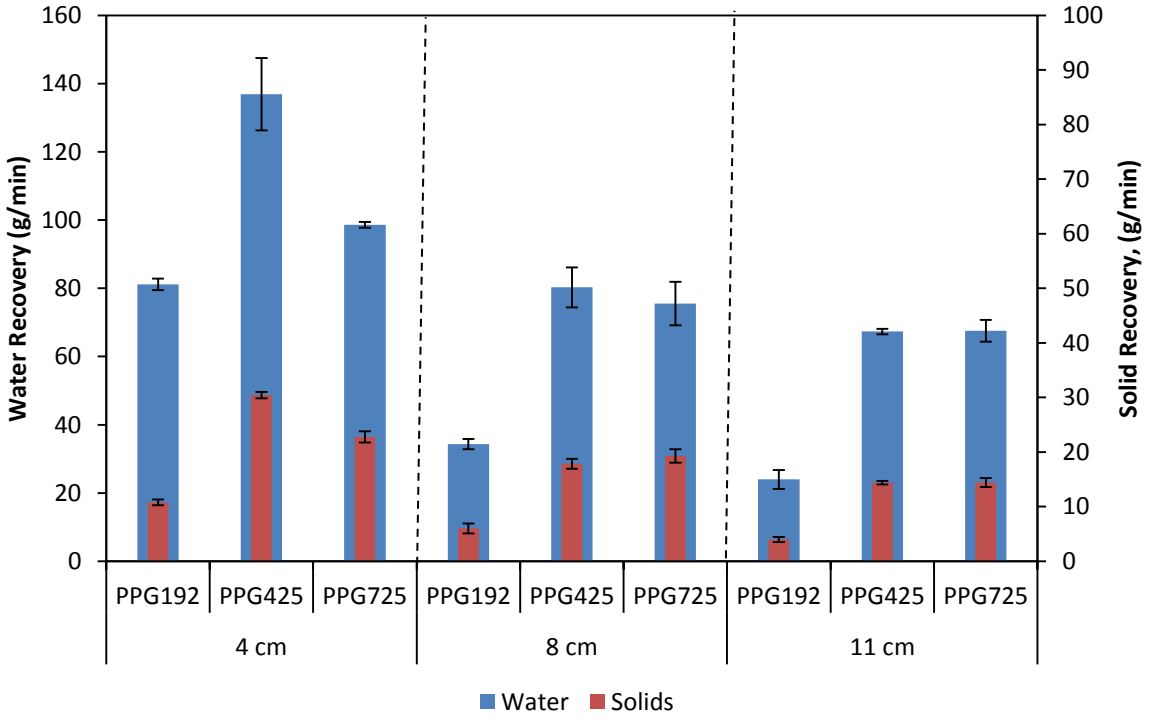


**Figure 4-26: Final solids and water recoveries from polyglycol frother flotation tests conducted at froth heights 4, 8 and 11 cm in the absence of a depressant at Jg of 1.70 cm/s and a total frother concentration of 0.314 mM.**

### 4.5.1. Effect of frother blends on flotation performance

For reasons mentioned in the preceding chapter flotation tests were carried out on the use of polyglycol-MIBC frother blends. A comparison of the solid and water recoveries on use of the same total molar concentration of single and polyglycol-MIBC dual component frothers can be conducted from observations reported in Figures 4-25 to 4-27. The comparison shows that the amount of solids and water recovered from tests using PPG192 alone and as a blend were virtually similar. However, it was interesting to note that the use of polyglycol-MIBC dual frother blends for PPG425 and PPG725 results in higher recoveries of both solid and water than on use of single component frothers. As it well established that water recovery is related to froth stability (Melo & Laskowski, 2007; Wiese et al., 2011; Araya et al., 2011) the results show that with the exception of PPG192 use of blends of PPG425 and PPG725 resulted in a more stable froth phase.

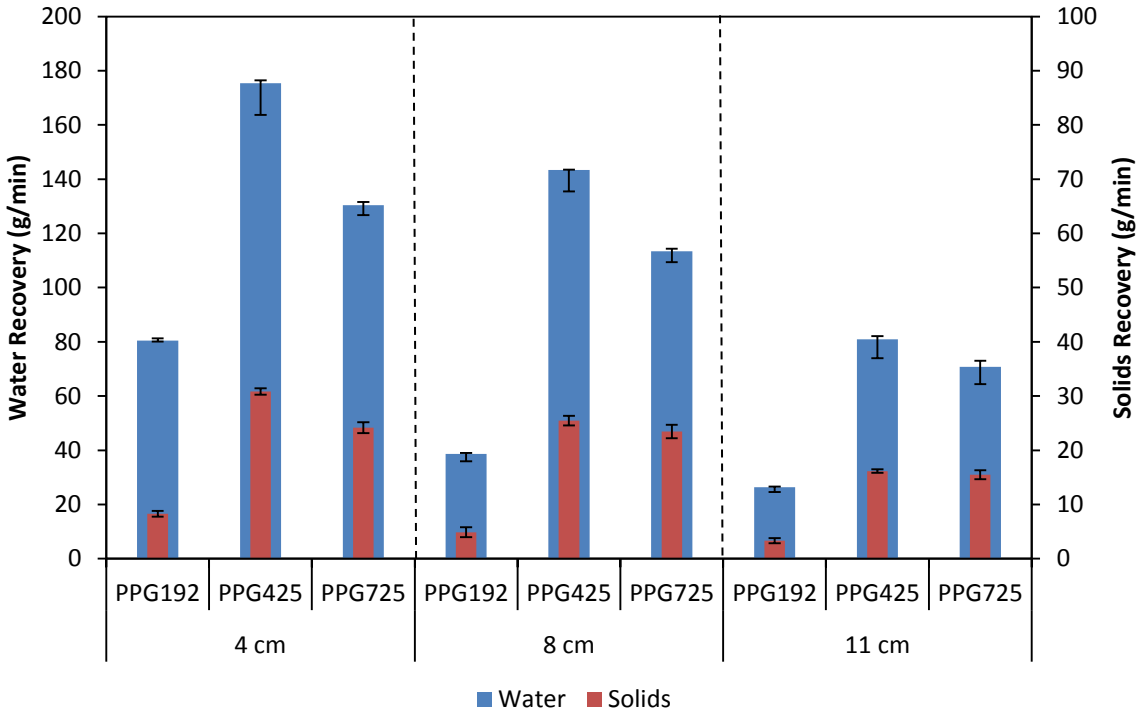


**Figure 4-27: Solids and water recoveries for polyglycol-MIBC blends (4:1) at different froth heights and total frother concentration of 0.314 mM.**

### 4.5.2. Analysis of flotation performance

The concentrate and tailings samples collected were analysed for PGM and chromite content. The results obtained were used to determine the recovery and grade of valuable minerals allowing for further investigations into other parameters such as froth recovery and degree of entrainment.

### 4.5.3. Effect of frother type on froth recovery

Using the technique proposed by Feteris et al (1987) flotation tests were carried at different froth heights to determine the froth recovery. Froth recovery was determined as a ratio of flotation rate constant to the collection zone rate constant (Equation 2-11), with the

collection zone rate constant determined by extrapolating the linear flotation rate constant – froth height relationship to zero froth height. The linear relationship shown in Figure 4-28 shows that use of PPG425 resulted in a higher flotation rate constant at 8 cm and 11 cm froth height compared to use of PPG192 and PPG725. PPG192 had the lowest rate constants.

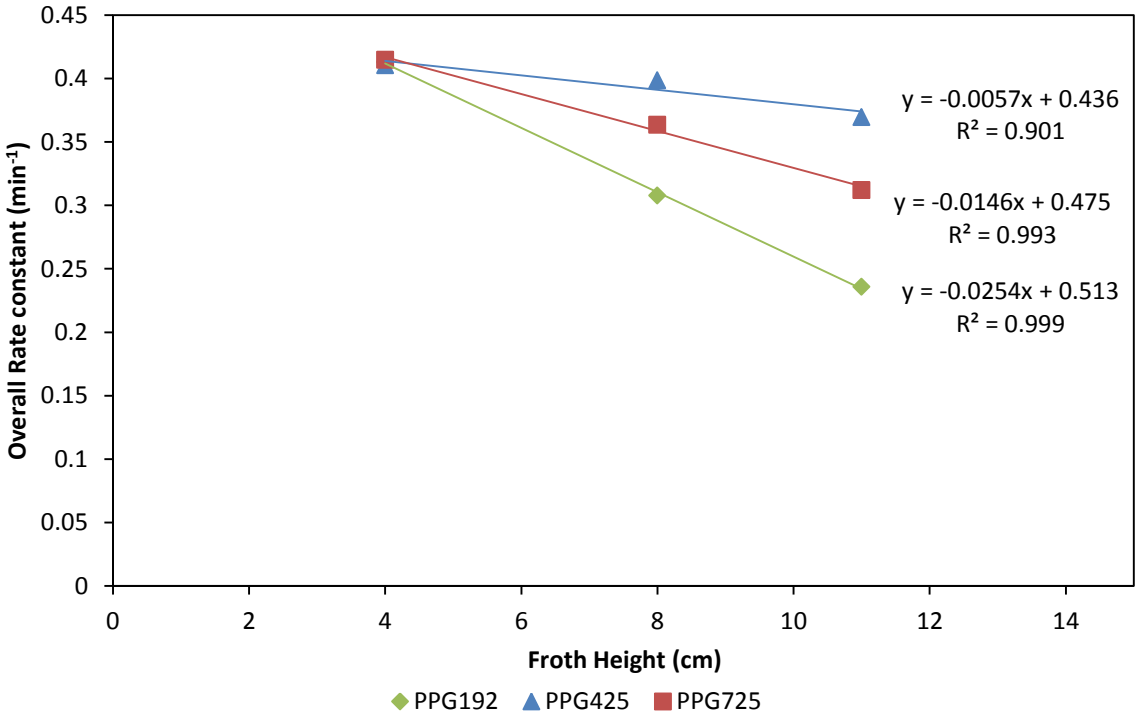


**Figure 4-28: Flotation rate constant as a function of polyglycol frother type and froth height at a frother molar concentration of 0.314 mM in the absence of a depressant and at a Jg of 1.70 cm/sec.**

Analysis of the flotation rate constant – froth height relationship of the alcohol frother types yielded the results shown in Figure 4-29. The figure shows use of pentanol resulting in the greatest flotation rate constant at all froth heights, followed by MIBC and hexanol.

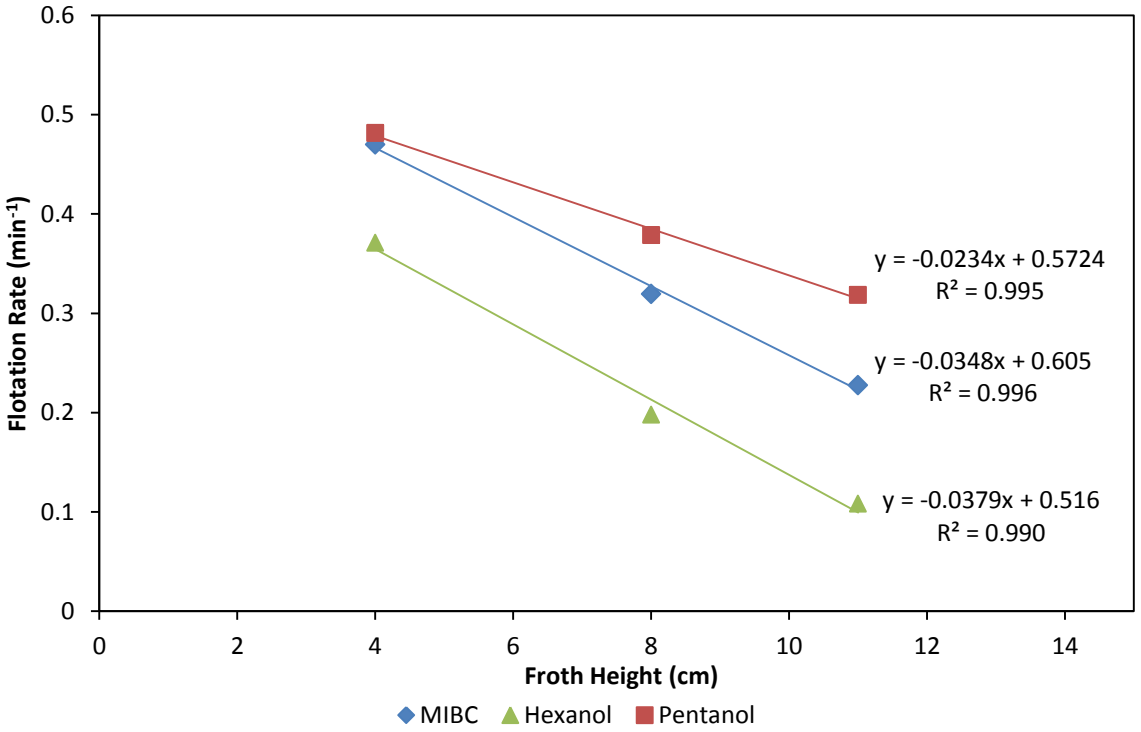


**Figure 4-29: Flotation rate constant as a function of alcohol frother type and froth height.**

The effect of frother type on froth recovery for the tests conducted is shown in Figures 4-30 and 4-31.The figures show that for any frother type as the froth height increases the froth recovery decreases and differences between the different frothers become more pronounced. For the polyglycol frothers, froth recovery increases with frother molecular weight to a maximum beyond which froth recovery decreases with increased frother molecule weight. Figure 4-31 illustrates that pentanol gave the highest froth recovery followed by MIBC and hexanol giving the least froth recovery. Although it was unexpected that pentanol yielded the highest froth recovery, this trend was similar to that observed for the solids and water recovery and the froth stability tests, which were performed in a different device. The froth recovery trend correlates to the froth stability trend.

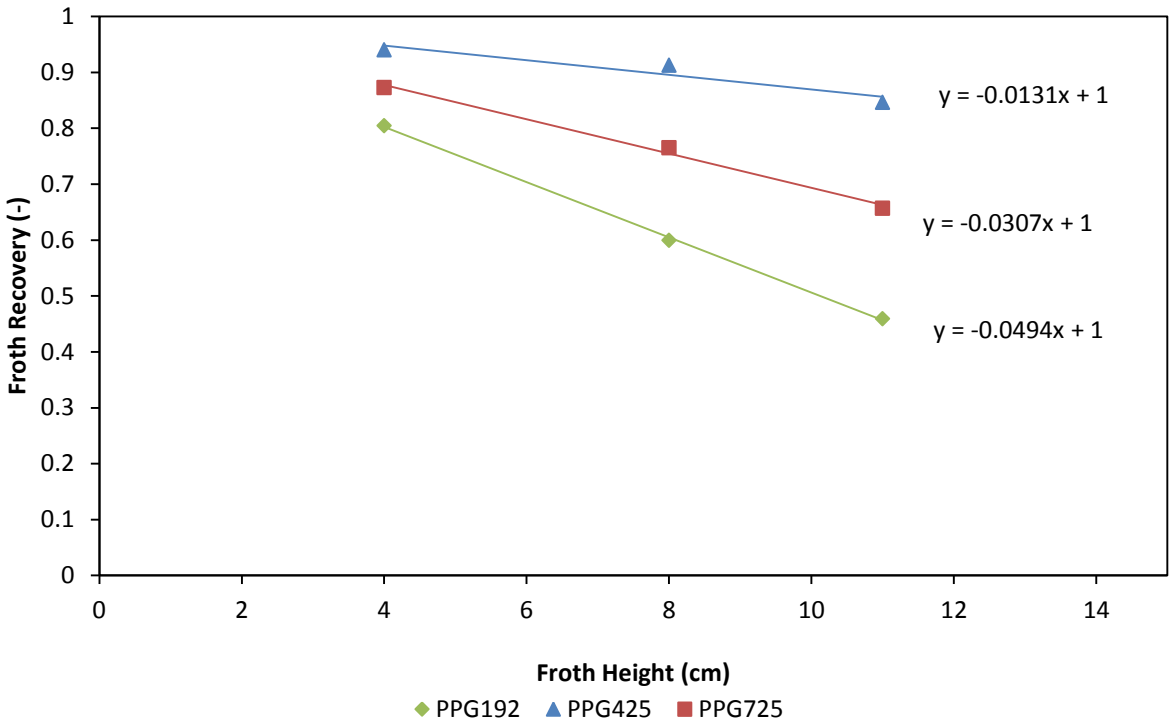


**Figure 4-30: Effect of polyglycol frother type on froth recovery.**

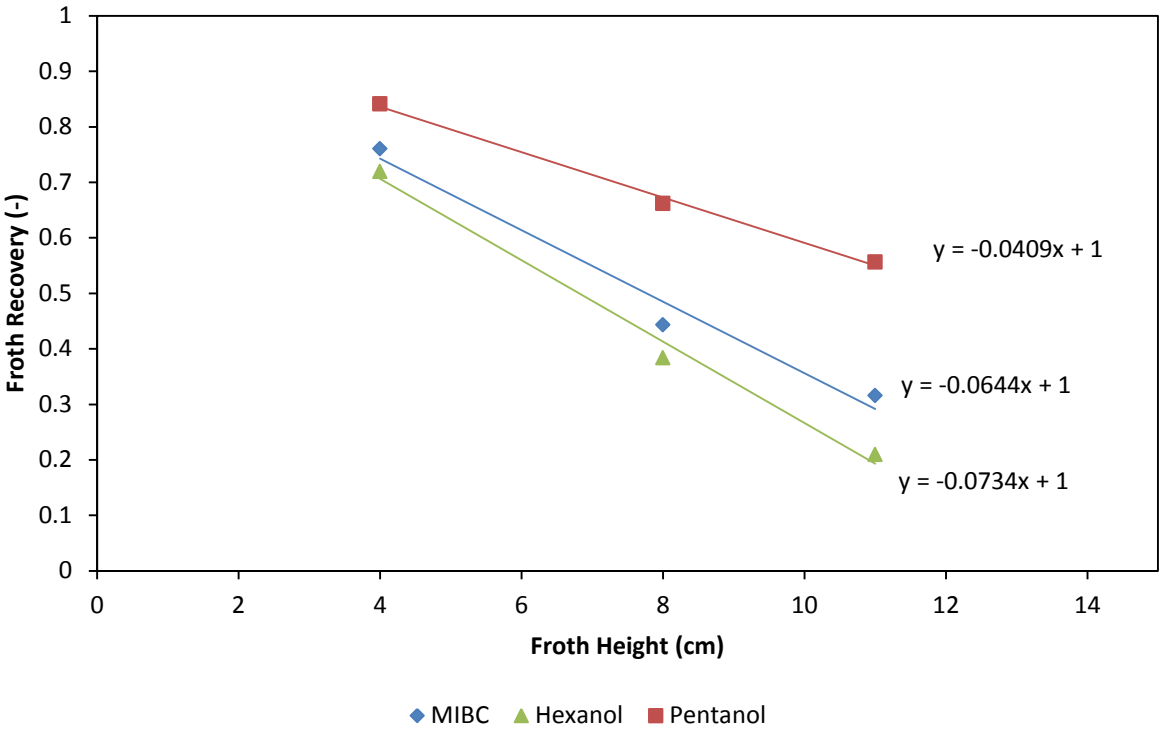


**Figure 4-31: Effect of alcohol frother type on froth recovery.**

Analysis of the effect of use of frother blends on froth recovery yielded results shown in Figures 4-30 to 4-34. With regards to use of PPG192 use of frother blends resulted in a low froth recoveries in comparison to the use of pure PPG192. Use of PPG425 blends generally showed a higher froth

recovery than the use of pure PPG425. These trends follow a similar trend that was observed on the effect of frother blends on froth stability.

.

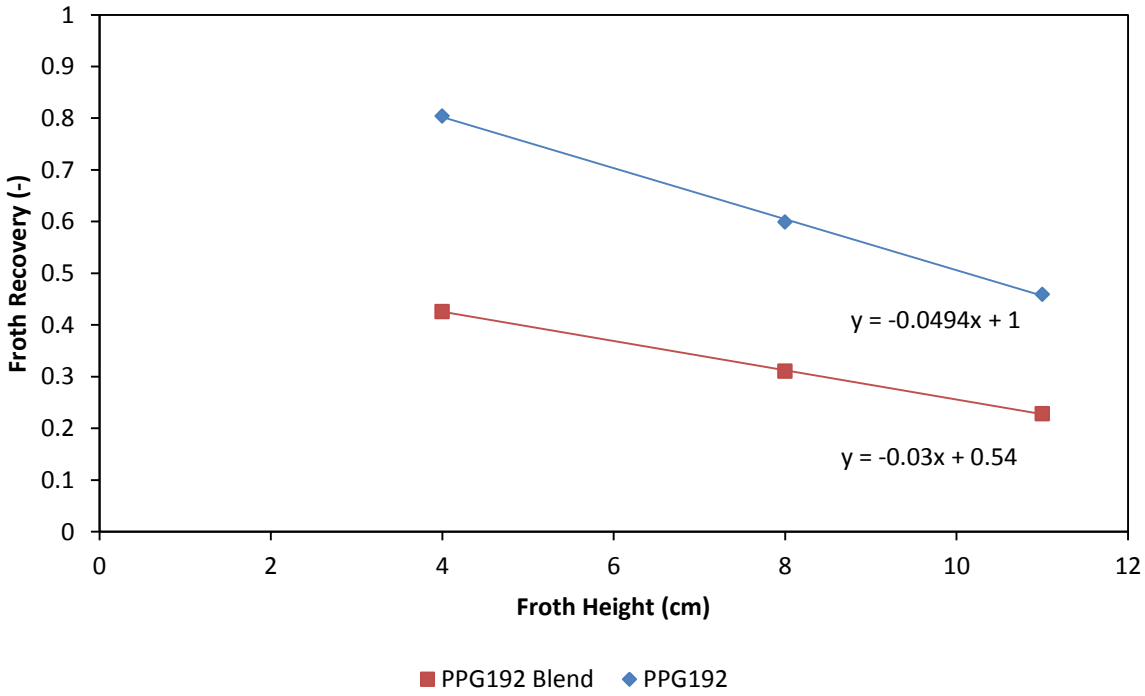


**Figure 4-32: Comparison of the use PPG192-MIBC frother mixture and pure PPG192 on froth recovery.**

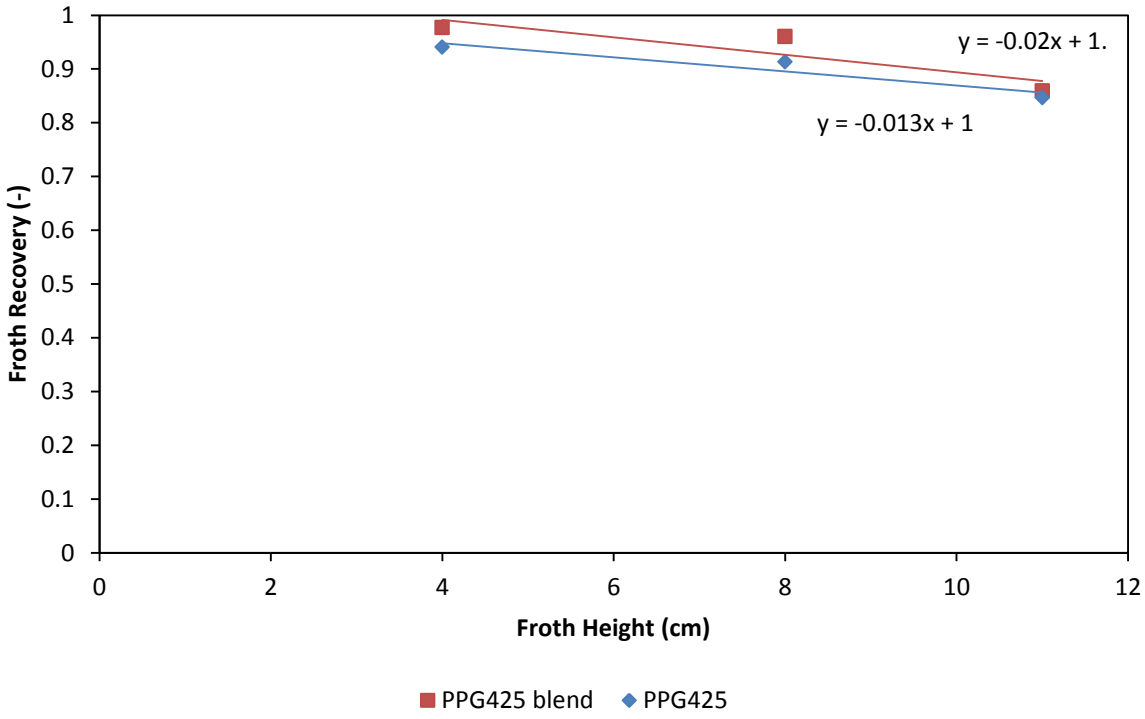


**Figure 4-33: Comparison of the use PPG425-MIBC frother mixture and pure PPG425 on froth recovery.**

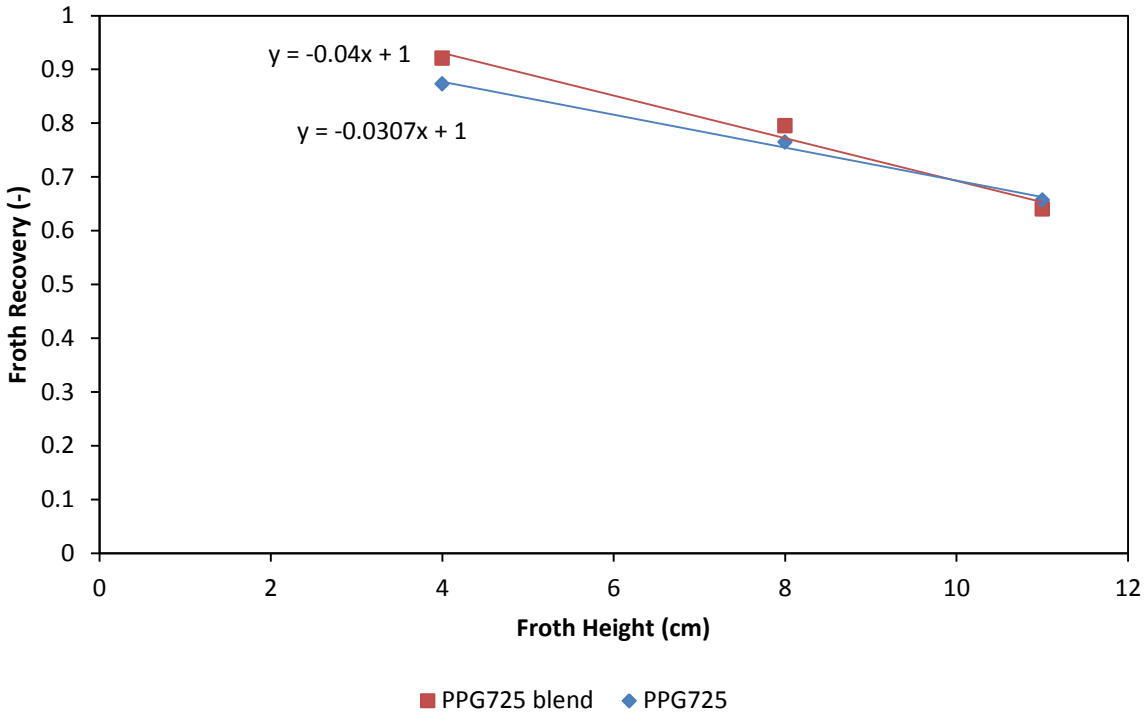


**Figure 4-34: Comparison of the use PP725-MIBC frother mixture and pure PPG725 on froth recovery.**

The froth recovery of the individual metals that made up the PGM assays were also determined on use of frother blends as shown by Figures 4-35 to 4-37. Generally the results show the highest froth recovery was for the metals palladium and platinum with the latter being slightly lower.

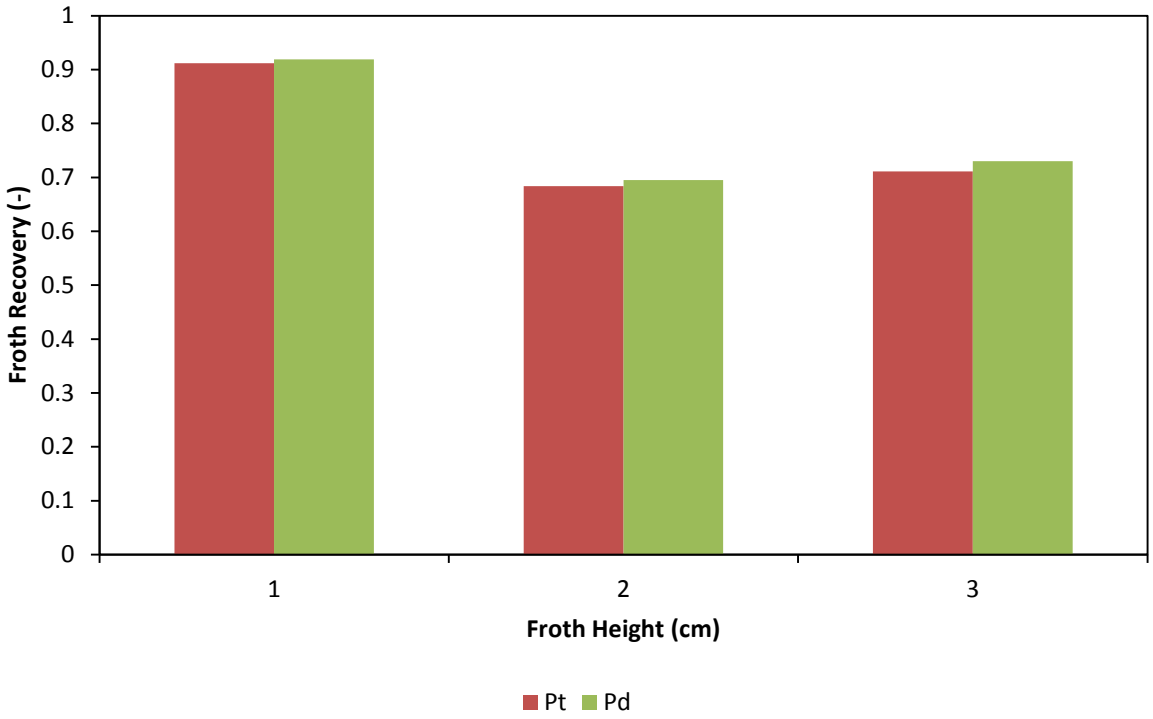


**Figure 4-35: Comparison of the froth recovery of the different PGM elements on use of PPG192-MIBC frother mixture.**

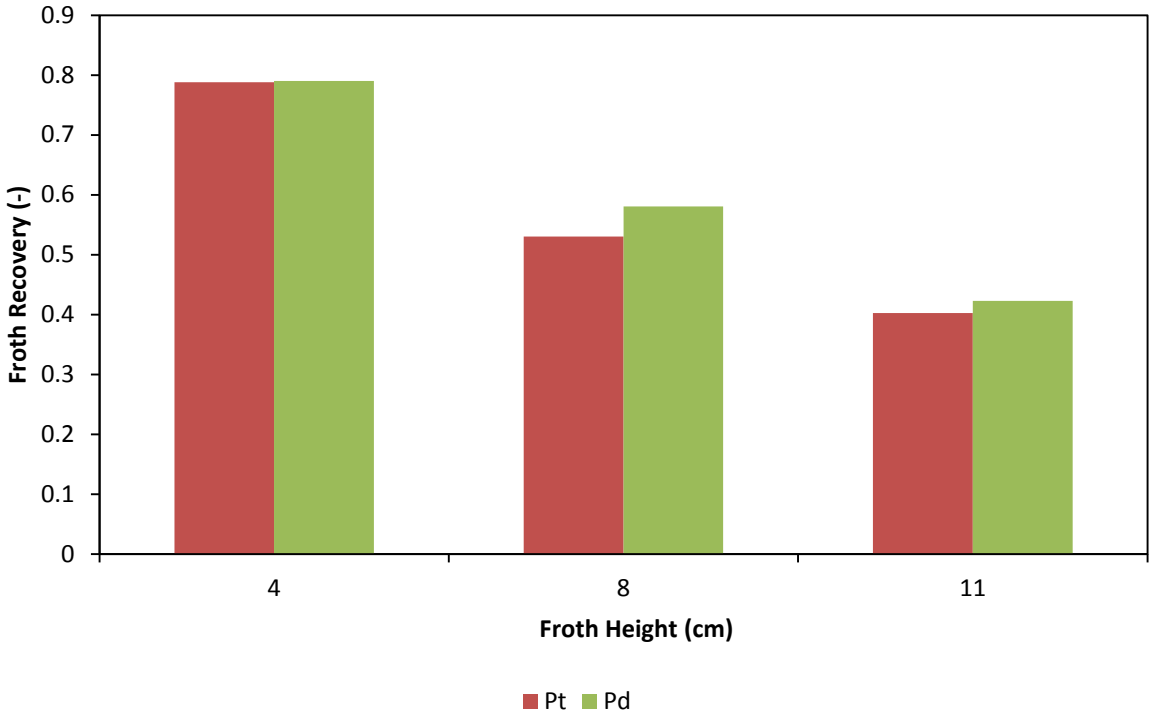


**Figure 4-36: Comparison of the froth recovery of the different PGM elements on use of PPG425-MIBC frother mixture.**

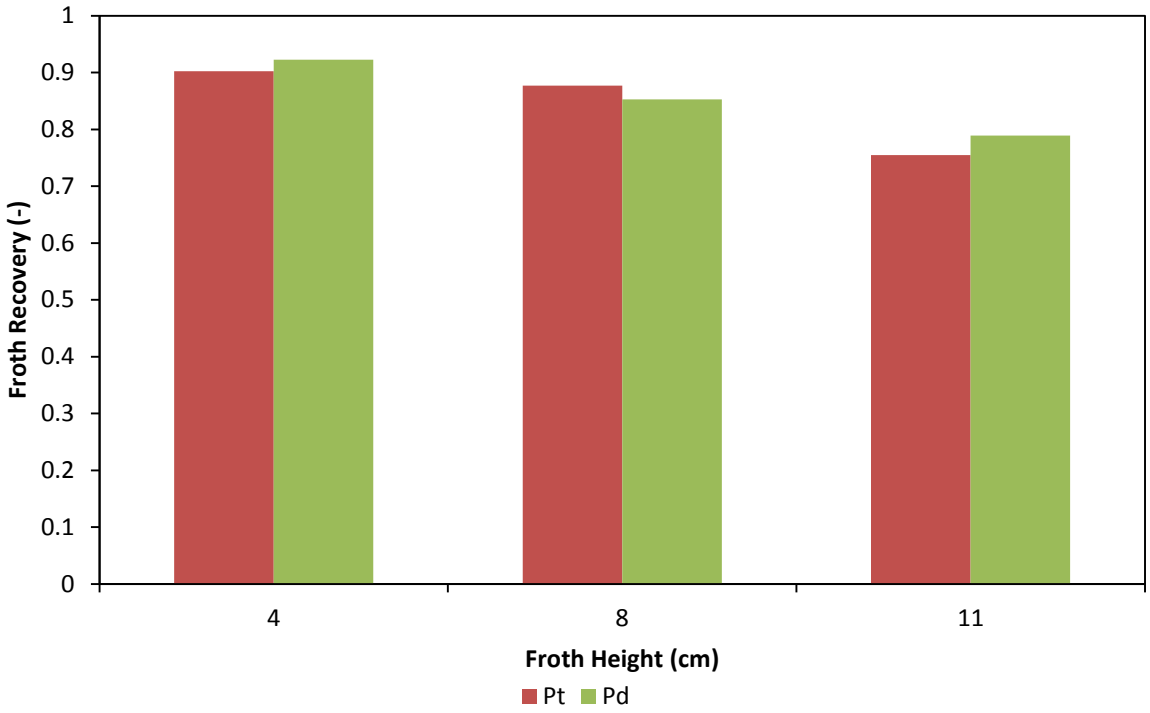


**Figure 4-37: Comparison of the froth recovery of the different PGM elements on use of PPG725-MIBC frother mixture.**

### 4.5.4. Effect of frother type on overall recovery and grade

Overall recovery is a function of froth recovery and Figures 4-38 to 4-41 show the effect of frother type on the PGM overall recovery and grade. At froth height of 4 cm there is very little difference in the overall recovery of PGMs, but at increasing froth heights it is evident that PPG425 gave a higher overall recovery and PPG192 gave the least recovery. This is expected, since differences in pulp zone recoveries for different frothers are expected to be minimal. The differences will be reflected by losses in the froth zone.

In general, the PGM recoveries were relatively lower than one would expect in a mechanical batch flotation device. This illustrates that the lower energy in the bench-scale column device was less efficient at generating bubble-particle collisions of the small grain-size PGM's. Evident from Figures 4-38 to 4-40 is that PPG425-MIBC and PPG725-MIBC mixtures resulted in higher recoveries. This trend is similar to the trend observed on investigating the effect of using the frother mixtures on froth stability.

Also shown in Figure 4-38 to 4-40 is that though use of the pure polyglycols resulted in fairly similar overall PGM recoveries the use of PPG192 resulted in a very high PGM grade compared to other frothers. PGM grades on use of PPG425 and PPG725 were not very different with use of the latter generally resulting in a slightly lower PGM grade. More interestingly was the observation that the use of PPG-MIBC blends consistently resulted in a higher PGM grade accompanying the high recoveries noted earlier.

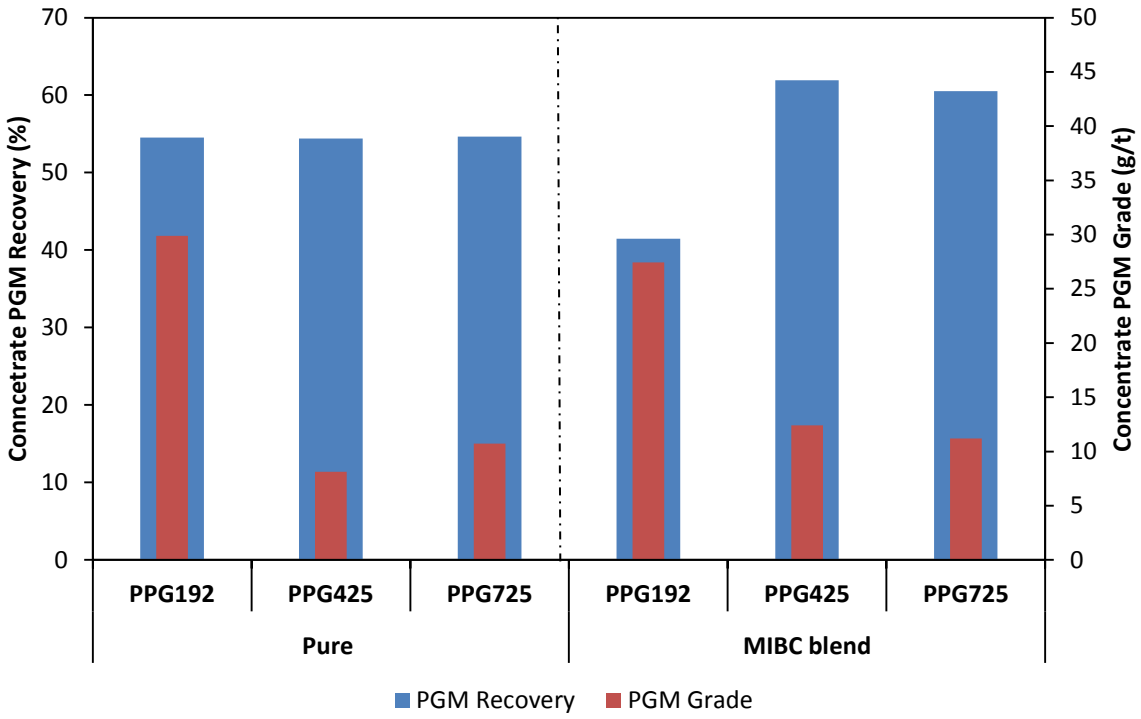


**Figure 4-38: PGM recoveries for flotation tests performed using polyglycol frothers at a froth height of 4 cm.**

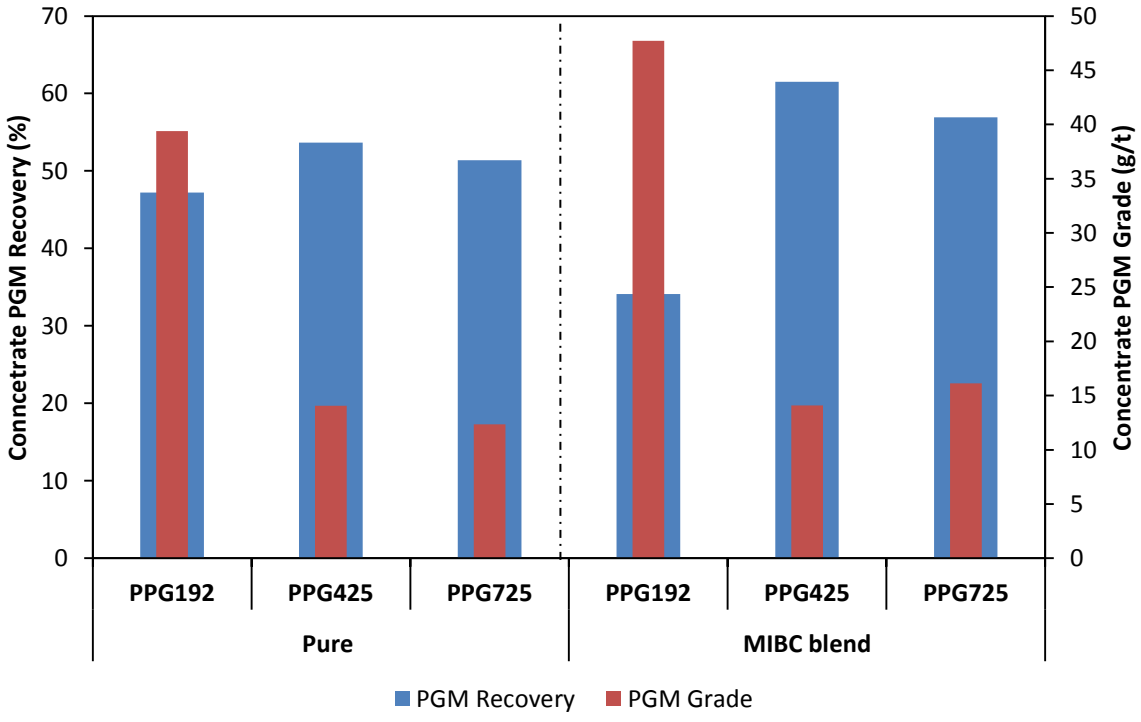


**Figure 4-39: PGM recoveries for flotation tests performed using polyglycol frothers at a froth height of 8 cm.**

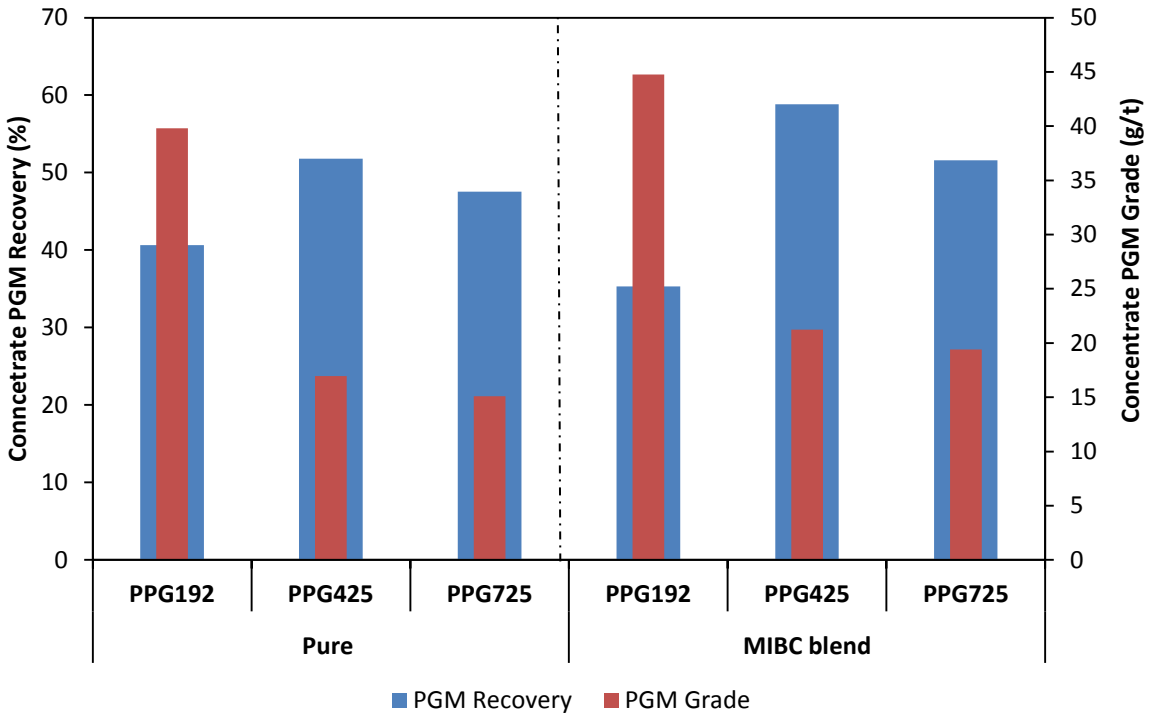


**Figure 4-40: PGM recoveries for flotation tests performed using polyglycol frothers at a froth height of 11cm.**

An analysis of alcohol frothers yielded results shown in Figure 4-41. Pentanol gave the highest overall recovery with use of hexanol resulting in the least overall recovery for the series of alcohol frothers. As expected an inverse relationship exists with the use of pentanol resulting in the least PGM concentrate grade and a high PGM grade on use of hexanol.

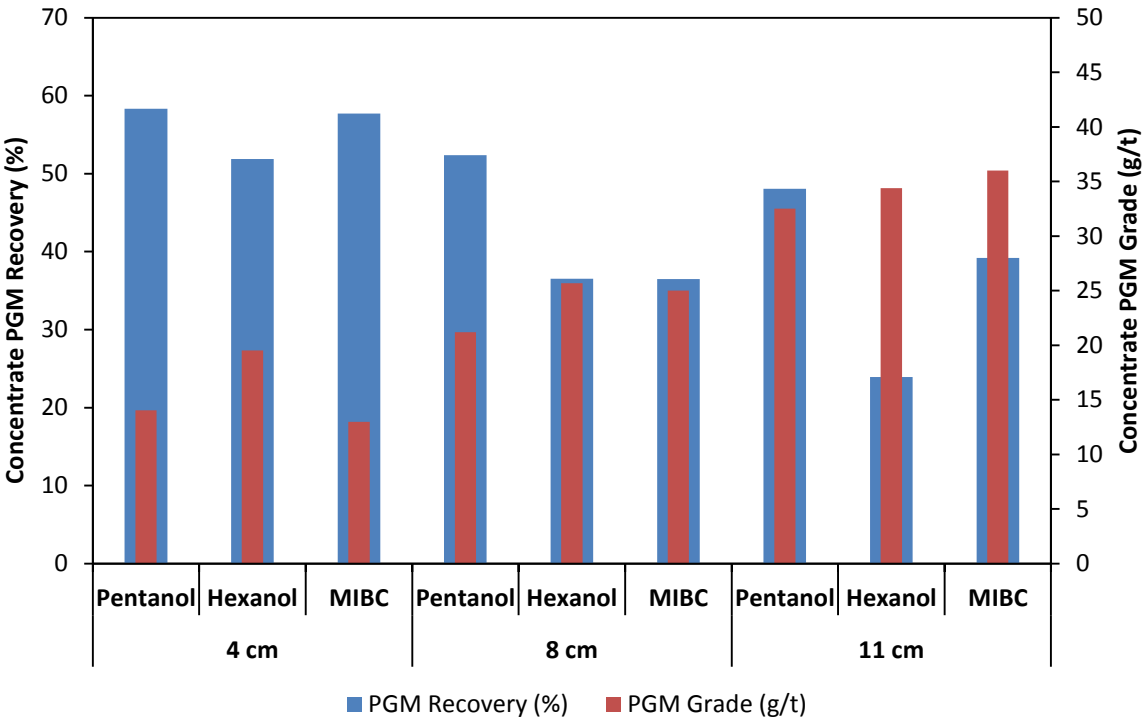


**Figure 4-41: PGM recoveries for flotation tests performed using alcohol frothers at froth heights of 8 and 11 cm.**

Figures 4-42 and 4-43 show the particle size distribution of the concentrate samples as a function of frother type and froth height. For any given frother type the concentrate particle size decreases as the froth height increases. The particle size distribution trend followed the froth stability trend.

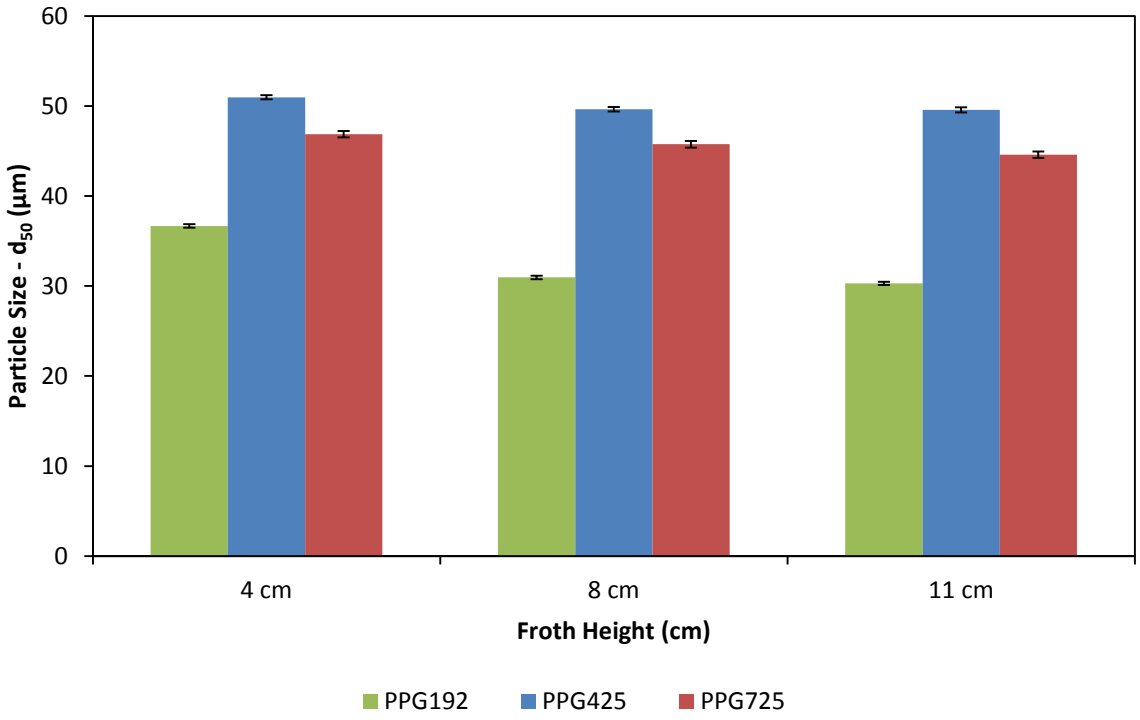


**Figure 4-42: Concentrate $D_{50}$ sizes for tests performed using polyglycol frothers at a frother dosage of 0.314 mM at froth heights of 4, 8 and 11 cm at Jg of 1.70 cm/s.**

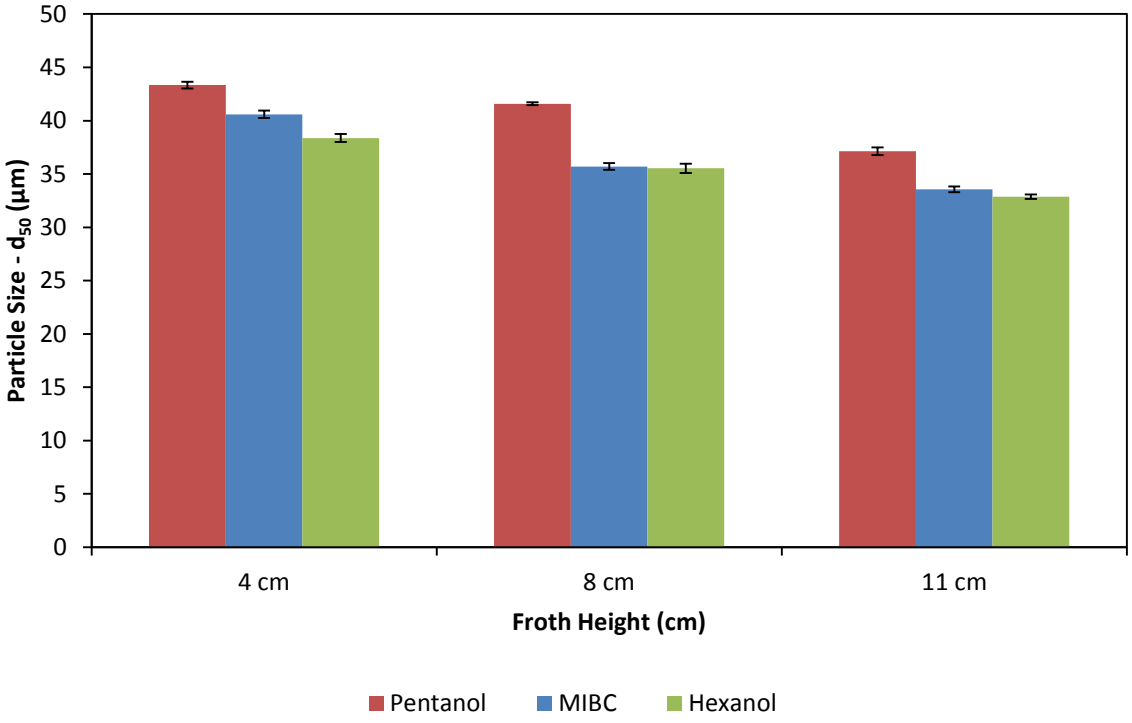


**Figure 4-43: Concentrate $D_{50}$ sizes for tests performed using alcohol frothers at a frother dosage of 11.3 mM at froth heights of 4, 8 and 11 cm at Jg of 1.70 cm/s.**

### 4.5.5. Effect of frother type on entrainment

The amounts of chromite recovered in the concentrate per unit of water recovered are an indication of the degree of entrainment since chromite is hydrophilic and has been shown not to report to the concentrate by true flotation. The amount of total chromite recovered as a function of water recovered on use of alcohol and polyglycol frothers are compared in Figures 4-44 and 4-45 respectively. The gradient of the lines is equivalent to the entrainment factor defined as the amount of entrained material recovered in the concentrate per unit water recovered. There was no attempt to force the lines through the zero intercept since it was shown by Engelbrecht and Woodburn (1975) and Neethling and Cilliers (2002) that this is only true for very fine particles, but that as particle size increases, so the intercept becomes more positive on the x-axis. The only case in which the line was forced through the origin was in the case of the PPG725 blend where there was some scatter in the data and leaving the data untouched resulted in a positive intercept on the y-axis.

Entrainment factor values obtained for the polyglycol and alcohol frother series are shown in Tables 4-6. For the polyglycol series, more chromite was recovered by entrainment during the use of pentanol (4.6 g per 100 ml water) than on use of hexanol (2.7 g per 100 ml water) which gave the least degree of entrainment. For the alcohol series, use of PPG725 resulted in the highest recovery of chromite (40.8 g per 100 ml water) and use of PPG192 resulted in the least chromite recovery (16.3 g per 100 ml water).

Investigations on the effect of frother blends on flotation performance carried out yielded results summarised in Figure 4-45 and Table 4-6. The results showed that, with the exception of PPG192, use of frother blends resulted in a reduced degree of entrainment compared to the single frothers. The use of PPG 425 and PPG725 blends resulted in a 34.7 % and 20.5 % decrease in the entrainability factor compared to the use of pure PPG425 and PPG725, respectively.

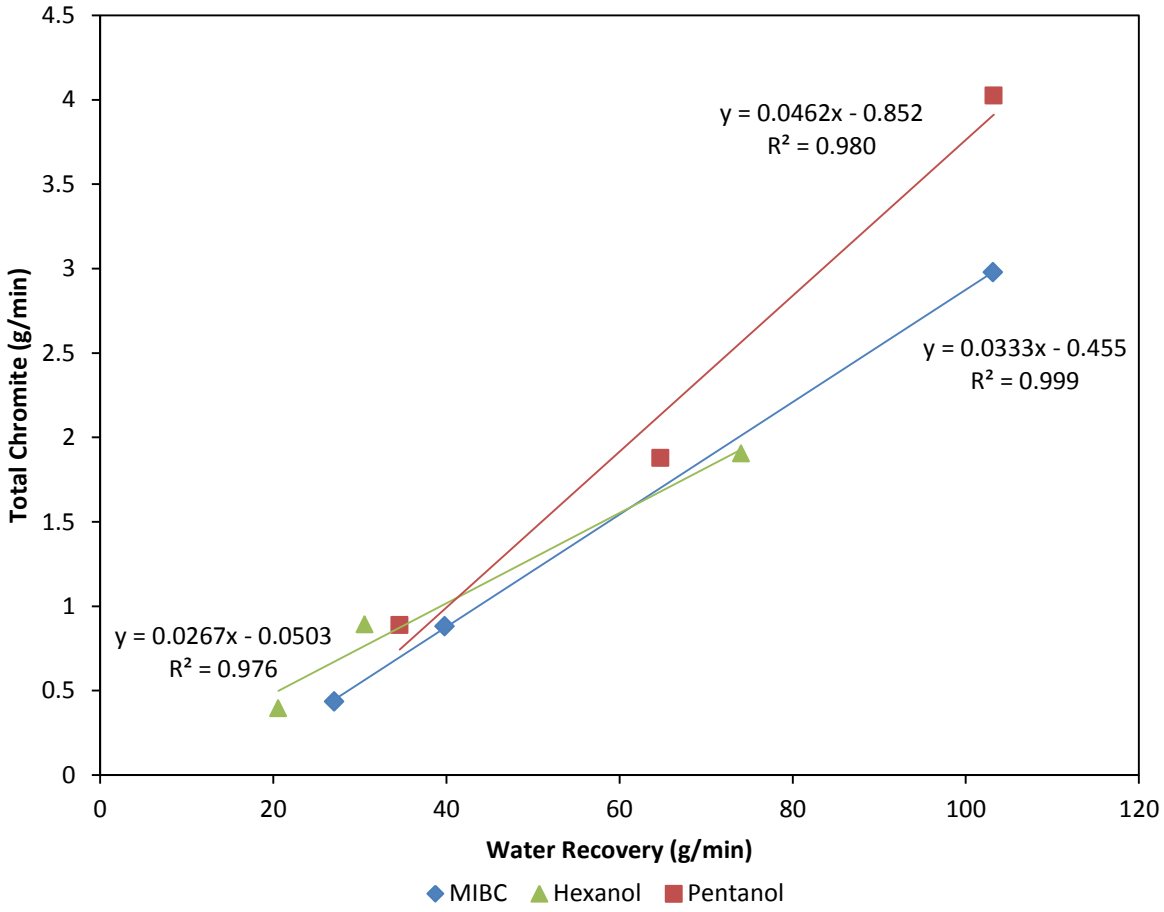


**Figure 4-44: Total chromite recovered in concentrate as a function of water recovered on use of alcohol frothers at a dosage of 11.3 mM with no depressant present.**

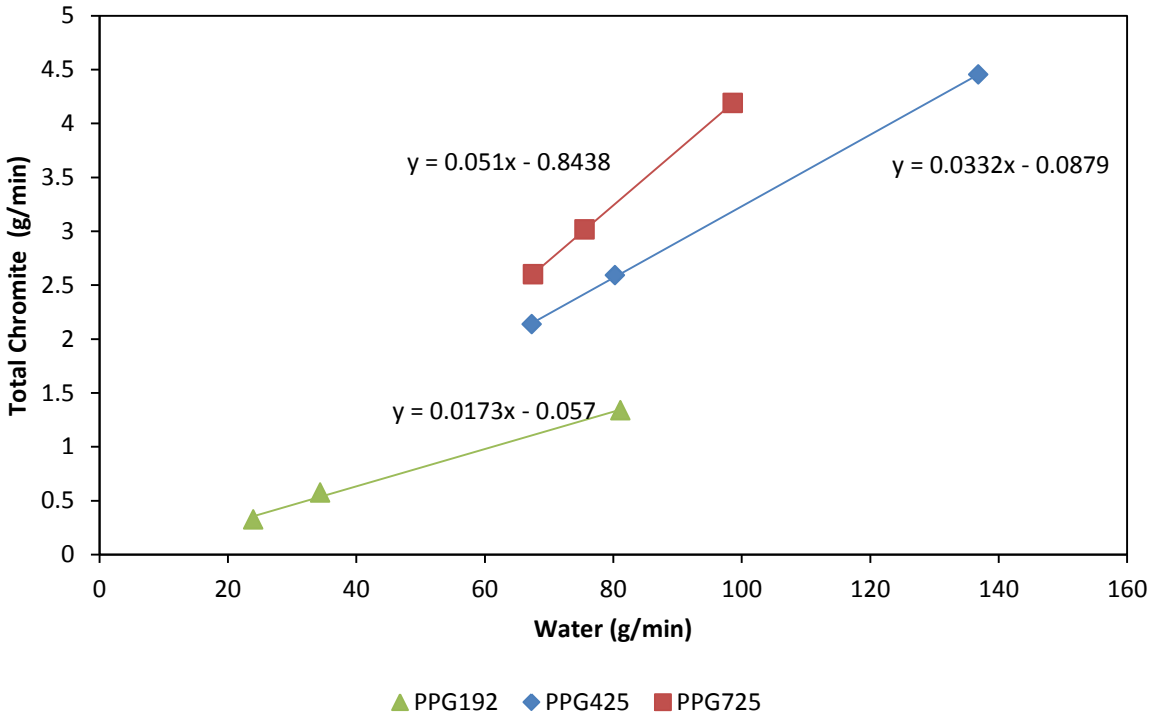


**Figure 4-45: Total chromite recovered in concentrate as a function of water recovered on use of polyglycol frothers at a dosage of 0.314 mM and with no depressant present.**

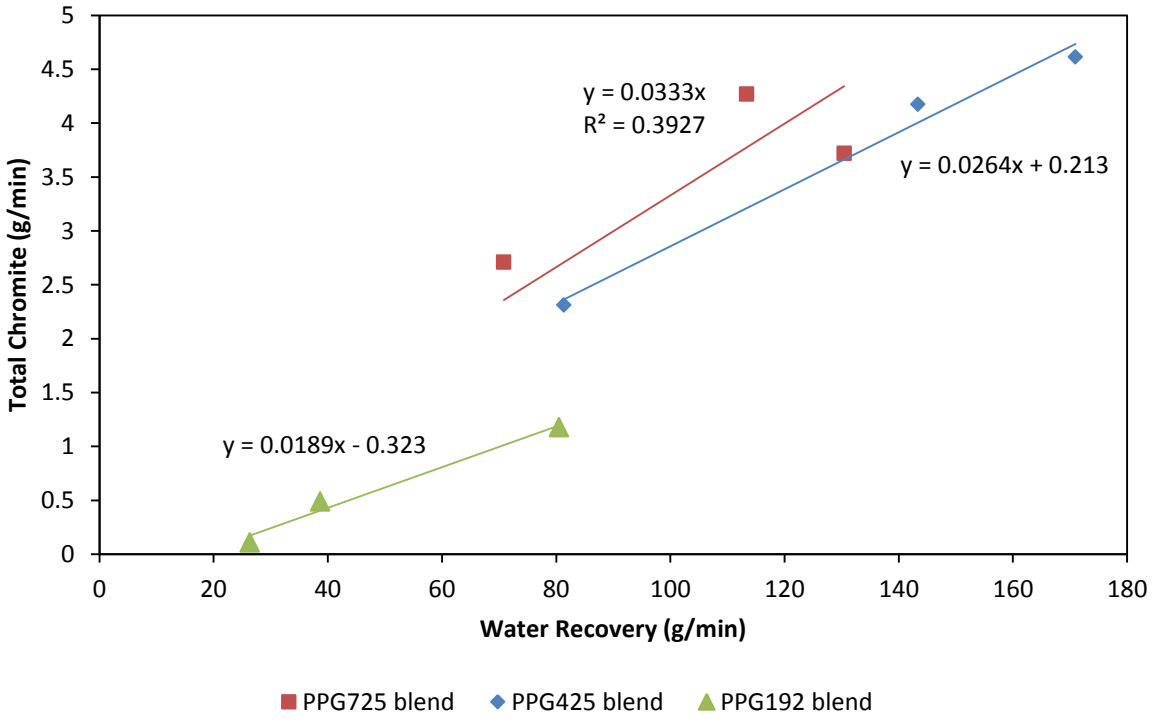


**Figure 4-46: Total chromite recovered in concentrate as a function of water recovered on use of polyglycol-MIBC frother mixtures at a dosage of 0.314 mM and with no depressant present.**

**Table 4-6: Entrainment values determined for the alcohol, polyglycol and polyglycol-MIBC frother series.**

| Frother type | Entrainment factor ( g chromite/g water) |
|---|---|
| Pentanol | 0.0462 |
| MIBC | 0.0333 |
| Hexanol | 0.0267 |
| PPG192 | 0.0173 |
| PPG425 | 0.0332 |
| PPG725 | 0.0510 |
| PPG192-MIBC | 0.0189 |
| PPG425-MIBC | 0.0264 |
| PPG725-MIBC | 0.0333 |

# Chapter 5

# Discussion

The aim of this study was to investigate the effect of frother type on froth stability, froth recovery and entrainment. The experimental approach taken to investigate the proposed hypotheses was described in Chapter 3 with the results obtained shown in Chapter 4. This chapter provides a discussion of the results shown in Chapter 3. The initial sections of the chapter focuses on results obtained from two phase experiments followed by a discussion focused on three phase experiment results.

## 5.1. Frother characterisation

Results shown in Figures 4-1 and 4-2 showed an increase in the excess Gibbs energy as the molecular weight of the frothers increased. An increase in excess Gibbs energy indicates an increase in the difference between the solution and an ideal solution. The increase in the excess property is due to the increasing difference in the molecular structures of the frothers compared to the molecular structure of water. Due to the increasing changes between the molecular structure of the frothers and water, interactions between the frother and water in response deviate from ideality (Sandler, 2006). Corin and O'Connor (2014) showed the existence of a linear relationship between hydrophile-lipophile balance (HLB) and excess Gibbs energy and proposed the use of the excess Gibbs energy as a measure of the hydrophilic/hydrophobic nature of surfactants. Figures 4-1 and 4-2 show an increase in the hydrophobic nature of frothers as the molecular weight of the frothers increased. As the alcohol frothers had lower values of the excess property in comparison to the polyglycol frothers this suggests that the latter is more hydrophobic in nature than the former. Figure 4-3 showed a similar trend of dual component frothers having lower values of the excess property compared to single component frothers. This suggests that dual component frothers are more hydrophilic in nature compared to single component frothers. The alcohol component of the mixture reduced the hydrophobic nature of the polyglycol frother.

## 5.2. Alcohol frothers

### 5.2.1. The effect of frother structure on surface activity

It is evident from Figure 4-5 that as the chain length increased, the ability of the alcohol frothers to lower the surface tension of the solution improved. Also shown in the figure is that the branched isomer MIBC lowered the surface tension to a lesser extent in comparison to the linear isomer, hexanol. The ability of surfactants to lower surface tension can be used as a measure of the surfactant activity. These findings confirm earlier observations on the effect of chain length and a branched structure on the surface activity of the frothers (Addison, 1945; Comley et al., 2001; Rosen, 2004; Le, 2012). This research has ascribed these findings to be as a result of their packing density at the interface as illustrated in

Figure 4-9 (Jachimska et al., 1995; Comley et al., 2001; Le, 2012). Branched chain surfactants cannot pack as tightly at the air-water interface as straight chain surfactants. The surface tension decreased as the frother concentration increased due to an increase in the number of surfactant molecules adsorbing at the interface. The point at which micelles begin to form (the critical micelle concentration) was not of interest and was not reached in this study. At this concentration, the surface tension becomes independent of frother concentration as the air-water interface is saturated with surfactant molecules. However, this point is very far from any realistic, practicable frother concentration.

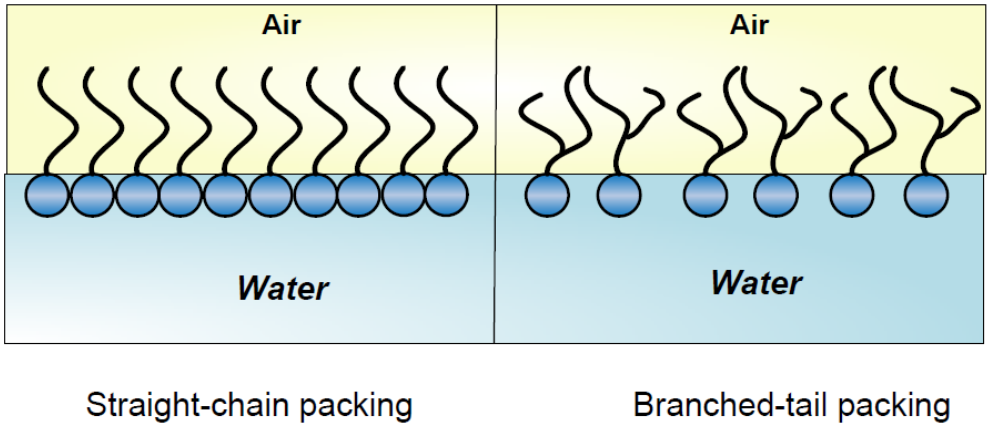


**Figure 5-1: Effect of the branched nature of surfactants on the compactness of surfactants at the interface (Le, 2012).**

Related to the above findings, was the calculated surface excess of the molecules (Table 4-3). The surface excess of the two straight-chain alcohols, hexanol and pentanol, was very similar. The longer chain, hexanol, had a marginally higher surface excess than the shorter chain, pentanol. However, the branched-chain MIBC molecules were not as highly packed as the hexanol and had a lower surface excess. These observations are in agreement with those made by previous researchers (Jachimska et al., 1995; Laskowski, 1998; Comley et al., 2001). Surface excess increased with an increase in chain length and consequently a decrease in the area occupied by the adsorbed molecule. This was attributed to the increase in Van der Waals forces between the molecules and the interface (Rosen, 2004). The increase in length of the hydrophobic chain leads to a decrease in the solubility of the surfactant and causes compact packing at the interface. The low surface excess on use of MIBC compared to the use of hexanol is ascribed to the branched structure MIBC which results in steric hindrance and does not allow the existence of a compact monolayer at the interface (Rosen, 2004; Wang & Yoon, 2008) as demonstrated in Figure 5-1. An increase in the packing of the surfactants at the interface results in a greater degree of disruptions of intermolecular forces between water molecules at the surface (Laskowski, 1998).

An analysis of the relationship between alcohol chain length with diffusion and adsorption coefficients as shown in Figure 4-14 and Table 4-4 respectively showed a decrease in the former and increase in the latter as the chain length increased. As expected a reciprocal

relationship exists between diffusion coefficient and surfactant size which can be attributed to a high drag force and hence resistance to the migration of surfactants to the interface.

Use of hexanol resulted in a higher adsorption constant in comparison to pentanol. This suggests that hexanol adsorbs more readily to the air-water interface than pentanol. A similar trend of the results was observed by other researchers (Chang et al., 1991; Comley et al., 2001; Wang & Yoon, 2008). This is possibly due to the higher hydrophobicity of the longer carbon chain of hexanol which induces a greater affinity of the surfactant to the interface. Also shown in Table 4-4 is that hexanol had a higher adsorption constant compared to MIBC. This is in agreement with all the other data showing that the packing of MIBC at the interface is less than for the straight-chain molecules.

### 5.2.2. Effect of frother structure on foam stability

The effect of alcohol molecular structure on foam stability is shown in Figure 4-18. For the straight-chain alcohols, an increase in molecular weight resulted in an increase in foam stability. These results confirm earlier well established findings on the effect of alcohol chain length on foam stability (Malysa et al., 1987; Aston et al., 1989; Sweet et al., 1997; Gupta et al., 2007; Zhang, 2012). The increase in stability can be attributed to an increase in elasticity and surface viscosity due to an increase in the Van der Waals force between the growing chain length and increase in entanglement associated with longer chains (Pugh, 1996; Khoshdast & Sam, 2011). Wang and Yoon (2008) showed that the elasticity of the air-water interface increased when using alcohol frothers of increasing chain length and also showed a linear relationship between foam stability and film elasticity proving the importance of film elasticity to ensuring a stable foam.

It is important to note that the foam stability results, in particular a comparison of MIBC and hexanol, are in contrast with the surface tension results which showed MIBC to be less surface active, being loosely packed at the interface and having the least affinity for the interface. However, the MIBC resulted in a more stable foam than hexanol. This suggests the existence of a different mechanism of action between the enhanced packing at the interface, which lowers surface tension, and the branched structure of MIBC which causes a decrease in water drainage through the thin films of the foam structure, resulting in a more stable foam.

### 5.2.3. Effect of frother structure on froth stability

Froth stability factors obtained to investigate the effect of frother type are depicted in Figure 4-21. It may have been expected that the order of froth stability would follow the foam stability trend. However, it was shown that the use of pentanol resulted in the most stable froth compared to the use of hexanol and MIBC. The order of froth stability was hexanol<MIBC<pentanol. In the presence of solids, the froth phase is significantly more stable than the two-phase foam. This is evident from the molar stability factors whose range from 2-14 sec/mol, in two-phase, to 40-160 sec/mol in the presence of solid particles. This increased stability in the presence of particles is due to reduced drainage from the

mineralised froth caused by an increase in roughness of bubble walls (Bulatovic, 2007) and by the structural stability imparted by particles that form a steric boundary between bubbles that prevents coalescence (Hunter et al., 2008).Thus, in the presence of solids, the froth stability is overwhelmingly dominated by the solids. However, having said this there must be some contribution from the frother otherwise the froth stability would be the same for all frother types. According to Pugh (2007), overdosing of frothers can lead to adsorption of frothers at the mineral surface. As a result of large concentrations of frother required to run the bench-scale column flotation cell, it is possible that frother molecules adsorbed at the mineral surface which can have an effect on particle attachment on air bubbles and has a decisive effect on froth stability (Bulatovic, 2007).

### 5.2.4. Effect of frother type on flotation performance

An analysis of the effect of frother type on water and solid recovery is depicted in Figure 4-24. At any given froth depth, solid and water recoveries followed a similar trend to froth stability. These findings corroborate earlier findings (Wiese et al., 2011; Araya et al., 2011; Corin & Wiese, 2014) which suggested the use of water recovery as a measure of froth stability during the flotation process. A negative relationship between froth depth and water recovery was observed in Figure 4-24. Research (Engelbrecht & Woodburn, 1975; Feteris et al., 1987) has shown that froth stability is dependent on froth depth due to film thinning due to drainage of liquid film with increasing froth depth. The amount of solids and water decreases with increased froth depth due to drainage of entrained solids and bursting of bubbles over an increasing froth residence time, which is defined as froth height/superficial air velocity.

Results on the effect of frother type and froth depth on froth recovery are shown in Figure 4-30. Extrapolation of the flotation rate constant versus froth depth to the pulp-froth interface converges at almost the same point, an indication that frother type did not affect kinetics within the pulp phase. At any given froth height, use of pentanol resulted in a higher froth recovery with use of hexanol resulting in the least froth recovery. The observed trend again is similar to the trend observed on the effect of frother type on froth stability and water recovery. The trend is as expected as froth recovery is significantly dependent on froth stability which is a function of frother type (Bisshop & White, 1976; Mathe et al., 1998; Tao et al., 2000). A stable froth phase during the flotation process ensures a high froth recovery, while an unstable froth phase results in rapid bubble bursting, particle drop back and low froth recoveries (Mathe et al., 1998; Zanin et al., 2009).

The overall recovery of valuable minerals is dependent on, amongst others, froth recovery. Therefore, it is expected that the trends of the overall PGM recoveries as a function of froth height should be similar to those of the froth recoveries. Since all tests were operated above the CCC of the frother in question, pulp recoveries were not expected to change from one frother to another. Thus, it was only the froth characteristics that would change valuable mineral recovery. Figure 4-40 showed that, as expected, the overall PGM

recoveries showed similar trends to the froth stability and froth recovery trends. As expected, associated with the high PGM recoveries on use of pentanol, is a lower PGM grade. This was possibly due to the more stable froth that carried gangue minerals which dilute the valuables. A more stable froth phase translates to high degree of gangue mineral entrainment. The least stable froth obtained on use of hexanol resulted in a relatively higher PGM grade than the other frothers. The grade-recovery results follow the well-established compromise between grade and recovery that is associated with the flotation process.

Due to the hydrophilic nature of chromite it is only recovered in the launder by means of entrainment. Investigations on the effect of frother type on degree of entrainment showed that the use of pentanol and hexanol resulted in the highest and least degree of entrainability, respectively. The entrainability values relate to the amount of chromite mineral entrained per unit water recovered. This finding was expected as the frothers had shown a similar trend with regards to froth stability (Tao et al., 2000; Neethling & Cilliers, 2002). Due to the high entrainment function and high water recovery associated with the use of pentanol a relatively large amount of entrained material was recovered in the concentrate, diluting the valuable mineral. This is reflected in the lower grades associated with the use of pentanol.

## 5.3. Polyglycol frothers

### 5.3.1. The effect of frother structure on surface activity

The surface tension of different solutions of varying frother type and concentrations are presented in Figure 4-4. It can be seen that, the activity of the frothers increases with frother molecular weight. Tan et al (2005) and Schwarz (2004) observed similar findings and suggested that this is due to the increasing number of hydrophobic repeating units per molecule associated with the larger chains. Table 4-3 illustrates that generally surface excess of surfactants increases with use of surfactants of shorter chain length. As a result of the alternating polar groups of polyglycols, the molecules favour a parallel alignment of the surfactants at the interface hence low surface excess values are observed as the chain length increases (Comley et al., 2001). It is also as a result of the favoured alignment position of the surfactants at the interface that alcohol frothers have a high associated surface excess, unlike polyglycols. Figure 4-11 illustrates that there is some degree of coiling of the larger polyglycols, but that this is not pronounced. PPG725 takes up approximately 75% of the surface area theoretically predicted from its straight chain conformation.

Surfactants of longer chain length have lower diffusion rates associated with them as illustrated in Figure 4-14. However, the dependence of diffusion rate on molecular weight becomes less after a molecular weight of about 200 g/mol. The surfactants of lower diffusion rate have a high affinity for the gas-liquid interface (as shown in Table 4-4). The decrease in rate of diffusion with an increase in chain length as discussed earlier is expected

due to the increase in resistance to the movement of the molecules. As a result of the increasing hydrophobic nature of surfactants with increase in chain length it is expected that the affinity for the interface increases.

### 5.3.2. Effect of frother structure on foam stability

The effect of surfactant chain length on foam stability is illustrated in Figure 4-18. The stability of the foam increased with the chain length of the surfactants. For a similar range of molecular weight polyglycols this behaviour has been observed by a number of authors, namely Laskowski et al (2003), Tan et al (2005) and Schwartz (2004). Similarly to the surface tension results, the extent of the increase in foam stability decreases as the molecular weight increases. Thus, there was a large increase in foam stability in moving from PPG192 to PPG425, but a small increase in foam stability on moving from PPG425 to PPG725. Similar trends of foam stability and surfactant surface activity indicates that there is a close correlation between them which has also been shown in other research (Melo, 2001; Tan et al., 2006; Melo & Laskowski, 2007). The stability of the foam is, among other factors, dependent on the number of polar groups at the interface that interact with the film water molecules. PPG725 has more polar units than the other frothers hence a greater ability to associate with water molecules. Interaction of the frother hydrophilic group and liquid phase increases the mechanical strength of the enveloping hydrating layer surrounding bubbles hence preventing destruction of the bubbles (Bulatovic, 2007).

### 5.3.3. Effect of frother structure on froth stability

From the test results, it was observed that the use of PPG425 generally resulted in the most stable froth phase (see chapter 4, Figure 4-23) with regards to single component frothers. This represents a departure from the earlier observed trend of the effect of frother type on foam stability where PPG725 gave a marginally more stable foam. The complex physicochemical sub-processes associated with flotation may generate alternative interpretations of the results. Tan et al (2006) suggested that the change in interfacial coiled nature of the frothers from a linear (PPG425) to coiled (PPG725) nature results in a decrease in the spreading rate of the molecules at the interface hence a less stable froth. However, results presented earlier on the effect of frother molecular weight on foam stability disproves this theory as an increase in foam stability was observed with increasing frother molar mass. Melo and Laskowski (2007) also found no correlation between froth stability and frother surface activity. The difference in stability trends as a function of frother type may be due to preferential adsorption of the frothers to the surface of the mineral. Due to the heteropolar nature of surfactants they may adsorb onto hydrophobic mineral surfaces as well as at the air-water interface. They can interact by means of Van der Waals forces between the hydrophobic part of the chain and the mineral surface (Fuerstenau & Pradip, 1982; Miller et al., 1983; Melo & Laskowski, 2007). Due to a higher surface activity of PPG725 in comparison to PPG425, the PPG725 molecules may adsorb preferentially at the mineral surface and cease to act as frothers. This would result in a decrease in PPG725 solution concentration and hence a decrease in froth stability when using PPG725. The

larger the frother molecule becomes, the more like a depressant molecule it may become due to possible interactions with the surface of the minerals hence ceasing to act as a frother. Figure 5-2 shows the mechanism of interaction proposed by Liu et al (2000) between a depressant and mineral surface. There is the possibility that the longer chain polyglycol frothers could interact with the mineral surface in a similar manner through the ether oxygen and/or hydroxide groups.

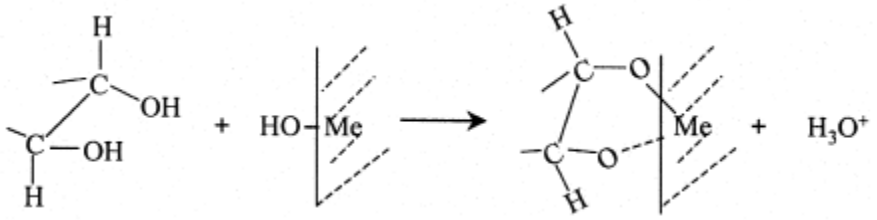


**Figure 5-2: Proposed reaction mechanism of depressants at the mineral surface (Liu et al., 2000)**

Leja and Nixon (1957) proposed the formation of a collector-frother complex which adsorbs onto the mineral surface removing the frother from solution. No work has been done thus far to verify this theory. This theory does not hold for alcohol frothers as the collecting properties of alcohols is practically similar (Malysa et al., 1987).

### 5.3.4. Effect of frother type on flotation performance

It was generally observed that use of PPG425 resulted in high solids and water recoveries as shown in Figure 4-25. This is an indication of a more stable froth on use of PPG425 supporting earlier results which gave a similar conclusion

Analysis of the effect of frother type on froth recovery is shown in Figure 4-29. Use of PPG425 resulted in a higher froth recovery than on use of PPG192 and PPG725, with the use of the former resulting in the least froth recovery. The slope of the froth recovery versus froth height graph shows that PPG425 loses 1.3% PGM's from the froth per centimetre of additional froth height whereas PPG192 loses 4.9% PGM's from the froth per centimetre of additional froth height. As expected the froth recovery trend followed the froth stability trend. Due to the relationship that exists between froth recovery and the overall recovery, a similar trend to the effect of frother type on froth recovery was observed on the effect of frother type on overall valuable mineral recovery. Consistently it was observed that use of PPG192 and PPG725 resulted in the highest and least concentrate PGM grade respectively possible reasons being the differing degree to which the froth transported the valuable and gangue mineral (entrainability).

The entrainability function showed that the entrainability was in the order PPG725>PPG425>PPG192 (Figure 4-44). The entrainability was expected to follow the froth stability trend and thus it was expected that the highest entrainability would come from the PPG425 frother. However, differences in both froth stability and entrainability are slight and not too much emphasis should be placed on these. Entrainability should not be

confused with the amount of entrained material. Entrainability is a property of the froth related to the froth structure whereas the amount of entrained material is the entrainability multiplied by the amount of water recovered. Thus, at 4cm froth height, the PPG425 recovered more water than the PPG725 and therefore had more entrained material present. However, the entrainability remained lower than that of the PPG725.

## 5.4. Polyglycol-MIBC frother mixtures

### 5.4.1. The effect of frother structure on surface activity

Binary mixtures of frothers were combined in a 4:1 molar ratio of PPG to MIBC. When comparing the surface tensions of the single component frothers to their binary mixtures, it was found that only the PPG192-MIBC mixture resulted in a clearly different surface tension. In the case of the PPG425 and PPG725, the surface tensions of the mixtures were almost identical with those of the stronger polyglycol frother (Figures 4-6 to 4-8). In the case of the PPG192-MIBC mixture, the surface tension isotherm lay approximately where one might expect from the dilution effect of the weaker surfactant (PPG192) with the stronger surfactant (MIBC). Previous research (Tan et al., 2005), also showed no significant change in surface tension was observed for mixtures of frothers of higher molecular weight compared to mixtures of low frother molecular weight. The results thus indicate no change in surfactant surface activity except on use PPG192.

Figure 4-10 shows an increase in surface excess on use of dual component blends calculated using the Hutchinson method compared to the use of single component polyglycol frother solutions. This was expected as more of the MIBC molecules would be found at the interface as a result of their small size. Due to the increasing differences in size between MIBC and polyglycols of long chain length, there is an increase in the difference between the surface excess between the single and dual component frother solutions. The dual frother solutions also showed a decrease in the adsorption constant in comparison to single component frother solutions. The low adsorption constant values associated with the frother mixtures seem to be simply the dilution effect of the weaker frother that reduces the affinity of the stronger frother for the air-water interface. Alternatively, Samantha and Ghosh (2011) suggested that alcohol surfactants penetrate between the polyglycol molecules, resulting in a greater distance between polyglycol molecules which results in a reduced interaction between the hydrophobic groups of polyglycols, inducing weaker adsorption at the interface. Importantly, there was nothing in the surface activity data that suggested that there was any synergistic interaction between the polyglycol and alcohol frothers.

### 5.4.2. Effect of frother structure on foam stability

A study of the foam stability data shows that the use of polyglycol – MIBC frother mixtures resulted in a more stable foam than on use of single component frothers (see Figures 4-19 to 4-20), which is an indication of a positive synergistic effect. Past research (Tan et al., 2005) showed similar results and suggested that a frother mixture of high and low HLB

components ensures a closely packed and cohesive film at the interface resulting in a more elastic film and hence more stable bubbles.

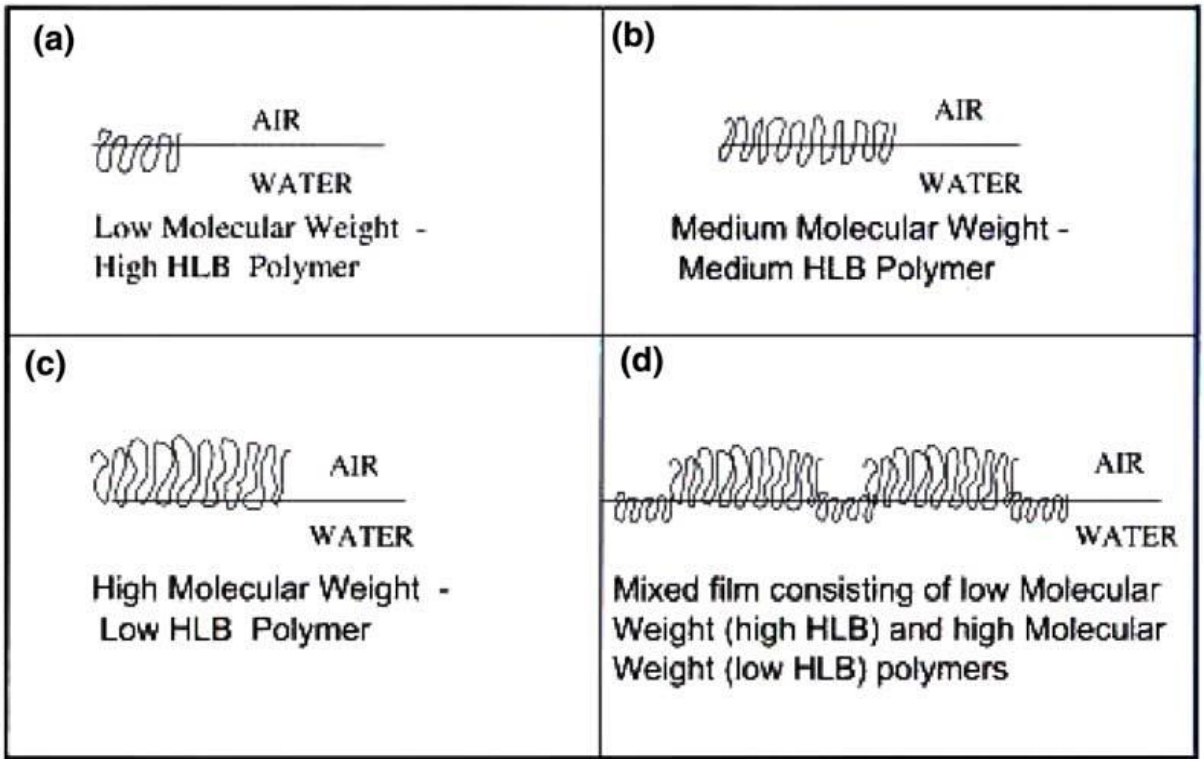


**Figure 5-3: Suggested configuration of polyglycols, MIBC and polyglycol-MIBC mixture at the air-water interface (Tan et al., 2005).**

By means of analysis of dynamic surface tension isotherms Tan et al. (2005) suggested that the use of frother mixtures ensured a foam of greater surface elasticity hence a more stable foam. These authors suggested that it was not only the equilibrium processes which were important in maintaining a stable foam, but also the rate processes. They suggested that the surfactant required the ability to maintain a high non-equilibrium surface tension to allow liquid surface flow to occur. These synergistic effects were not evident in the equilibrium surface tension measurements.

### 5.4.3. Effect of frother structure on froth stability

The increase in foam stability observed during the use of dual frother blends was carried through to the three-phase froth stability results. A significantly more stable froth phase was obtained on use of dual frother blends in comparison to single component frothers as shown in Figure 4-23. Past research (Elmahdy, 2011; Ngoroma et al., 2013; Pani et al., 2013) has also shown the existence of a positive synergy on use of frother blends. Possible reasons for the synergistic effect could be those highlighted on the effect of frother type on foam stability.

### 5.4.4. Effect of frother type on flotation performance

The results of the flotation tests, indicated by Figure 5-4, illustrate the effect of frother blends on the solids and water recoveries.

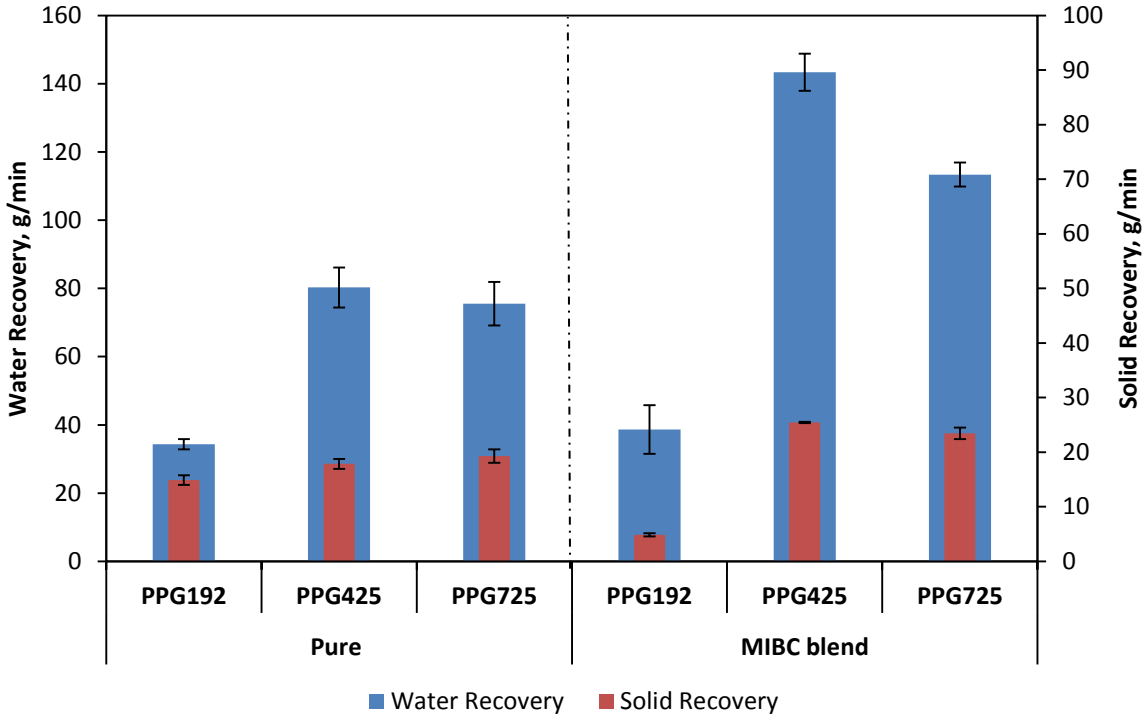


**Figure 5-4: Comparison of the effect of frother blends on solid and water recovery at a froth height of 8 cm.**

These results show that use of a dual frother suite resulted in an increase in the solids and water recovery. These results are consistent with the findings obtained by other researchers (Elmahdy, 2011; Ngoroma et al., 2013; Pani et al., 2013).

The froth recoveries show that there are marginal, but measurable increases in PGM recovery, particularly at the lower froth heights when using frother blends. For example, there was a 3.7% improvement in froth recovery when using a PPG425 blend at 4 cm froth height. These increases in the froth recovery are not enough to account for the overall improvement in recoveries shown Figures 4-31 to 4-33, where the improvement in recovery for the same condition was 7.5%. This, along with improvements in grade, suggests that that the frother blends are having a beneficial effect on the pulp phase flotation as well as the froth phase. This requires further investigation in future studies.

The greater froth stabilities of the dual frother blends were expected to translate to a higher entrainability factor. However, only the use of the PPG192 blend resulted in a higher degree of entrainment with the rest showing reduced degree of entrainment. Thus, if water were carefully managed, the amount of entrained material could be reduced when using frother blends. However, in this case, since the water recovery was also greater when using frother blends, the amount of entrained material was the same or more when compared to using the pure PPG425 or PPG725.

The use of frother blends resulted in generally a higher recovery and grade of valuable minerals as indicated by Figures 4-37 to 4-39.These findings support earlier reported results which showed that the use of frother blends results in an improved recovery and grade of valuable mineral (Ngoroma et al., 2013). High recoveries were obtained when using the PPG-MIBC frother blends. These blends also gave a high froth stability and high froth recovery.

## 5.5. **Summary**

In summary the results showed that the use of frother blends resulted in a more stable foam and froth phase. The much more stable froth phase obtained on use of frother blends correlated with high valuable mineral recovery and grade during the flotation process. Surface tension experimental results showed no indication of synergistic interactions on use of frother blends. This suggests that the better performance associated with a blend is not related to the surface activity of the frothers. The higher recoveries and grade of valuables possibly could be due to the existence of a froth structure enabling the attainment of high recovery and grade of valuables. Use of PPG-MIBC blends allows the constituent frothers to perform different roles due to their properties. PPG-MIBC blends result in a more closely packed and cohesive frother film at the air-water interface resulting in more stable bubbles hence a higher recovery (Tan et al., 2005). Unlike polyglycol frothers which ensure a persistent froth phase, alcohol frothers provide a more brittle froth phase hence ensuring a more selective separation process resulting in the high grade of valuable mineral (Wills & Napier-Munn, 2006). As a result the use of PPG-MIBC blends led to a high concentrate grade of valuable minerals. The froth structure that exists on use of the frother blends ensures low water drainage as indicated by the water recoveries and improved particle fall-back of gangue mineral as indicated by the low degree of entrainment. Elmahdy and Finch (2013) suggested that the use of frother blends allowed for more control over the function of frothers during the flotation process.

# Chapter 6

# Conclusions and Recommendations

This chapter summarizes the main findings from the test work performed investigating the effect of frother type on froth stability, froth recovery and entrainment. Conclusions drawn from the work are stated and recommendations for future work made.

## 6.1. Conclusions

The following conclusions may be drawn from the test work:

### 6.1.1. Frother characterisation

Characterisation of frothers was performed based on earlier work by Corin and O'Conner (2013) which proposed the use of $G^{ex}$ as a measure of the hydrophilic/hydrophobic nature of surfactants. For both series of frother types a linear relationship was observed between molecular weight and the $G^{ex}$. This correlated to an increase in the frother hydrophobic nature with increasing molecular weight. Frother blends showed a more hydrophilic nature compared to their single component polyglycol frothers but this pointed simply to the dilution effect of mixing a polyglycol frother, with a higher $G^{ex}$, with an alcohol of lower $G^{ex}$. The degree of hydrophobicity controls the adsorption kinetics associated with the frothers whilst the degree of hydrophilicity determines the degree of interaction between the frother and surrounding water molecules.

### 6.1.2. Effect of frothers on surface activity

The alcohol and polyglycol frother series showed an increase in the activity of frothers as the chain length increased. This was attributed to the increasing number of hydrophilic or hydrophobic groups hence an improved interaction at the air-water interface. Also evident from the alcohol series, was that the branched isomer (MIBC) was less surface active compared to its linear isomer (hexanol). This observation has been ascribed to the reduction in packing density of the branched chain isomer at the air-water interface. With the exception of the PPG192-MIBC mixture the frother blends did not show any significant change in surface activity compared to the polyglycol frother. This observation suggests no synergism exists on the use of frother blends which is contrary to foam and/or froth stability results. This could suggest that equilibrium surface activity is not the underlying mechanism in the improved foam and/or froth stability on use of frother blends. It should also be noted that the use of equilibrium surface tension data is limiting since the flotation process is dynamic.

Polyglycol experimental data showed an increase in the coiling nature, adsorption constant and a decrease in the surface excess with increasing molecular weight. Alcohol frother experimental data showed that an increase in molecular weight resulted in an increase in adsorption constant and surface excess. For both frother classes a linear relationship was

observed between $G^{ex}$ and the adsorption constant which suggests that the adsorption constant has a linear relationship to hydrophobicity. This relationship may allow for the simple classification of frothers without the need for large experimental work.

### 6.1.3. Effect of frothers on foam stability

An increase in frother molecular weight resulted in a more stable foam for both frother type series. For the polyglycol series as the molecular weight increased there was a greater interaction between the frother and enveloping hydrating layer hence a more stable bubble and foam. With respect to the alcohol frothers an increase in chain length corresponded to an increase in the positive inductive effect hence ultimately greater interaction between the polar group and enveloping hydrating layer.

Use of frother blends gave a more stable foam phase contrary to the surface activity trend which showed the single component polyglycol frother being more active. This finding shows that more factors apart from frother surface activity govern the effect of frothers on the foam stability. Tan et al. (2005) suggested that it was not only the equilibrium processes which were important in maintaining a stable foam, but also the rate processes. They suggested that the surfactant required the ability to maintain a high non-equilibrium surface tension to allow liquid surface flow to occur.

### 6.1.4. Effect of frothers on froth stability

Generally it was shown that an increase in frother molecular weight resulted in a more stable froth phase, but it also highlighted that the trends obtained were not mirror images to foam stability trends. Use of PPG425 and pentanol resulted in the most stable froth phase for the polyglycol and alcohol frother series, respectively.

At high frother concentration it is proposed that frothers adsorb at the mineral interface (Pugh, 2007)and, therefore ceases to act as frothers. They would then have an effect on particle attachment onto air bubbles and may have an adverse an effect on froth stability (Bulatovic, 2007).

With respect to alcohol frothers unexpected results which showed the use of pentanol resulting in the most stable froth were observed. It is proposed that, in terms of the above theory, that the low surface active nature of pentanol resulted in lower amounts of the pentanol being adsorbed on the mineral surface. This allowed for a greater portion of the pentanol frother to perform its frothing role and hence a more stable froth was observed. With regards to the polygycol series, it is proposed that, due to a higher surface activity of PPG725 in comparison to PPG425, the PPG725 molecules adsorb preferentially at the mineral surface and cease to act as frothers.

As with foam stability it was also observed that the use of frother blends resulted in a more stable froth in comparison to the use of constituent frothers. The same mechanism is proposed as for the enhanced foam stability when using frother blends. Similar findings of

the existence of synergistic interactions on use of frother blends have been reported in previous studies (Elmahdy, 2011; Ngoroma et al., 2013; Pani et al., 2013).

### 6.1.5. Effect of frothers on flotation performance

The use of frother blends resulted in a higher grade and recovery of valuable minerals. This observation could be due to the existence of an enhanced froth structure enabling the high recoveries and grade of valuables. Use of PPG-MIBC blends allows the constituent frothers to perform different roles due to their properties. The blends give a much more stable froth phase which translates to higher recoveries of the valuable minerals. Alcohol frothers provide a more brittle froth phase hence ensuring a more selective separation process resulting in the high grade of valuable mineral (Wills & Napier-Munn, 2006). As a result the use of PPG-MIBC blends led to a high concentrate grade of valuable minerals. The froth structure that exists on use of the frother blends ensures low water drainage as indicated by the water recoveries and improved particle fall-back of gangue mineral as indicated by the low degree of entrainment.

## 6.2. Recommendations

Based on the above stated key findings of this research, recommendations for future test work are outlined as follows:

- The dynamic nature of the flotation process ensures that adsorption of the frothers does not reach equilibrium conditions making the use of equilibrium surface tension data limited. As a result it is imperative that dynamic surface tension tests be carried out with particular interest on the use of frother blends.
- Frother blends can be comprised of an infinite combination of component frothers. Further research can be carried out investigating the optimum frother suite that ensures the best flotation performance to obtain the best technical and economic advantages.
- This research was focused on the effect of frothers on the froth phase. Frother adsorption density measurements at a hydrophobic solid surface are suggested. The tests would provide valuable insight into the proposed theory of frother adsorption onto the mineral surface at high frother dosages.

# Chapter 7

## References

Addison, C., 1945. The properties of freshly formed surfaces. Part iv: The influence of chain length and structure on the static and dynamic surface tensions of aqueous-alcoholic solutions. *Journal of Chemistry Society*, (98), pp.98-106.

Allen, T., 1997. *Particle size measurement Volume 1*. 5th ed. London: Chapman Hall.

Araya, R., Maldonado, M. & Finch, J.A., 2011. Technique to automate measurement of water overflow rate in frother characterization testing. *Minerals Engineering*, 24(8), pp.950-52.

Arbiter, C. & Harris, C.C., 1962. Flotation Kinetics. In D.W. Fuerstenau, ed. *Froth Flotation*. New York: AIME. pp.215-46.

Aston, J.R., Lane, J.E. & Healy, T.W., 1989. The solution and interfacial chemistry of nonionic surfactants uesd in coal flotation. In J.S. Laskowski, ed. *Frothing flotation*. 1st ed. New York: Gordon and Breach. pp.229-56.

Ata, S., 2012. Phenomena in the froth phase of flotation - A review. *International Journal of Mineral Processing*, 102, pp.1-12.

Ata, S., Ahmed, N. & Jameson, G.J., 2003. A study of bubble coalescence in flotation froths. *International Journal of Mineral Processing*, 72, pp.255-66.

Bamforth, C.W., 1985. The foaming properties of beer. *Journal of the Institute of Brewing*, 91(6), pp.370-83.

Barbian, N., Hadler, K., Ventura-Medina, E. & Cilliers, J.J., 2005. The froth stability column: linking froth stability and flotation performance. *Minerals Engineering*, 18, pp.317-24.

Barbian, N., Ventura-Medina, E. & Cilliers, J.J., 2003. Dynamic froth stability in froth flotation. *Minerals Engineering*, 16, pp.1111-16.

Bhakta, A. & Ruckenstein, E., 1997. Decay of standing foams: drainage, coalescence and. *Advances in Colloid and Interface Science*, 70(1), pp.1-124.

Bikerman, J., 1973. Foams. In *Applied Physics and Engineering*. London: Springer-Verlag. p.337.

Bisshop, J. & White, M., 1976. Study of particle entrainment in flotation froths. *Transactions of the institute of mining and metallurgy*, pp.191-94.

Bradshaw, D.J. & O'Connor, C.T., 1996. Measurements of the sub-process of bubble loading in flotation. *Minerals Engineering*, 9(4), pp.443-48.

Bulatovic, M., 2007. *Handbook of Flotation Reagents*. 1st ed. Petersborough: Elsevier.

Chang, C.-H. & Franses, E.I., 1995. Adsorption dynamics of surfactants at the air/water interface: a critical of mathematical models, data and mechanisms. *Colloids and Surfaces*, (100), pp.1-45.

Chang, C.H., Wang, N.L. & Franses, E.I., 1991. Adsorption dynamics of single and binary surfactants at air/water interface. *Colloids and Surfaces*, (62), pp.321-32.

Cho, Y.-S., 2001. *Effect of flotation frothers on bubble size and foam stability*. MSc Thesis. Vancouver: Department of Mining and Mineral Process Engineering The University of British Columbia.

Cho, Y.S. & Laskowski, J.S., 2002. Effect of flotation frothers on bubble size and foam stability. *International Jornal of Mineral Processing*, 64(1), pp.69-80.

Cilliers, J., 2006. Understanding Froth Behaviour With CFD. In *Fifth International Conference on CFD in the Process Industries*. Melbourne, Australia, 2006. Commonwealth Scientific and Industrial Research Organisation (CSIRO).

Colegate, D., 2009. *Structure-kinetics relationships in micellar solutions of nonionic surfactants*. PhD Thesis. Durham: Durham theses Durham University.

Comley, B.A., Harris, M.C., Bradshaw, D.J. & Harris, P.J., 2001. *Dynamic Surface Tension as a Means of Characterising Flotation Frother Performance*. MSc Thesis. Cape Town: University of Cape Town.

Corin, K.C. & O'Connor, C.T., 2014. A proposal to use excess Gibbs energy rather than HLB number as an indicator of the hydrophilic-liphophilic behavior of surfactants. *Minerals Engineering*, (58), pp.17-21.

Corin, K.C. & Wiese, J.G., 2014. Investigating froth stability: A comparative study of ionic strength and frother dosage. *Minerals Engineering*, 66-88, pp.130-34.

Craig , V.S., Ninham, B.W. & Pashley, R.M., 1993. Effect of electrolytes on bubble coalescence. *Nature*, 364(1), pp.317-19.

Cramer, L.A., 2008. What is your PGM concentrate worth ? In Rogers, M., ed. *Platinum in Transformation*. Rustenburg, 2008. SAIMM.

Czarnecki, J., Malysa, K. & Pomianowski, A., 1982. Dynamic frothability index. *Journal of Colloid and Interface Science*, 86, pp.570-72.

Derjaguin, B.V. & Landau, L., 1941. Theory of stability of strongly charged lyophobic sols and of the adhesion of strongly charged particles in solution of electrolytes. *Acta Physicochim*, 14(1), pp.633-62.

Dey, S., Pani, S. & Singh, R., 2014. Study of interactions of frother blends and its effect on coal flotation. *Powder Technology*, 260, pp.78-83.

Do, H., 2010. *Development of a Turbulent flotation Model from First Principles*. PhD Thesis. Virginia: Virginia Polytechnic Institute and State University.

Dyer, C., 1995. *An investigation into the properties of the froth phase in the flotation process*. MSc Thesis. Johannesburg: University of Witwatersrand.

Eastoe, J. & Dalton, J.S., 2000. Dynamic surface tension and adsorption mechanisms of surfactants at the air waterinterface. *Advances in Colloid and Interface Science*, (85), pp.103-44.

Ekmekci, Z., Bradshaw, D.J., Allison, S.A. & Harris, P.J., 2003. Effects of frother type and froth height on the flotation behaviour of chromite in UG2 ore. *Minerals Engineering*, 16, pp.941-49.

Elmahdy, M.A., 2011. *Frother Blends in Flotation: Polyglycols and Alcohols*. PhD Thesis. Montréal: Department of Mining and Materials Engineering McGill University.

Elmahdy, A.M. & Finch, J.A., 2013. Effect of frother blends on hydrodynamic properties. *International Journal of Mineral Processing*, 123, pp.60-63.

Engelbrecht, J.A. & Woodburn, E.T., 1975. The effect of froth height, aeration rate and gas precipitation on flotation. *Journal of the South African Institute of Mining and Metallurgy*, (76), pp.125-32.

Exerowa, D. & Kruglyakov, P.M., 1998. *Foam and Foam Films, Volume 5: Theory, Experiment, Application*. 1st ed. Amsterdam: Elsevier Science.

Falatsu, M. & Dobby, G., 1992. Froth performance in commercial sized flotation columns. *Minerals Engineering*, 5(1), pp.1207-23.

Farrokhpay, S., 2011. The significance of froth stability in mineral flotation- A review. *Advances in Colloid and Interface Sciences*, 166, pp.1-7.

Feteris, S.M., Frew, J.A. & Jowett, A., 1987. Modelling the effect of froth depth in flotation. *International Journal of Mineral Processing*, 20(1), pp.121-35.

Finch, J.A. & Dobby, G.S., 1990. *Column Flotation*. 1st ed. Oxford: Pergamon Press.

Fredenslund, A., Gmehling, J. & Rasmussen, P., 1977. *Vapour-Liquid Equilibria Using Unifac: A Group-Contribution Method*. 1st ed. Amsterdam: Elsevier.

Fruhner, H., Wantke, K. & Lunkenheimer, K., 1999. Relationship between surface dilational properties and foam stability. *Colloids and Surfaces A: Physicochemical and Engineering Aspects*, 162, pp.193-202.

Fuerstenau, D.W. & Pradip, 1982. Adsorption of frothers at coal/water interfaces. *Colloids and Surfaces*, 4(3), p.213–227.

Gibbs, J.W., 1928. *The Collected Works of J.W.Gibbs*. 1st ed. New York: Longmans, Greens and Co.

Grobler, W.A., Sondashi, S. & Chidley, F.J., 2005. RECENT DEVELOPMENTS IN FLOTATION REAGENTS TO IMPROVE BASE METAL RECOVERY. In *The Third Southern African Conference on Base Metals*. Kitwe, 2005. The South African Institute of Mining and Metallurgy.

Gupta, A.K., Jee, B.P. & Mishra, A., 2007. Effect of frothers on foamability, foam stability and subble size. *Coal preparation*, 27(1-3), pp.107-25.

Hadler, K., Barbian, N. & Cilliers, J.J., 2006. The relationship between froth stability and flotation performance down a bank of cells. In Onal, G., ed. *XXIII International Mineral Processing Congress*. Istanbul, 2006.

Hadler, K. & Cilliers, J.J., 2009. The relationship between the peak in air recovery and flotation bank performance. *Minerals Engineering*, 22(5), pp.451-55.

Hadler, K., Smith, C.D. & Cilliers, J.J., 2010. Recovery vs mass pull: The link to ir recovery. *Minerals Engineering*, 23, pp.994-1002.

Harris, G.H. & Jia, R., 2000. An improved class of flotation frothers. *International Journal of Mineral Processing*, 58(1-4), pp.35-43.

Heath, J., 2013. *Frothing at the lip - stability in your flotation cell*. Magazine. Output SEAP.

Hunter, T.N., Pugh, R.J., Franks, G.V. & Jameson, J., 2008. Ther role of particles in stabilising foams and emulsions. *Advances in Colloid adn Interface Science*, 137, pp.57-81.

Iglesias, E., Anderez, J., Forgiarini, A. & Salager, J.-L., 1995. A new method to estimate the stability of short-life foams. *Colloids and Interfaces*, 98, pp.167-74.

Jachimska, B., Lunkenheimer, K. & Malysa, K., 1995. Effect of position of the Functional Group on the Equillibrium and Dynamic Surface Properties of the Butyl Alcohols. *Journal of Colloid and Interface Science*, (176), pp.31-38.

Jiang, C., Wang, X.H. & Parekh, B.A., 2006. Ores, Flotation of. In P. Somasundaran, ed. *Encyclopedia of Surface and Colloid Science, Volume 6*. 2nd ed. New York: CRC Press. pp.4318-35.

Karakashev, S. & Nguyen, A.V., 2007. Effect of sodium dodecyl sulphate and dodecanol mixtures on foam film drainage: examining influence of surface rheology and intermolecular forces. *Colloids and Surfaces A: Physicochemical and Engineering Aspects*, 293(1-3), pp.229-40.

Kawatra, K.S., 2011. Fundamental Principles of Froth Flotation. In P. Darling, ed. *SME Mining Engineering Handbook*. 3rd ed. Colorado: Society for Mining, Metallurgy, and Exploration. pp.1517-32.

Khoshdast, H. & Sam, A., 2011. Flotation Frothers: Review of Their Classifications, Properties and Preparation. *The Open Mineral Processing Journal*, 4(1), pp.25-44.

Kirjavainen, V.M., 1996. Review and analysis of factors controlling the mechanical flotation of gangue minerals. *Mineral Processing*, 46, pp.21-34.

Kitchener, J.A. & Cooper, C.F., 1959. Current concepts in the theory of foaming. *Quarterly Reviews*, 40(1), pp.71-95.

Klimpel, R.R. & Isherwood, S., 1991. Some industrial implications of changing frother chemical structure. *International Journal of Mineral Processing*, 33(1), pp.369-81.

Koerner, C., 2008. *Integral Foam Molding of Light Metals*. 1st ed. Erlangen: Springer.

Laskowski, J.S., 1989. Thermodynamic and Kinetic Flotation Criteria. *Minerals Processing and Extractive Metallurgy Review*, 5(1), pp.25-41.

Laskowski, J.S., 1993. Frothers and Flotation Froth. *Minerals Processing and Extractive Metallurgy Review*, 12(1), pp.61-89.

Laskowski, J., 1998. Frothers and frothing. In J. Laskowski & E.T. Woodburn, eds. *Frothing in Flotation II: Recent Advances in Coal Processing*. 2nd ed. Amsterdam: Gordon and Breach Science. pp.1-50.

Laskowski, J.S., 2004. Testing Flotation Frothers. *Physicochemical Problems of Mineral Processing*, 38(1), pp.13-22.

Laskowski, J.S., Cho, Y.S. & Ding, K., 2003b. Effect of Frothers on Bubble Size and Foam Stability in Potash Ore Flotation Systems. *The Canadian journal of Chemical Engineering*, 81(1), pp.63-69.

Laskowski, J.S., Tlhone, T., Williams, P. & Ding, K., 2003a. Fundamental properties of the polyoxypropylene alkyl ether. *International Journal of Mineral Processing*, 72(1), pp.289-99.

Laskowski, J.S., Tlhone, T., Williams, P. & Ding, K., 2003. Fundamental properties of the polyoxypropylene alkyl ether flotation frothers. *International Journal of Mineral Processing*, 72, pp.289-99.

Le, N.T., 2012. *Influence of molecular structure on the adsorption of surfactants at water/air interface*. PhD Thesis. Curtin: Department of Chemical Engineering Curtin University.

Leja, J. & Nixon, J.C., 1957. Ethylene Oxide and Propylene Oxide compounds as a flotation reagents. In Schulman, J.H., ed. *Congress of Surface Activity*. London, 1957. Butterworths.

Leja, j. & Schulman, J.H., 1954. Flotation theory: molecular interactions between frothers and collectors at solid-liquid-air interfaces. *Tran.AIME*, 199, pp.221-28.

Liu, Q., Zhang, Y. & Laskowski, J.S., 2000. The adsorption of polysaccharides onto mineral surfaces: an acid/base interaction. *International Journal of Mineral Processing*, 60, pp.229-45.

Malysa, K., Czubak-Pawlikowska, J. & Pomianowski, A., 1978. Frothing properties of solutions and their influence on floatability. In *International Congress of Surface Active Substances*. Mowscow, 1978.

Malysa, K., Lunkenheimer, K., Miller, R. & Hartenstein, C., 1981. Surface Elasticity and Frothability of n-octanol and n-octanoic Acid Solutions. *Colloids and Surfaces*, 3, pp.329-38.

Malysa, E., Malysa, K. & Czarnecki, J., 1987. A method of Comparison of the Frothing and Collecting Properties of Frothers. *Colloids and Surfaces*, 23(1), pp.29-39.

Masutani, G. & Stenstrom, M.K., 2001. *A Review of surface tension measuring techniques, surfactants, and their implications for oxygen transfer in wastewater treatment plants*. Los Angeles: University of Califonia Water Resources Program School of Engineering and Applied Sciences.

Mathe, Z.T., Harris, M.C., O'Connor, C.T. & Franzidis, J.-P., 1998. Review of Froth Modelling In Steady State Flotation Systems. *Minerals Engineering*, 11(5), pp.397-421.

Melo, F., 2001. *Fundamental Properties of Flotation Frothers and Their Effect On Flotation*. MSc Thesis. Concepcion: The University Of British Columbia University of Concepcion.

Melo, F. & Laskowski, J.S., 2007. Effect of frothers and solid particles on the rate of water transfer to froth. *International Journal of Mineral Processing*, (84), pp.33-40.

Miller, J.D., Lin, C.L. & Chang, S.S., 1983. MIBC Adsorption at the Coal/Water Interface. *Colloids adn Surfaces*, (7), pp.351-55.

Morar, S.H., Bradshaw, D.J. & Harris, M.C., 2012. The use of the froth surface lamellae burst rate as a flotation froth stability measurement. *Minerals Engineering*, 36-38, pp.152-59.

Moyo, P., 2005. *Characterization Of Frothers By Water Carrying Rate*. PhD Thesis. Montreal: Canada Heritage McGill University.

Moys, M.H., Yianatos, J. & Larenas, J., 2010. Measurement of particle loading on bubbles in the flotation process. *Minerals Engineering*, 23(2), pp.131-36.

Murthy, V.S., Jena, A.K., Gupta, K.P. & Murty, G.S., 2005. *Structure And Propoerties Of Engineering Materials*. 2nd ed. New Delhi: Tata McGraw-Hill.

Nagaraj, D.R. & Ravishankar, S.A., 2007. Floatation Reagents - A Critical Overview from an Indutrial Perspective. In C. Maurice, C. Fuerstenau, G.J. Jameson & R.-H. Yoon, eds. *Froth Flotation: A Century of Innovation*. Colarado: Society for Mining, Metallurgy, and Extraction. pp.375-424.

Neethling, S.J. & Cilliers, J.J., 2002. The entrainment of gangue into a flotation froth. *Mineral Processing*, 64(2-3), pp.123-34.

Ngoroma, F., Wiese, J. & Franzidis, J.-P., 2013. The effect of frother blends on the flotation performance of selected PGM bearing ores. *Minerals Engineering*, 46-47, pp.76-82.

Pani, S., Dey, S. & Singh, R., 2013. Quantitative Evaluation of Frother Blend Interaction and Its Effect on Coal Flotation. In Tripathy, A., ed. *XIII International Seminar on Mineral Processing Technology*. Bhubaneswar, 2013. Indian Institute of Technology.

Pauley, R.C., Hashemi, R. & Caothlen, S., 1988. Analysis of Foaming Mechanisms in Amine Plants. In *American Institute of Chemical Engineer's Summer Meeting*. Denver, 1988. Pall Fuels and Chemicals.

Pugh, R.J., 1996. Foaming, foam films, antifoaming and defoaming. *Advances In Colloid and Interface Science*, 64(1), pp.67-142.

Pugh, R.J., 2005. Experimental techniques for studying the structure of foams and froths. *Advances in Colloid and Interface Science*, 114-115, pp.239-51.

Pugh, R.J., 2007. The Physics and Chemistry of Frothers. In M.C. Fuerstenau, G.J. Jameson & R.-H. Yoon, eds. *Froth Flotation: A Century of Innovation*. 1st ed. Colorado: Society for Mining, Metallurgy, and Exploration. pp.259-80.

Pugh, R.J. & Johansson, G., 1992. The influence of particle size and hydrophobicity on the stability of mineralized froths. *International Journal of Mineral Processing*, 34(1-2), pp.1-21.

Rajatanavin, P., 2005. *Solid-Stabilised Foams Produced Using a Mixed Surfactant System*. PhD Thesis. Victoria: Swinburne University of Technology.

Rosen, M.J., 2004. *Surfactants and Interfacial Phenomena*. 3rd ed. New York: John Wiley & Sons.

Runge, K., Crosbie, R., Rivett, T. & McMaster, J., 2010. An evaluation of froth recovery measurement techniques. In *XXV International Mineral Processing Congress*. Brisbane, 2010. IMPC.

Samanta, S. & Ghosh, P., 2011. Coalescence of air bubbles in aqueous solutions of alcohols and nonionic surfactants. *Chemical Engineering Science*, (66), pp.4824-37.

Sandler, S.I., 2006. *Chemical, Biochemical, and Engineering Thermodynamics*. 4th ed. Delaware: John Wiley & Sons.

Savassi, O.N., Alexander, D.J., Franzidis, J.P. & Manlapig, E.V., 1997. An Empirical Model for Entrainment in Industrial Flotation Plants. *Minerals Engineering*, 11(3), pp.243-56.

Savassi, O.N. et al., 1997. Measurement of froth recovery of attached particles in industrial cells. In Lorenzen, L. & Bradshaw, D.J., eds. *Sixth Mill Operators Conference*. Madang, 1997. AusIMM.

Schouwstra, R.P. & Kilnoch, E.D., 2000. *A short geological review of the Bushveld complex*. Amplats Reserch Center.

Schwartz, S., 2004. *The relationship between froth recovery and froth structure*. PhD Thesis. Adelaide: Ian Wark Research Institute University of South Australia.

Seaman, D.R., Franzidis, J.P. & Manlapig, E.V., 2004. Bubble load measurement in the pulp zone of industrial flotation machines—a new device for determining the froth recovery of attached particles. *International Journal Mineral Processing*, 74(1), pp.1-13.

Seaman, D.R., Manlapig, E.V. & Franzidis, J.P., 2006. Selective transport of attached particles across the pulp-froth interface. *Minerals Engineering* , 19(6-8), pp.841-51.

Sherrel, I.M., 2004. *Development of a Flotation Rate Equation from First Principles under Turbulent Flow Conditions*. Virginia: Virginia Polytechnic Institute and State University.

Smith, P.G. & Warren, L.J., 1989. Entrainment of particles into flotation froths. *Minerals Processing and Extractive Metallurgy Review*, 5, pp.123-45.

Sweet, C.J., van Hoogstraten, J. & Harris, M.C., 1997. The effect of frothers on bubble size and frothability of aqueous solutions. In Finch, J.A., Rao, S.R. & Holubec, I., eds. *Processing of Complex Ores*. Sudbery, 1997. CIMM & P Montreal Quebec.

Tabakova, S.S. & Danov, K.D., 2009. Effect of disjoining pressure on the drainage adn relaxation dynamics of liquid films with mobile interfaces. *Journal of Colloid and Interface Science*, 336(1), pp.273-84.

Tan, S.N., Fornasiero, D., Sedev, R. & Ralston, J., 2006. The interfacial conformation of polypropylene glycols and their foam properties. *Minerals Engineering*, (19), pp.703-12.

Tan, S.N., Pugh, R.J., Fornasiero, D. & Ralston, J., 2005. Foaming of polypropylene glycols and glycol/MIBC mixtures. *Minerals Engineering*, 18(1), pp.179-88.

Tao, D., Luttrell, G. & Yoon, R., 2000. A parametric study of froth stability and its effect on column flotation of fine particles. *International Journal of Mineral Processing*, 59, pp.25-43.

Taylor, R. & Krishna, R., 1993. *Multicomponent mass transfer*. 1st ed. New York: Wiley.

Tsatouhas, G., Grano, S.R. & Vera, M., 2006. Case studies on the performance and characterisation of the froth phase in industrial flotation circuits. *Minerals Engineering*, 19, pp.774-83.

Ventura-Medina, E., Barbian, N. & Cilliers, J.J., 2003. Froth stability and flotation performance. In Van Deventer, S.J., ed. *XXII International Mineral Processing Congress*. Cape Town, 2003.

Ventura-Medina, E. & Cilliers, J.J., 2002. A model to describe flotation performance based on physics of foams and froth image analysis. *International Journal of Mineral Processing*, 67(1-4), pp.77-99.

Vera, M.A., Franzidis, J.P. & Manlapig, E.V., 1999a. The JKMRC high bubble surface area flux flotation cell. *Minerals Engineering*, 12(5), pp.477-84.

Vera, M.A., Franzidis, J.P. & Manlapig, E.V., 1999b. Simultaneous determination of collection zone rate constant and froth zone recovery in a mechanical flotation environment. *Minerals Engineering*, 12(10), pp.1163-76.

Vera, M.A. et al., 2002. The modelling of froth zone recovery in batch and continuously operated laboratory flotation cells. *International Journal of Mineral Processing*, 64(1), pp.135-51.

Wang, L. & Yoon, R.-H., 2004. Hydrophobic Forces in the Foam Films Stabilized by Sodium Dodecyl Sulfate: Effect of Electrolyte. *Langmuir*, 20(1), pp.11457-64.

Wang, L. & Yoon, R.-H., 2008. Effects of surface forces and film elasticity on foam stability. *International Journal of Mineral Processing*, 85(1), pp.101-10.

Wiese, J.G., 2009. *Investigating depressant behaviour in the flotation of selected Merensky ores*. MSc Thesis. Cape Town: Department of Chemical Engineering University of Cape Town.

Wiese, J. & Harris, P., 2012. The effect of frother type and dosage on flotation performance in the presence of high depressant concentrations. *Minerals Engineering*, 36-38, pp.204-10.

Wiese, J.G., Harris, P.J. & Bradshaw, D.J., 2005. The influence of the reagent suite on the flotation of ores from the Merensky reef. *Minerals Engineering*, 18(2), pp.189-98.

Wiese, J.G., Harris, P.J. & Bradshaw, D.J., 2010. The efect of increased frother dosage on froth stability at high despressant dasoges. *Minerals Engineering*, 23, pp.1010-17.

Wiese, J., Harris, P. & Bradshaw, D., 2011. The effect of the reagent suite on froth stability in laboratory scale batch flotation tests. *Minerals Engineering*, 24(9), pp.995-1003.

Wills, B.A. & Napier-Munn, T.J., 2006. *Wills' Mineral Processing Technology*. 7th ed. Queensland: Elsevier Science and Technology Books.

Wills, B.A. & Napier-Munn, T., 2006. *Will's Mineral Processing Technology: An Introduction to the Practical Aspects of Ore Treatment and Mineral Recovery*. 7th ed. Oxford: Butterworth-Heinemann.

Yoon, R.H. & Aksoy, B.S., 1999. Hydrophobic Forces in Thin Water Films Stabilized by Dodecylammonium Chloride. *Journal of Colloid and Interface Science*, 211(1), pp.1-10.

Yunkai, X., 2000. *Dynamic Property Evaluation of Frother*. MSc Thesis. Morgantown: Department of Mining Engineering West Virginia University.

Zanin, M., Wightman, E., Grano, S.R. & Franzidis, J.-P., 2009. Quantifying contributions to froth stability in porphyry copper plants. *International Journal of Mineral Processing*, 91(1-2), pp.19-27.

Zhang, W., 2012. *Frothers and Frother Blends: A Structure - Function Study*. PhD Thesis. Montreal: McGill University.

Zhang, W., Nesset, J.E., Rao, R. & Finch, J.A., 2012. Characterizing Frothers through Critical Coalescence Concentration (CCC)95-Hydrophile-Lipophile Balance (HLB) Relationship. *Minerals*, 2(1), pp.208-27.

# Chapter 8

# Appendices

## A1. Equilibrium Surface Tension Measurements

**Table A1-1: Equilibrium surface tension measurement data on use of PPG192 and PPG425.**

| PPG192 | | PPG425 | |
|---|---|---|---|
| Concentration (mM) | Surface Tension (mN/m) | Concentration (mM) | Surface Tension (mN/m) |
| 52 | 62.3 | 18.8 | 48.9 |
| 46.8 | 62.8 | 16.5 | 49.7 |
| 41.6 | 63.4 | 14.1 | 50.3 |
| 36.4 | 63.7 | 11.8 | 50.6 |
| 31.2 | 64.4 | 9.41 | 51.6 |
| 26 | 65 | 7.06 | 52.7 |
| 20.8 | 65.7 | 4.71 | 53.8 |
| 62.4 | 61.5 | 1.88 | 56.2 |
| 72.8 | 60.8 | 1.13 | 57.7 |
| 83.2 | 60.3 | 0.678 | 58.9 |
| 93.6 | 59.7 | 0.407 | 60.8 |
| 104 | 59.3 | 0.244 | 62.8 |
| 125 | 58.5 | 0.146 | 64.4 |
| 156 | 57.2 | 0.0878 | 65 |
| | | 0.0527 | 66.9 |
| | | 0.0316 | 67.9 |
| | | 0.019 | 69.5 |
| | | 0.00683 | 70.3 |
| | | 0.0041 | 70.9 |
| | | 0.00246 | 71.2 |
| | | 0.00148 | 71.1 |

**Table A1-2: Equilibrium surface tension measurement data on use of PPG725 and PPG1000.**

| PPG725 | | PPG1000 | |
|---|---|---|---|
| Concentration (mM) | Surface Tension (mN/m) | Concentration (mM) | Surface Tension (mN/m) |
| 11.03 | 43.5 | 8.00 | 42.0 |
| 9.66 | 43.8 | 7.00 | 42.5 |
| 8.28 | 44.0 | 6.00 | 42.6 |
| 6.90 | 44.3 | 5.00 | 42.8 |
| 5.52 | 45.1 | 4.00 | 43.3 |
| 4.14 | 45.8 | 3.00 | 43.9 |
| 2.76 | 46.7 | 2.00 | 44.7 |
| 0.828 | 49.2 | 1.00 | 46.1 |
| 0.497 | 50.5 | 0.48 | 47.2 |
| 0.179 | 51.9 | 0.288 | 48.4 |
| 0.107 | 52.47 | 0.173 | 49.5 |
| 0.00834 | 58 | 0.104 | 50.1 |
| 0.00500 | 59.6 | 0.0622 | 50.7 |
| 0.00300 | 60.3 | 0.0373 | 51.6 |
| 0.00108 | 61.1 | 0.0224 | 52.5 |
| | | 0.0134 | 53.4 |
| | | 0.00806 | 54.7 |

**Table A1-3: Equilibrium surface tension measurement data on use of PPG-MIBC blends.**

| PPG192 & MIBC | | PPG425 & MIBC | |
|---|---|---|---|
| Concentration (mM) | Surface Tension (mN/m) | Concentration (mM) | Surface Tension (mN/m) |
| 5.40 | 68.4 | 29.4 | 47.9 |
| 41.6 | 59.9 | 17.6 | 49.8 |
| 25.0 | 62.9 | 10.6 | 51.4 |
| 15.0 | 65.3 | 6.35 | 53.1 |
| 9.00 | 67.2 | 3.81 | 54.9 |
| 130 | 51.5 | 2.29 | 56.0 |
| 143 | 50.8 | PPG725 & MIBC | |
| 156 | 50.1 | Concentration (mM) | Surface Tension (mN/m) |
| 169 | 49.5 | 17.2 | 41.8 |
| 182 | 48.9 | 10.3 | 43.6 |
| 117 | 52.4 | 6.2 | 44.8 |
| 97.6 | 53.8 | 3.72 | 46.19 |
| 85.6 | 54.9 | 2.23 | 47.35 |
| 71.6 | 56.3 | | |
| 65.1 | 56.8 | | |

**Table A1-4: Equilibrium surface tension measurement data on use of hexanol and pentanol.**

| Hexanol | | Pentanol | |
|---|---|---|---|
| Concentration (mM) | Surface Tension (mN/m) | Concentration (mM) | Surface Tension (mN/m) |
| 97.9 | 27.9 | 159.0 | 35.8 |
| 88.1 | 28.1 | 147.0 | 36.9 |
| 78.3 | 28.6 | 136.0 | 38.0 |
| 68.5 | 29.1 | 125.0 | 39.0 |
| 58.7 | 30.7 | 113.0 | 40.3 |
| 48.9 | 33.4 | 102.0 | 41.7 |
| 39.2 | 36.5 | 90.8 | 43.3 |
| 29.4 | 40.0 | 79.4 | 45.1 |
| 19.6 | 46.4 | 68.1 | 47.1 |
| 9.79 | 54.9 | 56.7 | 49.1 |
| 5.88 | 61.1 | 45.4 | 52.1 |
| 3.52 | 65.5 | 34.0 | 55.3 |
| 2.11 | 68.3 | 22.7 | 59.8 |
| 1.27 | 69.7 | 18.2 | 61.7 |
| 0.761 | 70.5 | | |
| 0.457 | 70.9 | | |
| 34.3 | 38.6 | | |
| 24.5 | 43.4 | | |
| 44.0 | 35.0 | | |

**Table A1-5: Equilibrium surface tension measurement data on use of MIBC.**

| MIBC | |
|---|---|
| Concentration (mM) | Surface Tension (mN/m) |
| 78.3 | 39.5 |
| 58.7 | 42.3 |
| 39.1 | 46.8 |
| 19.6 | 53.6 |
| 11.7 | 58.1 |
| 7.05 | 62.6 |
| 14.7 | 55.5 |
| 29.4 | 49.5 |
| 48.9 | 44.5 |
| 24.5 | 51.5 |
| 63.6 | 41.8 |
| 88.1 | 38.1 |
| 97.8 | 36.9 |

# A2. Foam Stability Measurements

**Table A2-1: Foam rise rate experimental data on use of PPG1000.**

| | Foam Height (cm) | | |
|---|---|---|---|
| Time (sec) | Run 1 | Run 2 | Run 3 |
| 10 | 14.6 | 15.2 | 19.2 |
| 20 | 24.1 | 25.7 | 28.3 |
| 30 | 32.3 | 34.5 | 35.3 |
| 40 | 37.1 | 40.6 | 40.6 |
| 50 | 41.5 | 45.4 | 45.1 |
| 60 | 46.5 | 49 | 48.3 |
| 75 | 50.3 | 54.2 | 53.6 |
| 90 | 54.3 | 58.4 | 56.2 |
| 105 | 57.5 | 61.7 | 59.6 |
| 120 | 61.3 | 64.8 | 62.2 |
| 140 | 63.7 | 67.3 | 65.3 |
| 160 | 68.2 | 68.6 | 67.4 |
| 180 | 68.2 | 68.6 | 69.5 |
| 210 | 70.3 | 71.5 | 72.1 |
| 240 | 71.8 | 73.2 | 74.6 |
| 300 | 71.9 | 73.2 | 74.6 |
| 480 | 72.5 | 73.2 | 74.6 |

**Table A2-2: Foam decay rate experimental data on use of PPG1000.**

| Time (sec) | Run 1 | Run 2 | Run 3 |
|---|---|---|---|
| 0 | 57.5 | 63 | 61.2 |
| 3 | 57.2 | 57 | 54.3 |
| 6 | 47.3 | 50.1 | 48 |
| 9 | 40.7 | 41.3 | 40.9 |
| 12 | 33.8 | 34.2 | 35.2 |
| 15 | 25.8 | 26.1 | 27.6 |
| 18 | 18.3 | 20.5 | 20.6 |
| 21 | 11.3 | 12.2 | 14.4 |
| 24 | 5.3 | 5.8 | 9.1 |
| 27 | 2.2 | 1.3 | 4.2 |

**Table A2-3: Summary of foam stability indicator measurements on use of PPG1000.**

| Stability measure | Mean | % Error |
|---|---|---|
| τ (sec) | 53.86 | 7.40 |
| Stability (sec) | 43.26 | 1.59 |
| Half-life (sec) | 11.19 | 4.12 |

**Table A2-4: Foam rise rate experimental data on use of PPG725.**

| | Foam Heights (cm) | | |
|---|---|---|---|
| Time (sec) | Run 1 | Run 2 | Run 3 |
| 10 | 12.8 | 10.2 | 11.1 |
| 20 | 20.2 | 19 | 20.3 |
| 30 | 25.4 | 24.3 | 25.8 |
| 40 | 27.2 | 26.6 | 27.7 |
| 50 | 29.3 | 27.8 | 29.4 |
| 60 | 30.6 | 28.2 | 30.1 |
| 75 | 31.2 | 29.1 | 30.9 |
| 90 | 31.2 | 29.2 | 31.4 |
| 105 | 31.2 | 29.2 | 30.7 |
| 120 | 30.7 | 29.2 | 29.4 |
| 140 | 30.7 | 27.4 | 29.3 |
| 160 | 30.2 | 24.8 | 27.5 |
| 180 | 30.2 | 24.8 | 27.3 |
| 210 | 28.4 | 24.6 | 27.3 |
| 240 | 27.4 | 24.6 | 27.1 |
| 300 | 23.9 | 24.1 | 26.7 |
| 360 | 23.5 | 24.1 | 23.3 |
| 420 | 23.6 | 23.9 | 23 |
| 480 | 23.5 | 24 | 23.3 |

**Table A2-5: Foam decay rate experimental data on use of PPG725.**

| | Foam height (cm) | | |
|---|---|---|---|
| Time (sec) | Run 1 | Run 2 | Run 3 |
| 0 | 23.5 | 24.1 | 23.3 |
| 3 | 15.9 | 14.9 | 17.2 |
| 6 | 10 | 9.7 | 11.9 |
| 9 | 3.2 | 3.7 | 6.7 |
| 12 | | 1.7 | 2.2 |

**Table A2-6: Summary of foam stability indicator measurements on use of PPG725.**

| Stability measure | Mean | % Error |
|---|---|---|
| τ (sec) | 14.61 | 1.07 |
| Stability (sec) | 16.34 | 4.09 |
| Half-life (sec) | 4.72 | 15.00 |

**Table A2-7: Foam rise rate experimental data on use of PPG425.**

| | Height (cm) | | |
|---|---|---|---|
| Time (sec) | Run 1 | Run 2 | Run 3 |
| 10 | 10.2 | 10.3 | 12.6 |
| 20 | 16.8 | 16 | 16.3 |
| 30 | 19.1 | 18.3 | 17.1 |
| 40 | 19.1 | 19.5 | 18.2 |
| 50 | 19.3 | | 17.3 |
| 60 | 19.5 | 19.1 | 17.1 |
| 75 | 20.6 | 17.7 | 18.2 |
| 90 | 20.8 | 17.4 | 17.3 |
| 105 | 20.8 | 16.1 | 17.1 |
| 120 | 20.8 | 17.2 | 15.6 |
| 140 | 19.7 | 14.6 | 15.7 |
| 160 | 19.7 | 14.7 | 14.6 |
| 180 | 19.5 | 14.7 | 15.3 |
| 210 | 19.6 | 14.7 | 15.5 |
| 240 | 19.5 | 13.4 | 14.6 |
| 300 | 19.7 | 13.9 | 14.7 |
| 360 | 19.7 | 13.7 | 14.5 |
| 420 | 16.7 | 13.7 | 14.7 |
| 480 | 17.3 | 13.7 | 14.6 |

**Table A2-8: Foam decay rate experimental data on use of PPG425.**

| | Foam height (cm) | | |
|---|---|---|---|
| | Run 1 | Run 2 | Run 3 |
| 0 | 17.3 | 13.7 | 14.6 |
| 3 | 10.8 | 9.1 | 9.2 |
| 6 | 4.6 | 3.2 | 3.1 |
| 9 | 0.5 | 0.9 | 0.7 |

**Table A2-9: Summary of foam stability indicator measurements on use of PPG425.**

| Stability measure | Mean | % Error |
|---|---|---|
| τ (sec) | 8.032 | 44.5 |
| Stability (sec) | 9.97 | 16.5 |
| Half-life (sec) | 3.83 | 3.02 |

**Table A2-10: Foam rise rate experimental data on use of MIBC.**

| | Height (cm) | | |
|---|---|---|---|
| Time (sec) | Run 1 | Run 2 | Run 3 |
| 5 | 6.2 | 9.6 | 6.7 |
| 10 | 10.5 | 13.4 | 10.3 |
| 15 | 12.3 | 15.9 | 12.5 |
| 20 | 13.6 | 17.2 | 14.3 |
| 30 | 16.2 | 20.1 | 16.8 |
| 40 | 18.3 | 21.5 | 18.9 |
| 50 | 19.2 | 22.4 | 20.3 |
| 60 | 20.4 | 23.6 | 21.2 |
| 75 | 20.7 | 25.2 | 23.1 |
| 90 | 21.2 | 25.7 | 23.1 |
| 105 | 22.2 | 26.3 | 23.1 |
| 120 | 22.6 | 26.3 | 23.1 |
| 135 | 23.7 | 26.3 | 23.1 |
| 150 | 23.9 | 26.3 | 23.1 |
| 165 | 24.2 | 26.3 | 23.1 |
| 180 | 24.4 | 26.3 | 23.1 |
| 210 | 24.4 | 26.3 | 23.1 |
| 240 | 24.7 | 26.3 | 23.1 |
| 300 | 25.1 | 26.3 | 23.1 |
| 360 | 25.6 | 26.3 | 23.1 |
| 420 | 25.6 | 26.3 | 23.1 |

**Table A2-11: Foam decay rate experimental data on use of MIBC.**

| | Height (cm) | | |
|---|---|---|---|
| | Run 1 | Run 2 | Run 3 |
| 0 | 25.6 | 26.3 | 23.1 |
| 3 | 21.1 | 19.3 | 17.3 |
| 6 | 12.6 | 11.3 | 8.7 |
| 9 | 4.2 | 4.1 | 2.1 |

**Table A2-12: Summary of foam stability indicator measurements on use of MIBC.**

| Stability measure | Mean | % Error |
|---|---|---|
| τ (sec) | 22.81 | 33.67 |
| Stability (sec) | 14.79 | 7.60 |
| Half-life (sec) | 4.98 | 8.33 |

**Table A2-13: Foam rise rate experimental data on use of PPG425-MIBC blend.**

| | Height (cm) | | |
|---|---|---|---|
| time (sec) | Run 1 | Run 2 | Run 3 |
| 0 | 0 | 0 | 0 |
| 10 | 11.7 | 10.1 | 10.8 |
| 20 | 19.2 | 18.6 | 19.4 |
| 30 | 24.6 | 24 | 25.3 |
| 40 | 28.2 | 28.2 | 29.5 |
| 50 | 30.5 | 31.1 | 31.7 |
| 60 | 31.5 | 33.4 | 31.7 |
| 75 | 33.6 | 35.4 | 34.2 |
| 90 | 34.1 | 35.3 | 34.2 |
| 105 | 35.5 | 35.9 | 36.1 |
| 120 | 34.7 | 35.4 | 35.6 |
| 140 | 34.7 | 35.6 | 35.6 |
| 160 | 34.7 | 35.7 | 35.6 |
| 180 | 34.7 | 35.7 | 35.6 |

**Table A2-14: Foam decay rate experimental data on use of PPG425-MIBC blend.**

| | Run 1 | Run 2 | Run 3 |
|---|---|---|---|
| 0 | 34.7 | 35.7 | 35.6 |
| 2 | 31.6 | 31.6 | 31.9 |
| 4 | 25.6 | 25.8 | 26.8 |
| 6 | 20.2 | 21.8 | 22.2 |
| 8 | 16.1 | 18.2 | 17.2 |
| 10 | 11.7 | 14.2 | 13.2 |
| 12 | 6.4 | 11.1 | 9.7 |
| 14 | 3.4 | 7 | 5.9 |
| 16 | 0.9 | 3.6 | 3.4 |

**Table A2-15: Summary of foam stability indicator measurements on use of PPG425-MIBC blend.**

| Stability measure | Mean | % Error |
|---|---|---|
| τ (sec) | 25.57 | 5.29 |
| Stability (sec) | 21.06 | 1.97 |
| Half-life (sec) | 31.95 | 5.27 |

**Table A2-16: Foam rise rate experimental data on use of PPG725-MIBC blend.**

| | Height | | |
|---|---|---|---|
| Time (sec) | Run 1 | Run 2 | Run 3 |
| 0 | 0 | 0 | 0 |
| 10 | 12.3 | 13.5 | 11.2 |
| 20 | 22.2 | 22.9 | 21.7 |
| 30 | 31.3 | 30.6 | 30.4 |
| 40 | 38.2 | 36.4 | 35 |
| 50 | 43.5 | 40.1 | 40.7 |
| 60 | 47.2 | 43.3 | 44.9 |
| 75 | 49.4 | 46.6 | 47.6 |
| 90 | 51.2 | 47.4 | 48.7 |
| 105 | 51.7 | 47.4 | 49.3 |
| 120 | 51.7 | 47.4 | 49.9 |
| 140 | 51.2 | 47.4 | 49.9 |
| 160 | 50.8 | 45.4 | 48.9 |
| 180 | 49.9 | 45.4 | 48.9 |
| 240 | 49.9 | 45.4 | 47.3 |
| 300 | 49.9 | 45.4 | 47.3 |

**Table A2-17: Foam decay rate experimental data on use of PPG725-MIBC blend.**

| | Height (cm) | | |
|---|---|---|---|
| | Run 1 | Run 2 | Run 3 |
| 0 | 49.9 | 47.4 | 45.4 |
| 2 | 46.3 | 43.2 | 39.5 |
| 4 | 40.6 | 38.6 | 35 |
| 6 | 35.6 | 34.2 | 30.2 |
| 8 | 30.6 | 29.7 | 25 |
| 10 | 25.1 | 24.2 | 20.8 |
| 12 | 19.7 | 20.1 | 16.1 |
| 14 | 15 | 16.3 | 12.2 |
| 16 | 10.7 | 11.8 | 8.1 |

**Table A2-18: Summary of foam stability indicator measurements on use of PPG725-MIBC blend.**

| Stability measure | Mean | % Error |
|---|---|---|
| τ (sec) | 30.60 | 8.71 |
| Stability (sec) | 29.70 | 4.37 |
| Half-life (sec) | 8.78 | 8.46 |

**Table A2-19: Foam rise rate experimental data on use of PPG425-Pentanol blend.**

| | Height (cm) | | |
|---|---|---|---|
| Time (sec) | Run 1 | Run 2 | Run 3 |
| 0 | 0 | 0 | 0 |
| 10 | 10.8 | 11.1 | 11.4 |
| 20 | 19.1 | 20.1 | 19.1 |
| 30 | 25.3 | 25.6 | 26.4 |
| 40 | 29 | 30.7 | 30.1 |
| 50 | 31.7 | 33.8 | 32 |
| 60 | 32.8 | 35 | 35.4 |
| 75 | 32.8 | 35.3 | 35.3 |
| 90 | 33.1 | 35.8 | 35.5 |
| 105 | 33.1 | 35.8 | 35.5 |
| 120 | 33.1 | 35.8 | 35.5 |

**Table A2-20: Foam decay rate experimental data on use of PPG425-Pentanol blend.**

| | Height (cm) | |
|---|---|---|
| Time (sec) | Run 1 | Run 2 |
| 0 | 35.8 | 35.5 |
| 2 | 32.6 | 32 |
| 4 | 29.9 | 27.2 |
| 6 | 24.5 | 23 |
| 8 | 19.2 | 18.1 |
| 10 | 14.9 | 14 |
| 12 | 10 | 10 |
| 14 | 5.8 | 6.2 |
| 16 | 2.8 | 3.5 |

**Table A2-21: Summary of foam stability indicator measurements on use of PPG425-Pentanol blend.**

| Stability measure | Mean | % Error |
|---|---|---|
| τ (sec) | 23.81 | 5.11 |
| Stability (sec) | 21.17 | 5.08 |
| Half-life (sec) | 7.16 | 2.10 |

**Table A2- 22: Foam rise rate experimental data on use of PPG725-Pentanol blend.**

| | Height (cm) | | |
|---|---|---|---|
| Time (sec) | Run 1 | Run 2 | Run 3 |
| 0 | 0 | 0 | 0 |
| 10 | 13.5 | 12.5 | 11.2 |
| 20 | 23.3 | 21.7 | 21.3 |
| 30 | 31.1 | 30 | 29.1 |
| 40 | 36 | 34.7 | 35.2 |
| 50 | 39.4 | 39.6 | 39.1 |
| 60 | 42.3 | 41.5 | 41.3 |
| 75 | 44.3 | 43.7 | 43.1 |
| 90 | 44.3 | 44.9 | 44.6 |
| 105 | 44.3 | 44.9 | 44.6 |
| 120 | 44.3 | 45.2 | 44.8 |
| 140 | | 45.2 | 44.8 |
| 160 | | 45.2 | 44.9 |

**Table A2-23: Foam decay rate experimental data on use of PPG725-Pentanol blend.**

| | Height (cm) | |
|---|---|---|
| Time (sec) | Run 1 | Run 2 |
| 0 | 44.3 | 44.8 |
| 2 | 41.6 | 41.1 |
| 4 | 38.1 | 35.6 |
| 6 | 33.5 | 29.5 |
| 8 | 30.1 | 24.2 |
| 10 | 25.3 | 19.5 |
| 12 | 20.7 | 14 |
| 14 | 15.8 | 9.7 |
| 16 | 11.1 | 5.1 |

**Table A2-24: Summary of foam stability indicator measurements on use of PPG725-Pentanol blend.**

| Stability measure | Mean | % Error |
|---|---|---|
| τ (sec) | 28.2 | 5.73 |
| Stability (sec) | 46.9 | 0.426 |
| Half-life (sec) | 9.03 | 16.9 |

**Table A2-25: Foam rise rate experimental data on use of pentanol.**

| Time (sec) | Foam Height (cm) |
|---|---|
| 0 | 0 |
| 5 | 4.6 |
| 10 | 7.1 |
| 15 | 8.7 |
| 20 | 10.1 |
| 30 | 10.6 |
| 40 | 10.8 |
| 50 | 10.8 |
| 60 | 11.6 |
| 75 | 11.4 |
| 90 | 11.8 |
| 105 | 11.6 |
| 120 | 11.4 |
| 140 | 11.8 |

**Table A2-26:Foam decay rate experimental data on use of pentanol.**

| | Foam height (cm) | | |
|---|---|---|---|
| | Run 1 | Run 2 | Run 3 |
| 0 | 11.5 | 10.6 | 11.5 |
| 2 | 9.6 | 8.1 | 9.2 |
| 4 | 5.4 | 4.3 | 5.6 |
| 6 | 2 | 1.5 | 1.9 |

**Table A2-27: Summary of foam stability indicator measurements on use of pentanol.**

| Stability measure | Mean | % Error |
|---|---|---|
| τ (sec) | 10.3 | N/A |
| Stability (sec) | 6.74 | N/A |
| Half-life (sec) | 3.46 | 6.03 |

**Table A2-28: Foam rise rate experimental data on use of hexanol.**

| Time (sec) | Foam Height (cm) |
|---|---|
| 0 | 0 |
| 5 | 4.2 |
| 10 | 8 |
| 15 | 10.2 |
| 20 | 11.8 |
| 30 | 14.6 |
| 40 | 15.2 |
| 50 | 15.2 |
| 60 | 15.2 |

**Table A2-29: Foam decay rate experimental data on use of hexanol.**

| Time (sec) | Foam Height (cm) |
|---|---|
| 0 | 15.2 |
| 2 | 11.4 |
| 4 | 7.4 |
| 6 | 2.7 |

**Table A2-30: Summary of foam stability indicator measurements on use of hexanol.**

| Stability measure | Mean | % Error |
|---|---|---|
| τ (sec) | 14.4 | N/A |
| Stability (sec) | 9.36 | N/A |
| Half-life (sec) | 3.44 | N/A |

# A3. Froth Stability Measurements

**Table A3-1: Froth rise rate experimental data on use of PPG192.**

| | Froth Height (cm) | |
|---|---|---|
| Time (sec) | Run 1 | Run 2 |
| 2 | 2.8 | 3.6 |
| 4 | | 5.6 |
| 6 | 6.2 | |
| 10 | 8.3 | 8.2 |
| 14 | 10 | |
| 18 | 11.3 | 9.9 |
| 30 | 12.4 | 11.5 |
| 50 | 13.4 | 13.3 |
| 60 | 14.7 | |
| 80 | | 15.4 |
| 120 | 14.7 | 16.2 |

**Table A3-2: Summary of foam stability indicator measurements on use of PPG192.**

| Stability measure | Mean | % Error |
|---|---|---|
| τ (sec) | 15.4 | 17.2 |
| Stability (sec) | 12.8 | 14.5 |

**Table A3-3: Froth rise rate experimental data on use of PPG425.**

| | Froth Height (cm) | |
|---|---|---|
| Time (sec) | Run 1 | Run 2 |
| 4 | 4.6 | |
| 6 | 8.5 | |
| 10 | 12.2 | 11.4 |
| 16 | 16.8 | |
| 20 | 19.1 | 16.5 |
| 24 | 21.4 | |
| 30 | 24.2 | 20.8 |
| 40 | 28.8 | 25.3 |
| 50 | 33.5 | 29.4 |
| 60 | 37.6 | 32.1 |
| 70 | 41.1 | 35 |
| 90 | 45.1 | 39.5 |
| 120 | 49.7 | 44.3 |
| 160 | 52.8 | |
| 180 | | 47.5 |
| 240 | 52.8 | 49.1 |
| 270 | | 50.2 |
| 300 | | 50.2 |

**Table A3-4: Summary of foam stability indicator measurements on use of PPG425.**

| Stability measure | Mean | % Error |
|---|---|---|
| τ (sec) | 52.5 | 16.1 |
| Stability (sec) | 48.5 | 3.6 |

`

**Table A3-5: Froth rise rate experimental data on use of PPG725-MIBC blend.**

| | Froth Height (cm) | |
|---|---|---|
| Time (sec) | Run 1 | Run 2 |
| | 11.2 | 12.1 |
| 20 | 17.5 | 17.5 |
| 30 | 23.2 | 23.1 |
| 40 | 28.3 | 28.5 |
| 50 | 32.7 | 32.5 |
| 60 | 36.2 | 35.1 |
| 80 | 42.1 | 40.6 |
| 100 | 43.7 | 42.7 |
| 120 | 45.7 | 44.9 |
| 140 | 48.4 | |
| 150 | | 46.2 |
| 160 | 48.4 | |
| 180 | | 47.3 |
| 240 | | 47.3 |

**Table A3-6: Summary of foam stability indicator measurements on use of PPG725-MIBC blend.**

| Stability measure | Mean | % Error |
|---|---|---|
| τ (sec) | 46.0 | 5.0 |
| Stability (sec) | 46.3 | 3.6 |

**Table A3-7: Froth rise rate experimental data on use of hexanol.**

| | Froth Height (cm) | |
|---|---|---|
| Time (sec) | Run 1 | Run 2 |
| 4 | 3.2 | 2.9 |
| 8 | 4.7 | 4 |
| 12 | 6 | 4.9 |
| 16 | 6.6 | 5.4 |
| 20 | | 5.8 |
| 32 | 7.2 | |
| 34 | 7.7 | |
| 44 | 7.7 | |
| 60 | 7.7 | 6.3 |
| 70 | 7.4 | |
| 80 | 7.7 | |
| 90 | | 7.9 |

**Table A3-8: Summary of foam stability indicator measurements on use of hexanol.**

| Stability measure | Mean | % Error |
|---|---|---|
| τ (sec) | 4.4 | 8.0 |
| Stability (sec) | 7.4 | 1.8 |

**Table A3-9: Froth rise rate experimental data on use of MIBC.**

| | Froth Height (cm) | |
|---|---|---|
| Time (sec) | Run 1 | Run 2 |
| 0 | 0 | |
| 2 | 4.1 | 4.6 |
| 4 | 6.3 | 6.8 |
| 6 | 7.8 | 8.1 |
| 8 | 8.6 | |
| 10 | | 9 |
| 12 | 9.2 | |
| 14 | 9.2 | |
| 18 | | 9.7 |
| 20 | 9.8 | 9.7 |
| 30 | 10.2 | |
| 40 | 10.2 | |
| 60 | | 9.7 |

**Table A3-10: Summary of foam stability indicator measurements on use of MIBC.**

| Stability measure | Mean | % Error |
|---|---|---|
| τ (sec) | 4.3 | 5.4 |
| Stability (sec) | 9.4 | 3.6 |

**Table A3-11: Froth rise rate experimental data on use of pentanol.**

| | Froth Height cm) | |
|---|---|---|
| Time (sec) | Run 1 | Run 2 |
| 4 | 3.8 | 4.8 |
| 8 | 7.5 | 8 |
| 10 | 9.1 | |
| 12 | | 9.9 |
| 14 | 10.8 | |
| 18 | 12.2 | 11.7 |
| 22 | 13.6 | |
| 30 | 15.2 | |
| 40 | 16.6 | 14.7 |
| 50 | 16.6 | |
| 60 | 16.6 | |
| 70 | | 16.5 |
| 100 | | 17.1 |
| 120 | | 17.1 |

**Table A3-12: Summary of foam stability indicator measurements on use of pentanol.**

| Stability measure | Mean | % Error |
|---|---|---|
| τ (sec) | 14.2 | 5.2 |
| Stability (sec) | 16.1 | 0.4 |

**Table A3-13: Froth rise rate experimental data on use of PPG425-MIBC blend.**

| | Height (cm) | |
|---|---|---|
| Time (sec) | Run 1 | Run 2 |
| 10 | 13.3 | 13.1 |
| 20 | 21.2 | 20.2 |
| 30 | 27.6 | 25.8 |
| 40 | 31.8 | 31.1 |
| 50 | 36.4 | 36 |
| 60 | 38.5 | 39.6 |
| 80 | 42.7 | 45.4 |
| 100 | 44.9 | 49.1 |
| 120 | 47.7 | 51.5 |
| 140 | | 53.6 |
| 180 | 51.3 | 56.6 |
| 240 | 53.2 | 56.6 |
| 300 | 54.3 | |
| 360 | 55.1 | |

**Table A3-14: Summary of foam stability indicator measurements on use of PPG425-MIBC.**

| Stability measure | Mean | % Error |
|---|---|---|
| τ (sec) | 47.5 | 8.3 |
| Stability (sec) | 51.9 | 5.4 |

**Table A3-15: Froth rise rate experimental data on use of PPG725.**

| | Froth Height (cm) | |
|---|---|---|
| Time (sec) | Run 1 | Run 2 |
| 4 | 5.1 | |
| 8 | 8.8 | |
| 10 | | 10.9 |
| 16 | | 14.8 |
| 20 | 15.2 | 17.5 |
| 26 | | 20.6 |
| 30 | 21.2 | 23.4 |
| 38 | | 26.1 |
| 40 | 25.8 | |
| 50 | 29.1 | 30.1 |
| 60 | 31.2 | |
| 70 | | 34.7 |
| 80 | | 36.5 |
| 90 | 34.7 | |
| 100 | | 38.1 |
| 120 | 37.1 | 39.6 |
| 150 | 39.7 | |
| 180 | 40 | 45.2 |
| 240 | 41.5 | 45.2 |
| 260 | 41.5 | |

**Table A3-16: Summary of foam stability indicator measurements on use of PPG725.**

| Stability measure | Mean | % Error |
|---|---|---|
| τ (sec) | 36.7 | 8.5 |
| Stability (sec) | 35.5 | 7.7 |